The behaviour of heavy metals and nutrients from stormwater in the Bluebloqs Biofilter in Spangen, Rotterdam

MSc Thesis

By

Kirsten van Lienden (4357183)

Thesis Committee

Dr. Boris van Breukelen
Prof. Dr. Ir. Luuk Rietveld
Dr. Julia Gebert
Joshua Gallegos (PDEng)

Delft University of Technology

August 20, 2021

Abstract

Climate change, population growth and urbanisation contribute to an increasing demand for freshwater resources. In order to face this challenge, stormwater harvesting for aquifer storage and recovery has gained interest over the past decades. However, pollutants from various surfaces are transported with the runoff, posing a threat for receiving groundwater upon aquifer infiltration. Biofiltration is a low-cost and low-energy technology that uses natural processes to improve the stormwater quality. Heavy metals are a contaminant of concern, because of their lack of degradability and toxicity at low levels. So far, removal potential has been shown in lab and column tests, but field research is limited. Furthermore, most biofiltration studies focused on removal of total metals, whereas dissolved metals are known to have higher bioavailibilities and thus toxicities.

This research aims to gain more insight in the processes in field scale biofilters, by monitoring and analysing the concentrations of metals (Fe, Mn, As, Co, Cr, Cu, Ni, Pb, Zn) in the inlet and the outlet of a stormwater biofilter in Spangen, Rotterdam. In the analysis, a distinction was made between the total metal concentrations, consisting of dissolved and suspended metals, and dissolved metal concentrations. The main chemical water composition was also monitored, to get a better picture of the conditions in which the biofilter was operated. This information was used to identify how the design and operation of the system can be improved with regards to metal removal. Additionally, a transport model in PHREEQC was used to estimate the lifetime of the biofilter before breakthrough occurs, and how operational choices affect this lifetime.

Preferential flows and short-circuiting as a result of design- and operational choices were uncovered by analysis of the electrical conductivity. Heterogeneous distribution of water on the filter and the inlet located closely to the outlet contributed to this. A great variation in hydraulic conductivity supported these observations. The hydraulic conductivity was generally much higher than is recommended for biofilters. Additionally, the system was irrigated with recovered water from the aquifer to avoid a foul smell of extracted water and keep the biofilter wet during longer dry periods. This means that the system was not only fed with stormwater, but also with water from the aquifer. Feeding of two different water sources with different compositions lead to the increase of total and dissolved concentrations of As, Co, Cu, Ni & Pb in the outlet, as well as higher dissolved Zn concentrations. Phoshate, ammonium, and total and dissolved concentrations of Fe, Mn, and Cr on the other hand decreased. The effect of mixing of two different waters was accounted for, by estimating the expected concentration of each pollutant if mixing was the only mechanism effecting their concentration. This was done using mixing fractions based on the electrical conductivity. Differences in estimated and measured concentrations showed that the release and removal of various pollutants was not a mere result of mixing only. The change in water composition and subsequent competition for sorption spots was found to be the main mechanism involved. The transport model showed that preferential flows resulted in C/C0 = 0.8 breakthrough of metals occurring much faster than in a plug flow. These observations show that the current design and operation of the biofilter do not provide adequate removal of metals in the biofilter.

i

Preface

This document presents the master thesis "The Behaviour of Heavy Metals and Nutrients from Stormwater in the Bluebloqs Biofilter in Spangen, Rotterdam". The thesis is based on water quality analysis and monitoring of the system, and application of a PHREEQC surface complexation model. It was written as the final assignment to obtain the graduation requirements for the master Environmental Engineering at Delft, University of Technology. The research and writing of the thesis took place between June 2020 and August 2021.

The research was undertaken in collaboration with Field Factors, who designed the biofilter that was the system of interest for this project. The research aimed to evaluate this system and suggest design and operational guidelines for optimisation. The system operation was more complex than anticipated. Fortunately, there was always a team of people willing to discuss difficulties and share informationand knowledge.

I would like to thank Boris van Breukelen for his guidance as my main supervisor during this project and Joshua Gallegos for his time and support in the field and during constructive discussions. Furthermore I would like to thank the rest of my committee: Julia Gebert and Luuk Rietveld, for their valuable feedback and support.

In addition to my committee members, I would like to thank the team at Field Factors for enabling this research, with a special mention for Wilrik Kok, whose time and persistence made sure that the field work could continue, despite difficulties with access to the site. Thanks also, to Bert the Doelder for providing access to the site adjusting operation of the system in favour of the sampling rounds. Thanks to Jean-Luc and Erwin Boer, who were always super helpful with practical issues on site and answering questions about the system, and thanks to Teun van Dooren for providing access to historical data and the PLC readings. Tessa Jonker, thanks for being a great team mate in the field and Pim Versteeg, thank you for your assistance with the hydraulic conductivity measurements and for being available to discuss any questions I had about PHREEQC.

All the staff at the waterlab: Armand Middeldorp, Patricia van den Bos & Jane Erkemeij, thank you so much for your clear briefings on using the lab equipment and assisting me with my analysis. Thanks also to Emiel Kruisdijk for helping with the "regression method" on the IC.

Last, but not least, thank you to my family and friends for supporting me throughout this project. Graduating is a long process with ups and downs, and graduating during the Covid-19 pandemic came with challenges that sometimes emphasised the downs. Thank you for putting up with me. My boyfriend, Sander, derserves a special word of thanks for cheering me up and pulling me through and always being there when I needed it.

I hope you enjoy reading it.

Kirsten van Lienden
Delft, August 27, 2021

Contents

List of Figures

List of Tables

Acronyms and abbreviations

Ca^{2+} calcium

Cl^- chloride

HCO_3^- bicarbonate

HNO_3 nitric acid

K^+ potassium

Mg^{2+} magnesium

NH_4^+ ammonium

NO_2^- nitrite

NO_3^- nitrate

Na^+ sodium

PO_4^{3-} phosphate

SO_4^{2-} sulphate

ASR Aquifer Storage and Recovery

BB Bluebloqs Biofilter

BV bed volumes

CBE Charge Balance Error

CEC cation exchange capacity

DA Discrete Analyser

DO Dissolved Oxygen

DOC Dissolved Organic Carbon

EC Electrical Conductivity

HFO hydrous ferric oxides

HM heavy metal

IC Ion Chromatography

ICP-MS Inductively Coupled Plasma Mass Spectrometer

IOCS iron-oxide coated sand

MAR Managed Aquifer Recharge

OM organic matter

PLC Programmable Logic Controller

RSD relative standard deviation

SI Saturation Index

TSS total suspended solids

UWB Urban Water Buffer

1 Introduction

1.1 Background

Water management in urban areas is facing new challenges as a result of a growing population, urbanisation and climate change [10]. Urban growth and prolonged droughts lead to an increasing demand for freshwater resources [11], whereas soil sealing is reducing the ability of the soil to filter and store water, leading to higher runoff and pollution loads as well as higher flooding potential, especially in combination with the increasing frequency of intense rainfall events [12]. At the same time, groundwater overdraft leads to sinking cities [13] and saltwater intrusion [14], especially in delta cities and coastal areas. To meet the increasing water demand in a sustainable way, conserving water and diversifying the sources is of importance [15]. Managed Aquifer Recharge (MAR) for stormwater recycling is a promising technique that may contribute to this sustainable water management. Aquifers can retain large volumes of water and provide natural treatment (e.g. sorption, filtration and degradation) [16] at low costs, low energy and a low spatial footprint. In coastal aquifers it has the additional advantage of assisting in the prevention of saltwater intrusion [15]. Aquifers have been used for for water storage for millennia, however in recent years more scientific research has been carried out to show the effectiveness of aquifers as sustainable water treatment systems, often combined with treatment in a wetland [17].

Treatment is necessary, because urban stormwater runoff can contain various pollutants, such as pathogens, organic matter, nutrients, sediment and metals [18]. These pollutants are transported from surfaces in residential, commercial and industrial areas where water cannot pond and infiltrate. Heavy metals are an important pollutant, because of their prevalence in nature, their effects on the aquatic environment and their lack of degradability [19]. They can be toxic at very low concentrations and their accumulation in soils poses a threat to the environment [20]. Copper, zinc and nickel are measured in the highest concentrations in runoff. They originate from building materials such as roofs and traffic-related sources such as brake linings and tire wear [21]. The purpose of MAR is the recharge of water to aquifers for subsequent recovery or environmental benefit. Aquifer Storage and Recovery (ASR) is a type of MAR in which water is injected into a well for storage and is later recovered from the same well [22]. To prevent pollution of the aquifer stormwater treatment technologies are increasingly being developed. One of these technologies is the stormwater biofilter [23].The extent to which the source water needs to be treated depends on the quality of the source water, aquifer type and the groundwater quality in the aquifer as well as local regulations and the purpose of the recovered water [17].

Biofiltration is a technology that embraces natural processes in an engineered system. It typically combines the properties of wetlands and slow sand filtration in a sand-based, porous filter medium, covered by a vegetated swale. Underneath the filter layer, a transition layer and drainage layer of a coarser material ensure a proper drainage to the drainage pipe at the bottom. The biofilter can retain water during high rainfall peaks and treats the stormwater by means of physical, chemical and biological processes [24]. The use of a

biofilter in combination with stormwater harvesting and ASR forms the basis of the Urban Water Buffer (UWB) concept. Such a system, has been implemented in Spangen, Rotterdam. This neighbourhood has a surface level of 1.3 m below sealevel [2]. This low surface level, in combination with high amounts of paved surfaces lead to flooding problems during heavy rainfall, despite the presence of a separate sewer system [25]. In addition, soccer club Sparta, located in the same neighbourhood, uses freshwater to spray the artificial grass field for better play [1]. Together forming an ideal situation for the UWB. Stormwater from the stadium roof and surrounding areas is now connected to the UWB Spangen: it is collected in an underground retention basin, before passing through the Sedipoint pre-treatment system (Fraenkische, DE), followed by the Bluebloqs biofilter (FieldFactors). A schematic overview of the biofilter, including various processes that can occur in the filterlayer, is shown in Figure 1. Stormwater is distributed over the surface of the biofilter, where it can pond before infiltrating down the into the vegetated filter media. Here, the filter media, vegetation and microbes present facilitate a combination of physical, chemical and biological treatment, before water is collected at the drainage pipes at the bottom of the filter. After treatment, the stormwater is infiltrated into the aquifer.
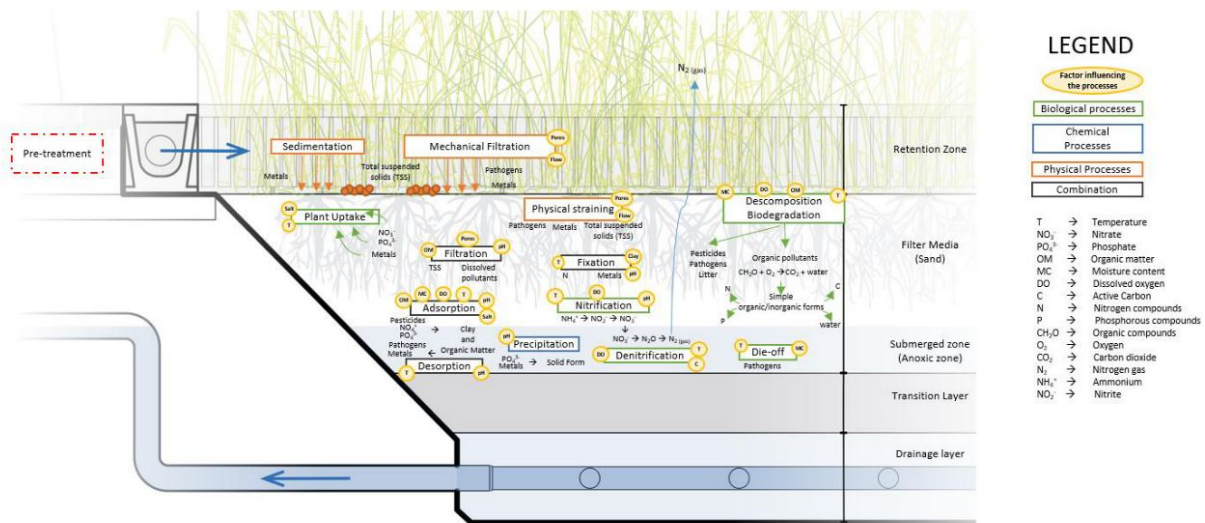
Figure 1: Biofilter design and removal processes. Adapted from [1]

1.2 Problem Statement

As urban water buffers seem to be a promising technique to contribute to solving aforementioned problems, a larger interest in research on the topic has developed over recent years. Consistently high removal percentages for metals have been reported in earlier studies ([26, 27, 28, 29, 30, 31]), showing that biofilters indeed have great potential to efficiently remove metals from stormwater. However, most of this research was based on lab- or column experiments, using small sized experimental set-ups and (semi)-synthetic stormwater

dosage in a controlled environment. Field data from full scale system on metal removal in biofilters are limited, especially in relation to the removal of dissolved metals. Although load reductions exceeding 90% for Cu, Pb & Zn were also found in a study monitoring several full scale systems in Australia [32], no distinction was made between total and dissolved metals and the contribution of the different processes responsible for this removal remains fairly unknown. A large fraction of heavy metals in stormwater runoff is generally associated with suspended solids, which can be removed by filtration, resulting in high metal removal. While lead was found to indeed be mainly particle bound [33, 34, 35, 36], other heavy metals were typically found in the particulate and dissolved phases. Several studies have shown that the presence of salt can increase concentrations of some metals in the dissolved form and negatively impact removal [35, 37, 38]. Maniquiz-Redillas et al (2014) showed that partitioning in the heavy metal load of runoff was also influenced by flow rate and total suspended solids (TSS) load, and that this fractionation played an important role in the performance of bioretention systems [39]. Results from previous research show more variation with respect to dissolved metals, compared to total metals. Søberg et al (2017) found in a column study that total and particulate Cd, Cu, Pb and Zn were well removed, but reported negative removal for dissolved Cu and Pb, especially when dosed with salt-containing stormwater [40]. Muthanna et al (2007) reported good removal of total Zn & Pb, but found varying results for total Cu, with removal percentages as low as 40%, the reduced removal is suggested to be related to Cu in the dissolved fraction [36]. This findings are in line with those of Trowsdale (2011), who reported removal for total Cu, but no removal and even leaching for dissolved Cu [41] in a full scale system in New Zealand. Hatt et al (2007), also found good removal for total Zn, Cu & Pb in a laboratory study, but found more variability in their dissolved forms, especially for Cu, for which leaching was observed [42]. As metals in their dissolved form are generally more toxic and bioavailable than when they are particle-bound [35], more research into their removal is needed.

Another problem, in which metal speciation also plays a role, is metal accumulation and breakthrough during long-term operation of biofilters. Accumulation of metals is mainly seen in the top layer of the biofilter as a result of mechanical filtration of particle-bound metals and adsorption of dissolved metals ([43, 28, 44, 31, 45, 46]. Although filtration of particulate metals can slowly clog the filter media over time, this is not expected to negatively impact the filtration capacity through the media. However, when the adsorption capacity of the top layer is exhausted, adsorbed metals may migrate through the filter until breakthrough occurs [47]. Hatt et al (2011) simulated this by accelerated metal dosing in a column test and found that breakthrough of Zn may be a concern. Although breakthrough of Pb, Cd & Cu were unlikely to occur before physical clogging, accumulation of these metals in the filter media may exceed guidelines for human and ecological health [47]. Søberg et al (2019) reported that metals primarily adsorbed to different filter materials in the exchangeable fraction, so desorption of these adsorbed metals may pose a delayed threat [48]. Research on other pollutants in three ten-year-old field-scale biofilters in Australia by Lucke et al (2017) showed reduced removal potential and even release of pollutants, and emphasises the need for international research on long term pollutant removal [49].

The Bluebloqs biofilter in Spangen has been operational since September 2018 and has been monitored by KWR on a monthly basis to maintain a permit which allows the infiltration into the aquifer. These monitoring rounds have shown removal of heavy metals to levels that generally comply with Dutch infiltration regulations [1]. Nevertheless, both Zn & Cu concentrations occasionally surpassed the permit target value, whereas both Ni and As concentrations at the outlet have occasionally been reported higher than at the inlet, although still well below their target values[1]. Iron concentrations were also reported to be very high, as a result of contamination of the stormwater in the buffer with phreatic groundwater [1]. Fe and Mn are not generally considered in stormwater biofiltration, as they are not directly relevant to aquatic health. However, they are of concern for ASR, because of their potential to clog injection and recovery wells [46]. After addition of iron-oxide coated sand (IOCS) to the Bluebloqs biofilter, the Fe concentrations have been strongly reduced [1]. The contamination with groundwater has also lead to a rather high salinity of the inlet water.

The previous monitoring at Spangen has only been done on a monthly basis (and even less frequently after longer operation). Additionally, these samples were taken from the inlet and outlet of the biofilter simultaneously, so that no relation between inlet and outlet sample exists. Only total metals were measured. As variability in the treatment capacity of certain metals has already occurred, and the system should be able to remove HMs consistently under different circumstances, more research into the processes that govern metal removal on this site is necessary.

In addition to this irrigation of the biofilter with water from the aquifer has been initiated before the study period and may have an influence on the treatment capacity. These irrigation rounds were implemented when extracted water started to present a foul smell. The irrigation rounds prevent water from standing too long. Besides, the irrigation rounds are used to keep the biofilter wet during longer dry periods. It was also noted that distribution of inlet water over the biofilter was not homogeneous. Kluge et al (2018) reported on the impact that a heterogeneous distribution of inlet water can have on the accumulation of metals at different distances from the water inlet [45]. This insinuates that the filter volume is not used optimally and may result in earlier breakthrough.

Versteeg (2020) [50] has constructed a surface complexation model in PHREEQC, which was calibrated using experimental data from Genç-Fuhrman (2007) [21]. This model was applied to the KWR monthly monitoring data at Spangen [1] to predict metal breakthrough on this site. Jonker (2020) constructed a similar model for pathogen breakthrough at Spangen, where heterogeneous distribution of inlet water was simulated using a multipathway approach [3]. To improve the breakthrough prediction for HMs in Spangen, the heterogeneous water distribution should be implemented in the PHREEQC model for dissolved metals.

1.3 Objectives

The monitoring data from KWR provide a basic overview of the water quality at the inlet and outlet of the biofilter. However, actual removal efficiencies cannot be calculated, because there is no relationship between the sample at the inlet and the outlet when taken at the same time. Taking multiple samples at frequent intervals from both the inlet and the outlet while the system is running can provide a better insight into the removal processes in the biofilter. In addition to this, a distinction between total and dissolved metals can show more about the processes that occur in the biofilter to facilitate metal removal. Knowledge of these factors can be used to make better predictions on the future of metals in the biofilter as well as to suggest ways to improve the system. As chemical adsorption is an important removal mechanism for dissolved metals, this removal mechanism will be the main focus. Sorption processes are not limited to metals, thus physicochemical parameters as well as main ion and nutrient concentrations are also considered. The aim of this study is to provide a better insight into the removal of heavy metal (HM) and nutrients in the Bluebloqs biofilter in Rotterdam, Spangen in order to validate, predict and optimise effectiveness of the heavy metal removal in the biofiltration system.

This leads to the following research question:

> **Research Question:** *How does the Bluebloqs biofilter perform with respect to removal of heavy metals and nutrients under environmental and operational conditions as found in Spangen, Rotterdam in spring and summer of 2020?*

> **Subquestions:**
> 1. To what extend are heavy metals (Fe, Mn, Pb, Cr, As, Co, Cu, Ni, Zn) removed during operation of the biofilter?
> 2. Which factors in the operation and design of the biofilter contribute negatively to heavy metal removal?
> 3. What changes can be made to the system to enhance heavy metal removal?

1.4 Approach and Research Outline

A schematic overview of the approach that was taken in order to answer the research questions is visualised in Figure 2.
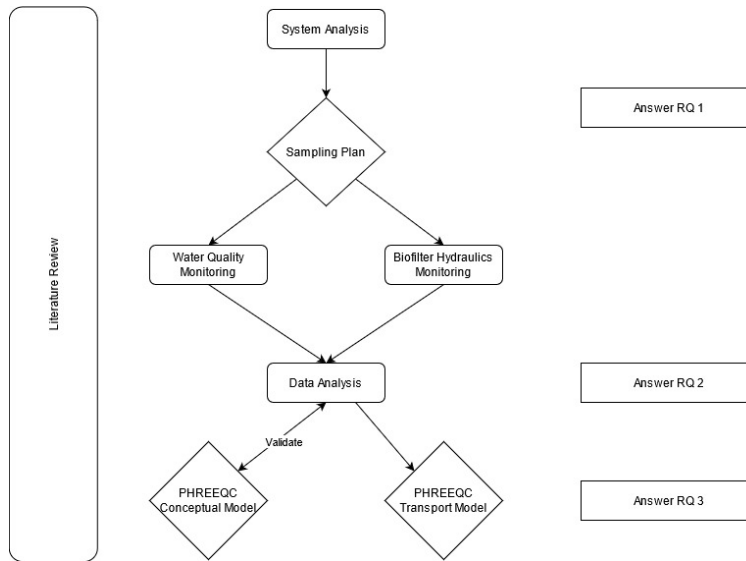
Figure 2: Schematic overview of research approach

The background and context of the topic are described in Chapter 1, along with the problem and its relevance and importance. Chapter 2 will elaborate on the conditions under which the system has been operated. After this, the methods used in this research are explained in more detail in Chapter 3. The results of the research are reported and discussed in Chapter 4 and the final conclusion drawn in Chapter 5. Finally recommendations for further research are mentioned in Chapter 5.2.

2 System Analysis

As the system of interest concerns a field scale system that had been operational before the start of this research, gaining an insight into how it operates and has been operated over time is essential to set-up a research plan. The analysis may reveal factors to take into consideration when taking samples and analysing the data obtained during the research. This chapter will give more information about the field site, biofilter design and system operations.

2.1 Research Site

The Bluebloqs biofilter is part of the UWB in Spangen, a neigbourhood in Rotterdam, with approximately 10200 inhabitants [51]. The area lies 1.3 m below sealevel and 22 km from the coast [2]. The UWB is connected to the rainwater sewer, which collects water from various areas, specified in Table 1, although the park may not be connected yet. Research by Zuurbier et al seems to indicate that the connected area was even smaller, based on how much water reached the buffer [1]. Figure 3 shows the areas that are assumed to be connected outlined in red, along with the location of the UWB and the underground retention basin, where water is stored before treatment in the biofilter. The next sections will expand further on this. Overflow to the surface water only occurs if the retention basin is completely full [1].

Table 1: Areas that are connected to the stormwater sewer [1, 2]

Surface Type	Area (m^2)
Roof (Sparta + Westervolkshuis)	6000
Paved (Parking + Square)	18300
Soccer Field	13200
Park	8400
Total	45900
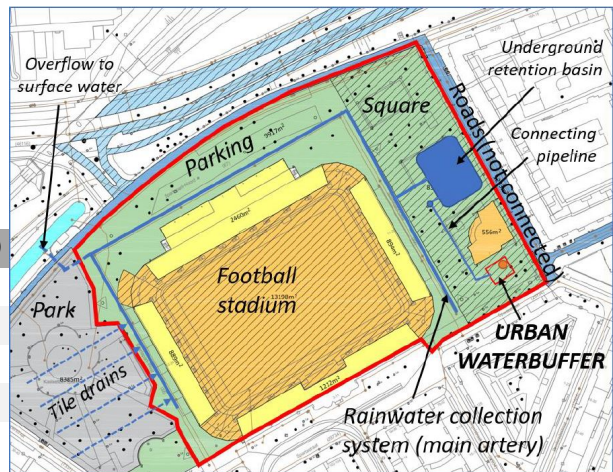
Figure 3: Area that is connected to the rainwater sewer, outlined in red. Figure from [2]

The collected and treated water is meant for use by Sparta, to spray their fields. The freshwater demand for this is approximately 15000 $m3$ per year, with a higher demand in summer than in winter. Other uses of the water are an ornamental water column from which water pours down three times a day and when people pull the handle that is attached to

it [1]. Furthermore water is used for backflushing and irrigation of the biofilter, which is discussed in more detail in Section 2.4.

2.2 System Set-up and Design

2.2.1 Urban Water Buffer

The UWB-system as is implemented in Spangen consists of a stormwater collection system with pre-treatment, before infiltration into the aquifer for ASR. The stormwater from Sparta is first stored temporarily in a 1400 m^3 Rigofill underground retention basin that is lined with foil to prevent any interaction with the groundwater [52]. This storage allows the distribution of water to the aquifer at a lower rate than the rainfall intensity as to not overload the infiltration rate to the aquifer during rain events [2]. In the pipeline leaving the retention basin, a Sedipoint system is installed as a first treatment step to remove coarse material and light, non-aqueous phases [53]. The next treatment step is the biofilter itself. This is a natural system to treat stormwater, based on a combination of slow sand filtration and a vertical flow constructed wetland [2], focused on removing suspended solids and adsorbed metals [1]. The surface of the biofilter in Rotterdam is 90 m^2 with a maximum discharge onto the filter of 30 m^3/h. After filtration, the water is pumped to a standpipe 3.3 m above surface level, to create extra head for infiltration into the ASR well. The water can be extracted for use at the Sparta stadium [1] after sufficient retention time in the aquifer. A schematic overview of the UWB is shown in figure 4.
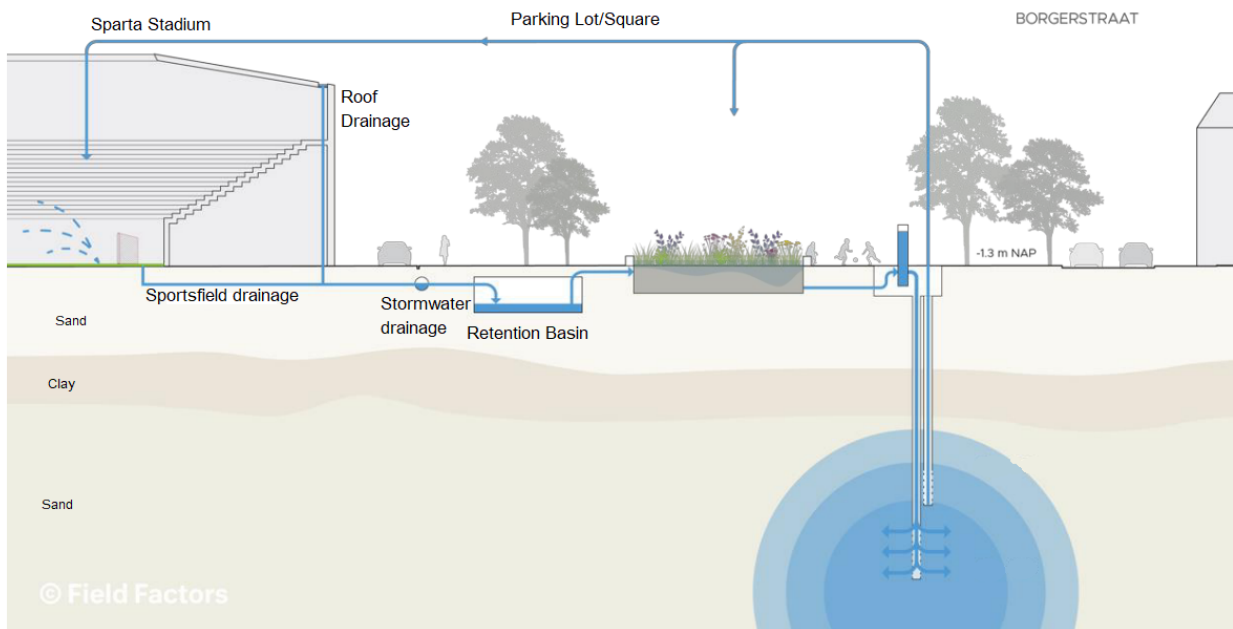
Figure 4: Schematic Overview of Field Site. Adapted from [1].

The ASR well consists of two two partial wells in a single borehole, separated by a clay layer to avoid short-circuiting [54]. The shallowest well (W1) has its screening at a depth of 17-19 m below surface level. The well screening of the deeper well (W2) is 20 - 26.5 m below surface level [2]. W2 is used for infiltration and W1 is used for recovery, to make use of the density difference between brackish and freshwater. The latter has a lower density, causing it to float on the brackish water in the deeper levels of the well. The influence of the infiltration and extraction of stormwater is monitored via the monitoring wells, located at seven metres away from the ASR well [1].
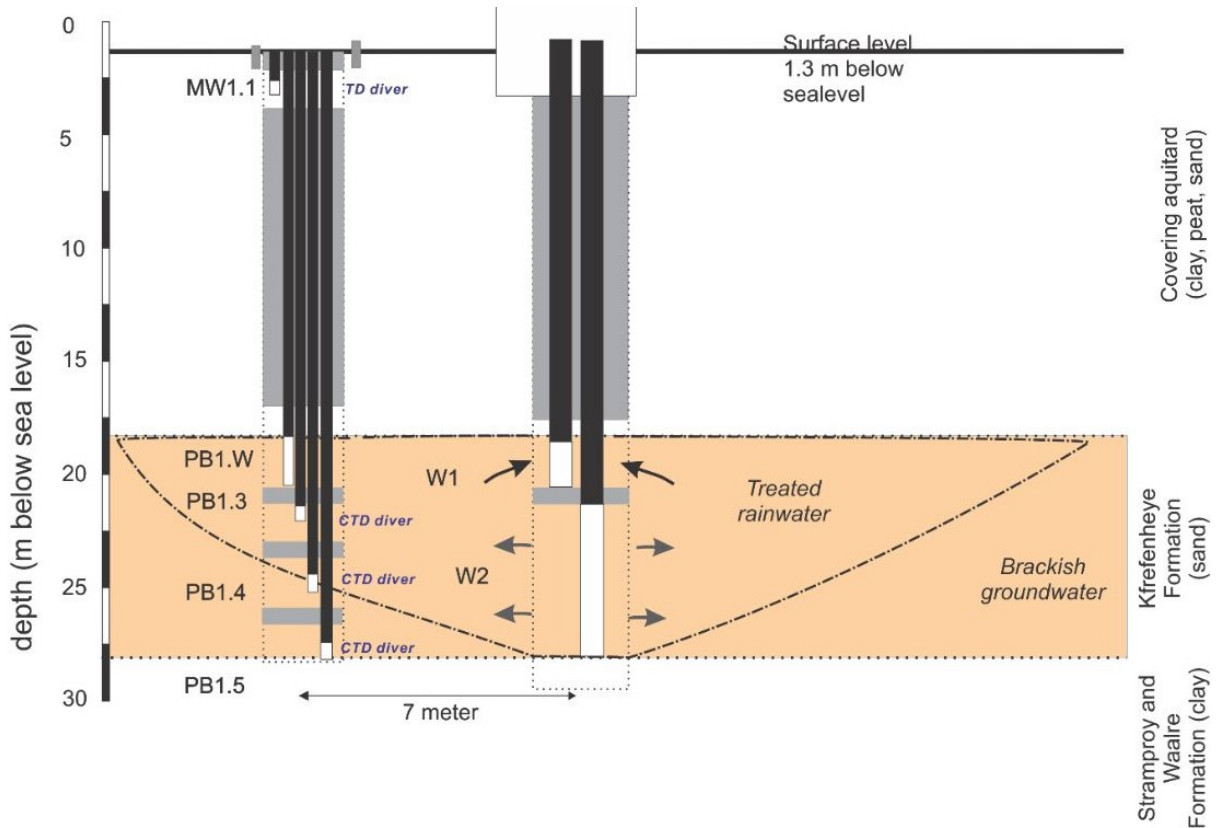
Figure 5: Cross-section of the ASR well and the monitoring well at the Urban Water buffer Spangen. From [2].

2.2.2 Biofilter

Bluebloqs biofiltration system is a natural system to treat stormwater, based on a combination of slow sand filtration and a vertical flow constructed wetland [2]. The filter has a top surface area of 94.4 m^2 and consists of three main sand layers of different grain sizes as is shown schematically in Figure 6. The coarsest sand (1.2-2.0 mm) on the bottom of the filter is 30 cm thick and functions as a drainage layer, above that is a 20 cm thick transition layer of coarse sand (0.8 - 1.25 mm), above which the 60 cm thick filter layer of medium -

Table 2: Filter sand grain size

Layer	Thickness (m)	Grain Size (mm)
Filter	0.6	0.4 - 0.8
Transition	0.2	0.8 - 1.25
Drainage	0.3	1.2 - 2.0
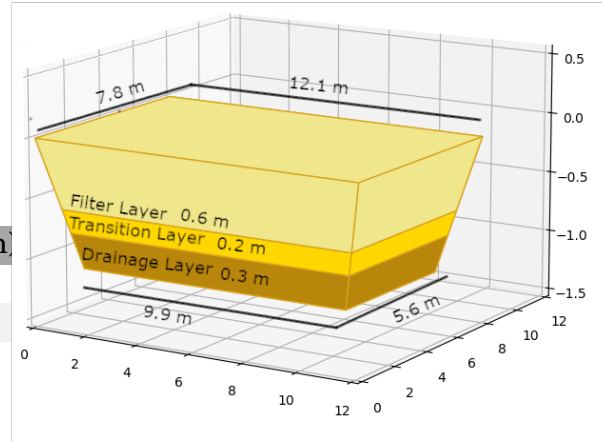
Figure 6: Schematic overview of the dimensions of the biofilter

coarse sand (0.4 - 0.8 mm) is located (Table 2). All of the sands are dried and calibrated and are commercially known as AcquaSilica®. The filter layer is covered with approximately 5 cm of iron-oxide coated sand (IOCS). As iron oxides have a relatively high surface area and surface charge, this is expected to enhance sorption processes [55]. Additionally, a mulch layer is added on top of the filter to retain moisture [56]. Vegetation is an important part of biofilters as it reduces flow, enhances sedimentation and takes up nutrients and other pollutants, including some metals, as growth components [24]. The vegetation in the BB at Sparta originally contained *Carex nigra, Carex testacea, Panicum virgatum, Calamagrostis acutiflora*, and *Mentha aquatica*. On the 16-07-2020 new plants were added: *Carex acuta, Persicaria bistorta, Filipendula ulmaria, Valeriana officinalis, Lythrum salicarium, Cardamine pratensis, Myosotis scorpiodes, Centaurea jades*, and *Allium suaveolens*. A saturated zone is created by raised outlet, causing standing water in the biofilter. This saturated zone provides water to the plants and microbes in drier periods and creates an anaerobic zone. Furthermore, the saturated zone can provide a prolonged retention time for a volume of stormwater [24].

2.3 System Operations

2.3.1 Overview

The flows from the buffer to the biofilter and from the biofilter to the standpipe are regulated based on the water levels in the different components of the UWB. These water levels are measured using pressure sensors that send a signal to a Programmable Logic Controller (PLC) which subsequently triggers frequency regulated pumps to adjust their flow rates. The flow is also measured, using magnetic flow meters [1] as well as the EC of the water that is infiltrated and extracted. All processes are regulated by the PLC that also logs the parameters every 30 minutes. A schematic overview of this regulation system is given

schematically in Figure 7.
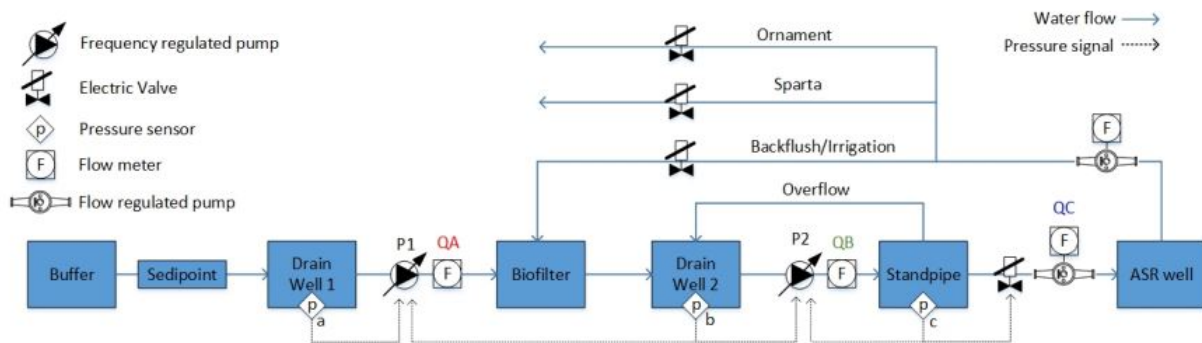
Figure 7: A schematic overview of the UWB Spangen and its flow regulation system. Figure from [3]

Retention buffer

The collected stormwater is stored in the retention buffer before being fed to the biofilter. This feeding event starts when the water level in the buffer surpasses a certain threshold. The water level of the buffer is measured using a pressure sensor (p_a) in connected drain well 1. The pressure-regulated pump ($P1$) adjusts its discharge (QA) onto the biofilter based on the pressure signal from pressure sensor p_a. The event finishes when the water level in the buffer drop to a certain value.

Biofilter

The biofilter is, in its turn connected to drain well 2, also equipped with a pressure sensor (p_b) to measure the water level in the biofilter. The discharge from the buffer onto the biofilter (QA) continues until the water level in the biofilter reaches its maximum desired value in order to prevent flooding. When this is reached, the flow from the buffer (QA) is paused and water from the biofilter is pumped ($P2$) into the standpipe to be subsequently infiltrated into the aquifer. The discharge onto the biofilter (QA) is higher than the discharge from the biofilter (QB), so during a longer event the flow from the buffer is paused several times in order for the water level in the biofilter to lower sufficiently. After the feed event has finished, water is pumped from the biofilter to the standpipe (QB) until the water level in the biofilter is back to a set level, to create a saturated zone.

Standpipe

The standpipe is made of PVC with a height of 3.3 m and a diameter of 400 mm. In the standpipe, the water builds up until it reaches the pressure needed to infiltrate water into the subsurface (QC). This happens when the water level reaches 90% [1]. Another pressure sensor (pc) registers the water level and gives a signal that opens an electric valve leading to the ASR well. The maximum pressure in the standpipe is limited in two ways: the same pressure sensor also gives feedback to the pump that pumps water from the biofilter to the

standpipe ($P2$) and reduces the flow (QB) when necessary. An additional measure is the overflow from the standpipe back to drain well 2 [1].

Extraction
Once infiltrated into the aquifer, the water is stored in the subsurface until it is recovered. The main extraction of water from the aquifer is used by Sparta Stadium, using the water to spray the field. Other purposes for extracted water are the water ornament, backflushes and irrigation of the biofilter. The purpose of the backflush is to minimise the well clogging potential. Backflush water is extracted from W2 for about 5 minutes after infiltration of every 20 m^3 of water [1]. This happens automatically as the flow is registered by a magnetic flow meter (QC). Irrigation is done three times a day to remove the smell of standing water and to supply the plants with water in dry periods [1].

Infiltration to the aquifer cannot happen simultaneously with extraction from the aquifer. This means that when Sparta is extracting water from the aquifer while the biofilter and standpipe are full, no water can infiltrate in to the aquifer, so the water level in the biofilter cannot go down until extraction is finished. As a result the discharge onto the filter during a feeding event is paused for a longer amount of time.

2.3.2   Settings

The logged data from the PLC was used for a preliminary investigation into the system and its operation. Some settings have been changed over time or were adjusted in favour of sampling for this research. This section gives a brief description of the relevant settings.

Event Frequency and Duration
The amount of water in the retention buffer is dependent on the amount of stormwater that is collected. Thus the duration and frequency of feeding events is dependent on rain events as well as the settings for the threshold values in the buffer and the biofilter (see Figure 8). The frequency and duration of feed events, as well as dry periods between events, thus varies a lot. Furthermore, the threshold levels that trigger feed events have been changed over time, contributing to even more variation. This has an effect on the retention time of the water in the buffer as well as in the biofilter and it poses a challenge to set up a sampling plan, as the system needs to run in order to be able to take water samples. Hence the settings were changed before the sampling rounds started (see Table 3). These changes allowed feed events to only start on Tuesdays, between 08.00 and 12.00, unless there had been so much rain that the water level in the buffer reached 75%, to prevent overflow of the retention buffer. The change in settings is clearly visible in figure 10, where the buffer level changes halfway through the month and events start happening on a weekly basis.
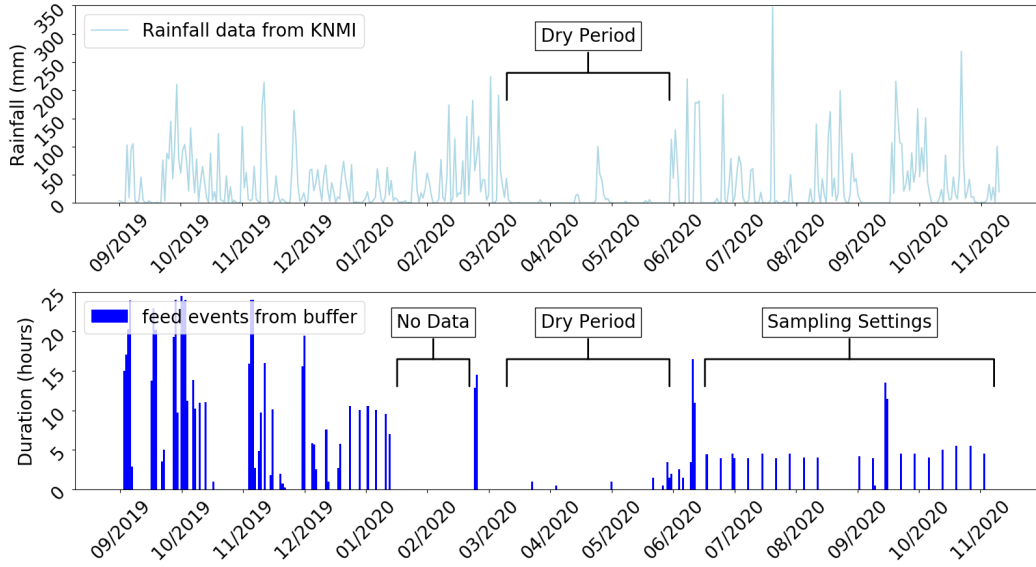
Figure 8: An overview of the duration of feeding events from the buffer to the biofilter and dry periods in between events (bottom). The Rainfall data from [4] (top) is used to show how rain events compare to feed events in the BB

Table 3: Waterlevel in retention buffer and biofilter (on PLC) to trigger flow from the retention buffer to the biofilter and from the biofilter to the standpipe. This table compares the original* settings [1] to the new settings during sampling. *original settings already changed multiple times before sampling rounds.

	original settings		sampling settings		
	Buffer	Biofilter	Buffer		Biofilter
	Any day		Any day	Tuesday	Any day
Start flow from retention buffer to biofilter	$\geq 50\%$	$\leq 92\%$	$\geq 75\%$	$\geq 50\%$	$\leq 90\%$
Stop flow from retention buffer to biofilter	$\leq 20\%$	$\geq 96\%$	$\leq 55\%$	$\leq 40\%$	$\geq 96\%$
Stop flow from biofilter to standpipe	-	$\leq 60\%$	-	-	$\leq 88\%$

Saturated Zone

After a feeding event, the water in the biofilter is pumped to the standpipe, until it the water level in the biofilter is back to its set level of the saturated zone. Like the thresholds in the buffer, the level of the saturated zone has also been changed over time. However these changes were not made in favour of the sampling rounds, but for other reasons, such as the root length of the vegetation. An example of such changes is clearly visible in figure 9 and 10. In December 2019 the saturated zone was set to 60% as can be seen from the water level in the biofilter in between events. During events it went up to between 92 and 96%. In June 2020 new vegetation was recently added to the biofilter and the saturated zone was kept above 80% continuously. This was also the month in which the settings were changed in

favour of the research. This switch is visible halfway through the month, where the Buffer level rises and the events start to happen on a weekly basis.
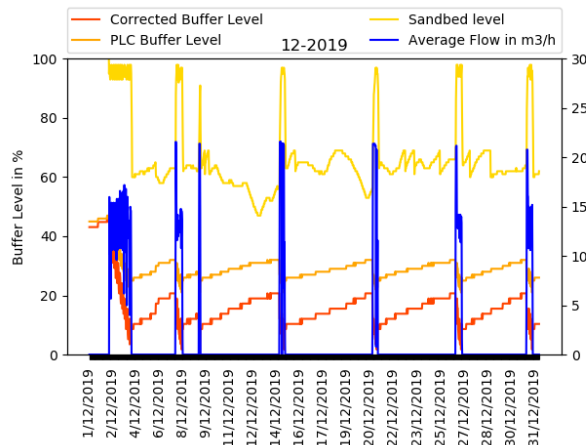
Figure 9: Feed events from the buffer to the biofilter (Average Flow in m3/h) and the corresponding water levels in the buffer and the biofilter (sandbed level) in December 2019. The water level in the buffer was 92-96% during an event, but the saturated zone remained at 60% in between events.
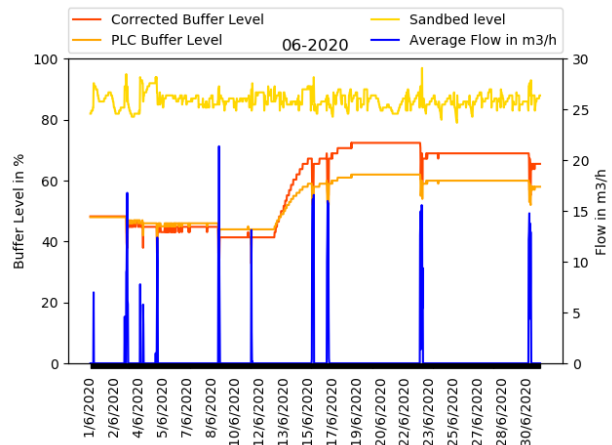
Figure 10: Feed events from the buffer to the biofilter (Average Flow in m3/h) and the corresponding water levels in the buffer and the biofilter (sandbed level) in June 2020. The water level in the buffer remained above 80% constantly.

2.4   Irrigation with Aquifer Water

Another operational change was made not long before starting the measuring rounds. In order to keep the biofilter wet during longer dry periods, such as the one indicated in figure 8, water from the aquifer was used to irrigate the biofilter. Another reason to introduce these irrigation rounds was to get rid of a foul smell that was present in the extracted water. The water for these irrigation rounds was extracted from well 1 (the upper well) three times a day. The result is visible in Figure 11, where the flow from the retention buffer to the biofilter is plotted as inflow and the flow from the biofilter is plotted as outflow. The higher outflow peaks that coincide with the inflow are due to feed events. The outflow peaks in between events happen three times daily as a result of irrigation with water from the aquifer. The daily irrigation cycles are set to happen once in the morning (07.00 - 08.30), one at noon (12.00 - 13.00) and one in the late afternoon (17.00 - 18.00). The average inflow volumes from the aquifer during these cycles were $5.26m^3$, $3.94m^3$ and $6.31m^3$ respectively. The average volume of stormwater entering the biofilter during a feed event is $34.4m^3$. This is enough to fill the pores in the submerged zone, approximately $88m^3$ completely with stormwater during an event. During the irrigation events, however, this water gets replaced by water from the aquifer. Based on the mentioned average volumes per irrigation

cycle, it takes less than two days for the stormwater to be replaced by aquifer water, as is demonstrated in figure 12. Figure 11 also shows that the EC drops during a feeding event and rises during the irrigation cycles, as a result of a higher salinity in the aquifer compared to the stormwater. The mixing of different waters can impact the the treatment by the biofilter and will be further discussed in Section 4.2.
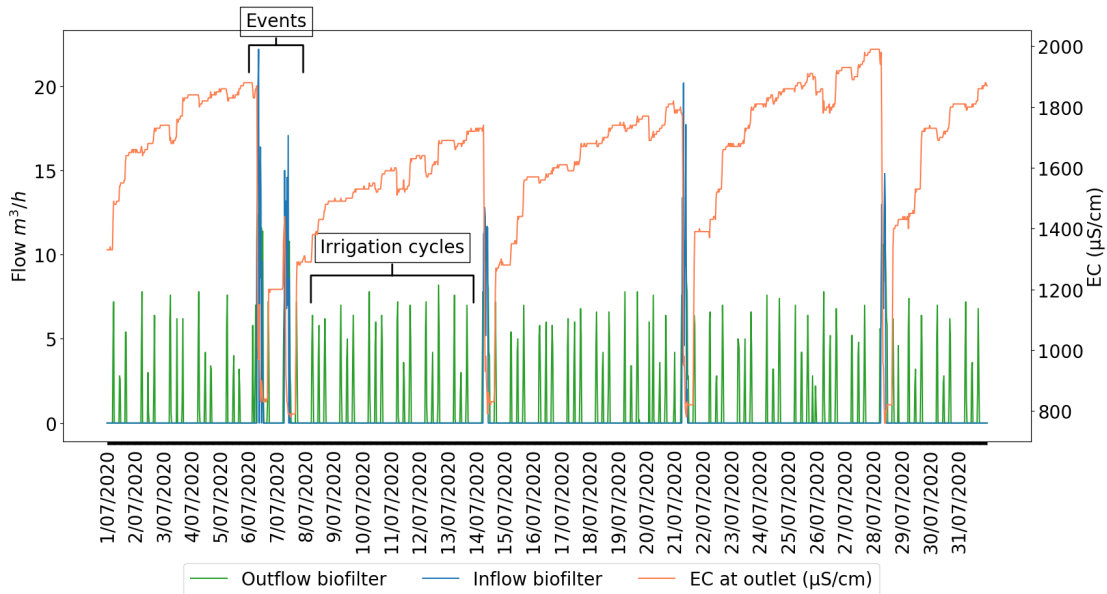
Figure 11: Outflow of the biofilter as the result of feed events (inflow) and three-times-daily irrigation with aquifer water in July 2020. The irrigation has an effect on the EC.
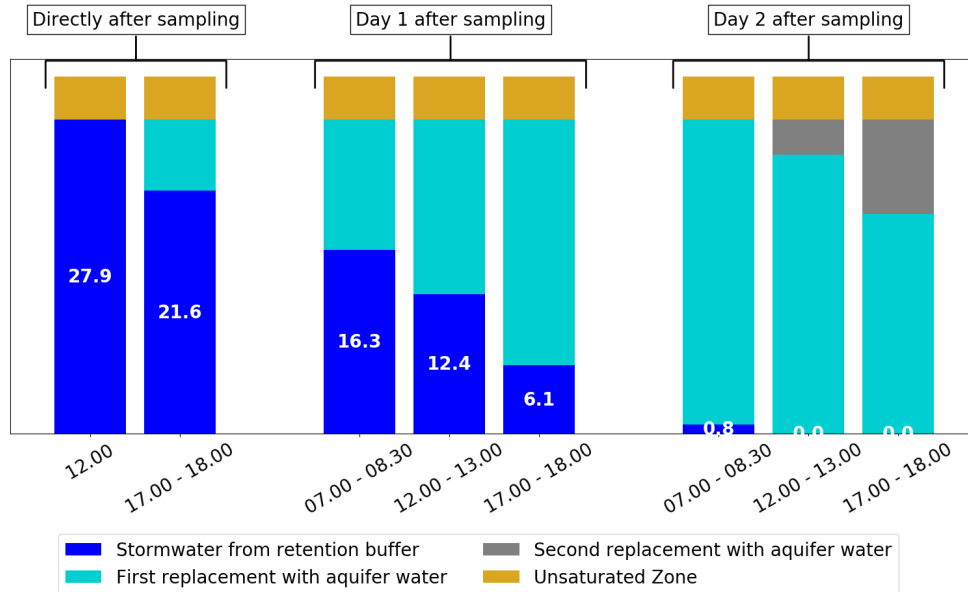
Figure 12: Replacement of stormwater by aquifer water as a result of three-times-daily irrigation events.

2.5   Water Distribution and Ponding Zone

The water from the retention buffer is distributed to the biofilter via channels surrounding the perimeter of the biofilter as are shown in Figure 13. Even though the channels surround the biofilter, the water is only discharged onto the biofilter in the corners indicated by the blue inlet arrows in figure 14. This design in combination with the current settings, that stop the inflow once the water level reaches the threshold that is below the subsurface, does not allow for water to pond onto the biofilter. Instead, only the inflow corners are wet in the case of an event, these are also the corners where the vegetation flourishes more than on the rest of the filter as is visible in figure 15. The effect of this will be discussed in Section 4.2 and 4.2.1.

Figure 13: Water Distribution Channels
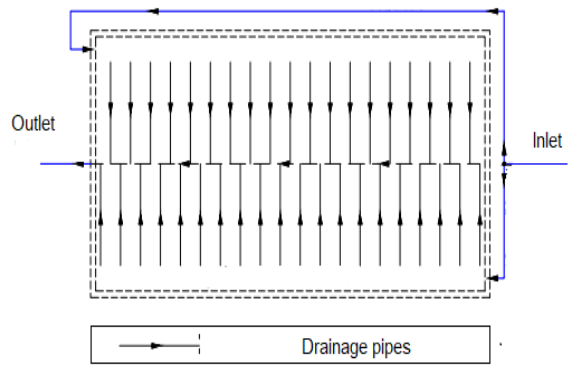
Figure 14: Drainage system of biofilter

Figure 15: Vegetation growth in inlet corners

3 Materials and Methods

3.1 Water Quality

Water quality is the main parameter of interest in this research, hence it was measured extensively. These measurements were done on Tuesdays between 08.00 - 12.00, to make sure that sampling was possible, based on the water level in the retention buffer, as was discussed in Section 2.3. Sampling rounds took place in spring and summer of 2020. Twice in June, twice in July and once in August.

3.1.1 Sampling Frequency

During its time of operation, water quality data had already been recorded by KWR and the municipality, but the measurements were done quite infrequently. The water quality has been monitored on a monthly basis during the first year of operation and once every three months after that [57]. These data do not only have a low density, but are also taken at the inflow and outflow of the BB at the same time. The hydraulic retention time is thus not taken into account and calculating the removal efficiency of the biofilter is thus not accurate. These historical data do thus not give sufficient insight in the processes in the biofilter.

Taking samples at frequent intervals at both the inlet and outlet during an event can give more insight into the actual removal efficiency in the filter. In-situ measurements using sensors were taken every five minutes minutes for this purpose, whereas grab samples to be analysed in the lab were taken approximately every 15 minutes. This was not always possible with the system starting and stopping as described in Section 2.3, leading to varying amounts of samples per event. Grab samples were used, because they can give an insight into the variations in the inlet and outlet water over time. Not all the samples that were taken were also analysed. The data from in-situ measurements was analysed first, to find patterns and retention times in the biofilter. Based on this, the first samples were analysed in the lab, as a well-spread subset of the taken samples. Based on this, a decision could be made on which additional samples to analyse. The schedule with actual measurements and analysis can be found in Appendix F.

3.1.2 In the Field

The in-situ data that were collected were pH, DO, EC & temperature. These were measured using various Greisinger metres, depending on their availability. The sensors were inserted in beakers that functioned as flow-through cells, as can be seen in Figure 16. One beaker contains inlet water, while the other contains outlet water. The other end of the tubes ending in the beakers is connected to sampling valves in the underground control room. These sampling valves are connected to pipes in the UWB, one at the inlet of the biofilter and one at the outlet. The valves were open throughout the event to create a continuous flow in the cell. The DO sensor was calibrated on the day before sampling, whereas the EC and pH sensors were calibrated within 30 minutes before the sample round started. Grab

samples could be collected from the overflow of the beaker. Water was caught in a 180 ml polypropylene container, out of which it was divided into separate vials in preparation for analysis in the lab. The procedure for different parameters will be explained in the next section.

Figure 16: Two flow-through cells to measure pH, DO, EC and temperature in the water at the inlet and outlet

3.1.3 Sample Preservation and Analysis

Main Cations and HMs

Two 15 ml vials were filled with water from each grab sample. One vial was filled with unfiltered water, whether the water in the other vial was first filtered using a syringe and 0.45 μm filter. The unfiltered sample is used for analysis of total metals, whereas the filtered sample is used for analysis of dissolved metals. Samples for metal analysis should ideally be acidified to pH < 2 immediately after sampling [8]. For logistic and safety reasons, the samples were not acidified on-site, but were instead stored cooled and acidified within 8 hours in the water lab at TU Delft, using 1 vol% of HNO_3 69% (Rotipuhran). The samples were then stored at 4 °Celsius for at least 48 hours, so that any precipitates had the time to dissolve, before analysis of main cations and heavy metals on the Inductively Coupled Plasma Mass Spectrometer (Analytik Jena PlasmaQuant MS). The unfiltered sample was filtered before analysis, to make sure that no insoluble particles can damage the ICP-MS. Samples were also diluted prior to analysis, so that the expected concentration remained below the upper detection limit of the machine (100 ppb for trace elements, 7500 ppb for other elements). An overview of the most important ions that were measured is given in Table 4.

Table 4: Cations analysed on ICP-MS

HMs	Main Cations
As	Ba
Cd	Ca
Cr	K
Cu	Mg
Fe	Na
Mn	Sr
Ni	
Pb	
Zn	

Main Anions

Another 15 ml vial was filled on-site, from the main grab sample. This was also filtered trough a 0.45 μm filter and stored at 4 °Celsius, but not acidified. The sample was used for main anion analysis on the Ion Chromatography (IC) (Methrohm 818 anion system). Because of expected high chloride (Cl^-) concentrations, the "regression with polynomials"-method [58] was used for calibration and samples did not need to be diluted. The measured parameters are shown in Table 5.

Table 5: Anions analysed on IC

Main anions
Cl
Br
SO4
NO2
NO3
F
PO4

Phosphate and Ammonium

Phosphate and ammonium were analysed on the Discrete Analyser (DA). For this method the sample needs to be filtered and acidified, like was done for one of the vials for cation-analysis. Because analysis on the ICP-MS does not use the full 15 ml of sample, the leftover water from the same vial could be used for analysis on the DA. Phosphate was also analysed with the other main ions on the IC, but the DA is more accurate. Acidification of the sample makes sure that all Fe in the sample occurs in dissolved form and cannot sorb part of the PO_4^{3-}.

DOC

Samples to analyse for Dissolved Organic Carbon (DOC) were taken less frequently than

the other samples, for economic reasons. One or two samples of 30 ml were taken during each event. They were filtered on-site, and acidified in the lab using 1.6 ml of 2M HCl, after which they were stored at 4 °C. Unfortunately the samples may have been stored too long before analysis on the TOC analyser. This resulted in concentrations that were so far out of the expected range, based on earlier reports on the same site [1], that the data were not used.

Turbidity & Alkalinity

The water from the grab sample that was left in the original container was stored unfiltered for turbidity analysis and alkalinity titration. Turbidity was analysed in the Hach 2100N laboratory turbidimeter. A titration was used to determine the total alkalinity of the sample. This was done using the Metroohm AG SM Tritino 702. The initial pH and volume of the sample was measured, before slowly adding 0.1M HCl, while the sample was being stirred. Acid was added until the pH reached 4.3. Using the initial volume of the sample, the volume of acid added and the normality of the acid, the total alkalinity could be calculated with Equation 1, in which V_{acid} is the volume of acid need to reach pH 4.3 (ml), N_{sample} is the normality of the acid that is used (eq/L), $50 * 10^3$ is the mass of $CaCO_3$ per eq, and V_{sample} is the volume of the intial sample.

$$Alkalinity = \frac{V_{acid} * N_{sample} * 50 * 10^3}{V_{sample}} \tag{1}$$

3.1.4   Accuracy

The accuracy of the water analysis was tested by the principle of electro-neutrality. The principle requires that the sum of the anions must equal the sum of the cations in meq/L (Eq. 2).

$$\sum cations = \sum anions \tag{2}$$

However, unanalysed species and analytical errors can introduce electrical imbalances in the data. This error can be quantified by the Charge Balance Error (CBE), a relative error in percent used to determine the quality of the water analysis (Eq. 3). A small error is acceptable (Table 6) [59].

$$CBE = \frac{\sum cations - |\sum anions|}{\sum cations + |\sum anions|} * 100 \tag{3}$$

Table 6: Acceptable Charge Balance Error [8]

sum Anions (meq/L)	Acceptable CBE
0 - 3.0	± 0.2 meq/L
3.0 - 10	± 2 %
10 - 800	± 5 %

Another method is estimating the EC from the sum of the anions and the cations separately, using a rule of thumb (Eq. 4) [8]. The estimated EC can then be compared to the measured EC.

$$\sum anions(meq/L) = \sum cations(meq/L) = EC/100 \tag{4}$$

3.2   Mixing Fractions

Section 2.4 explained that irrigation of the biofilter with water from the aquifer leads to filling of the biofilter with water from the aquifer. At the start of an event, this aquifer is initially present and is replaced by water from the inlet as the event continues. As a result of this, water at the outlet will first consist of aquifer water, before the inlet water comes trough. In order to analyse the actual removal and release of pollutants it is important to know the composition of the initial water and the inlet water, as well as the fraction of inlet water that is coming out at the outlet. This can be tracked using a tracer. Electrical Conductivity (EC) can function as an inexpensive, natural tracer [60], and because both waters have a different EC it can be used to calculate the fraction of inlet water, using a method from Appelo & Postma [61]. The fraction of inlet water is calculated using Equation 5, in which f_{inlet} is the fraction of inet water, $m_{EC,sample}$ is the measured EC in the sample, $m_{EC,initial}$ is the EC initially measured in the biofilter at the start of the run, and $m_{EC,inlet}$ is the EC measured at the inlet of the biofilter. The calculated fraction of inlet water can in turn be used to estimate the concentration of other ions, using Equation 6, where $m_{i,mix}$ is the estimated concentration of the ion of interest, based on mixing only. $m_{i,inlet}$ is the concentration of the same ion that was measured at the inlet and $m_{initial}$ is the concentration of the same ion is was initially present in the biofilter. The difference between the measured and estimated concentrations ($m_{i,sample}$ and $m_{i,mix}$ respectively) is calculated using Equation 7 and indicates whether the ion has been removed or released by a reaction other than mixing of the two water types.

$$f_{inlet} = \frac{m_{EC,sample} - m_{EC,initial}}{m_{EC,inlet} - m_{EC,initial}} \tag{5}$$

$$m_{i,mix} = f_{inlet} * m_{i,inlet} + (1 - f_{inlet}) * m_{i,initial} \tag{6}$$

$$m_{i,react} = m_{i,sample} - m_{i,mix} \tag{7}$$

It is important to note that under certain conditions, the EC may behave as non-conservative [62]. Interactions of cations within the saline tracer and the filter media by processes such as ion exchange, surface complexation and via physical mass-transfer phenomena can influence the accuracy of the tracer [63]. Using a truly conservative, natural tracer such as Cl^- was considered, but in the end EC was chosen. The easier and more economical in-situ

monitoring resulted in many more data points of EC compared to Cl^-. Deviations in EC as a result of cation-reactivity are expected to be too small to severely impact the results. Nevertheless this should be kept in mind when analysing the results. On 18-08-2020, the EC-sensor was malfunctioning, thus on this day the Cl^- concentration was used, rather than the EC.

3.3 Hydraulic Conductivity

To answer the question of how the heavy metal removal is affected by operational conditions, it is important to investigate the design of the biofilter. The hydraulic conductivity can give an insight into the flow and hydraulic retention time in the biofilter, which are important parameters to take into account.

3.3.1 Lab

The hydraulic conductivity of the material was measured in the lab using a constant head permeability test. The setup consists of a vertical, cylindrical column in which the material to be tested is placed. Above the soil sample, water flows into the column, which can overflow at the top, keeping the head constant. The head difference can be seen using the piezometers that are attached to the column at different heights, see figure 17 for a schematic drawing of the set-up. The three different sands of the Bluebloqs Biofilter were tested separately, as to determine the hydraulic conductivity for each layer. During a timed interval, the water going through the sample was caught in a measuring cup, which was weighed to determine the exact volume of water. This information, together with the dimensions of the sample and the head difference could be used to determine the hydraulic conductivity using Darcy's law (equation 8), where k is the hydraulic conductivity (m/s), Q is the discharge (m^3/s), z is depth (m) and h is the pressure head (m). The porosity can be calculated using equations 9 and 10, where p is porosity (-), V is volume (m^3), m = mass (kg) and ρ is the particle density of the sand particles (kg/m^3). The test was carried out in triplicate.

$$k = -\frac{Q * \Delta z}{A * \Delta h} \quad (8)$$

$$p = \frac{V_{bulk} - V_{grains}}{V_{bulk}} \quad (9)$$

$$V_{grains} = \frac{m_{sand}}{\rho_{particle}} \quad (10)$$
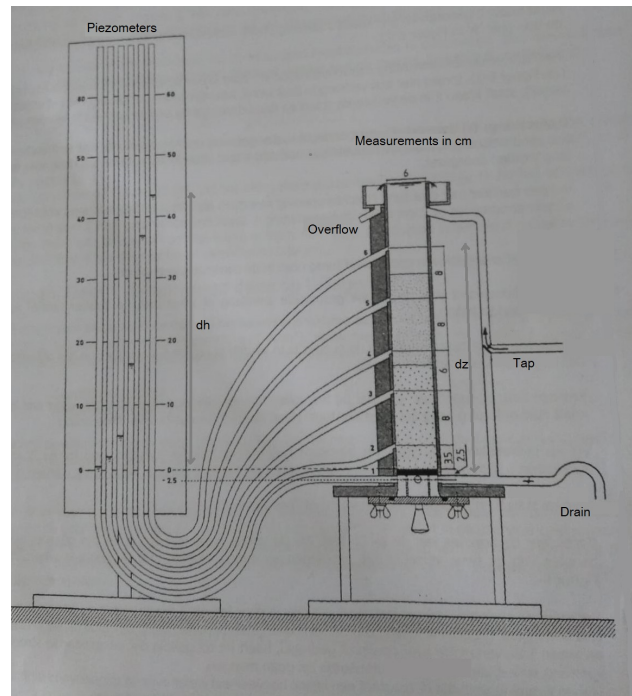
23.
Figure 17: Constant Head Permeability Test in the laboratory. (Adjusted from [5])

The test was repeated three times for each
different grain size. A laboratory hydraulic
conductivity test can give valuable infor-
mation about the initial conductivity of the
original media, which has shown to be one of the most important variables in how the hy-
draulic conductivity of the biofilter develops over time [64].

3.3.2 In-Situ

As a laboratory has some limitations, such as that the impact of in-situ soil compaction,
growth of plant roots and preferantial flow is not measurable, an in-situ hydraulic con-
ductivity test was also carried out. This was done using a single ring infiltration test as
recommended by Australian adoption guidelines for stormwater biofiltration [24]. Using
this method, the hydraulic conductivity at the surface of the soil is measured, using a plas-
tic ring with a diameter of 100 mm that is driven 50 mm into the soil [65]. The head is
then kept constant by pouring water in using a graduated cylinder. The time interval and
volume required to keep the head constant are noted down. The test is carried out for two
different heads (50 mm and 150 mm). For fast draining media, such as the Bluebloqs Biofil-
ter in Spangen, the time interval should be maximum one minute. The infiltration rate
should remain steady for at least 30 minutes before stopping the experiment [66]. This test
requires three measuring points for a biofilter with a surface area of $50m^2$ or less and an
additional measuring point for every extra $100m^2$. As the surface area of the BB is 90 m^2,
four points, spatially distributed over the biofilter were chosen, see figure 18. The points
were not chosen at random. A visual inspection already gave away that the corners near
the inlet received more water than the rest of the biofilter as was discussedin Section 2.5.
Hence one of the testing points was chosen near one of the inlets, one near the outlet, one
in the driest corner of the filter and one in the middle, to see the influence of heterogeneous
water distribution on the hydraulic conductivity.

To calculate the field saturated hydraulic conductivity ($K_f s$), Gardner's behaviour of the soil
is assumed (eq. 11) and the conductivity can be calculated using the analytical expression,
equation 12 for steady flow [66].

$$K(h) = K_{fs} * e^{\alpha h} \tag{11}$$

in which K is the hydraulic conductivity, α is a soil structure parameter and h is the negative
pressure head.

$$K_{fs} = \frac{G}{a} * \frac{Q_2 - Q_1}{H_2 - H1} \tag{12}$$

in which a is the ring radius, H1 and H2 are the two pressure heads (50 mm and 150 mm),
Q1 and Q2 represent the discharge for the two pressure heads and G is a shape factor
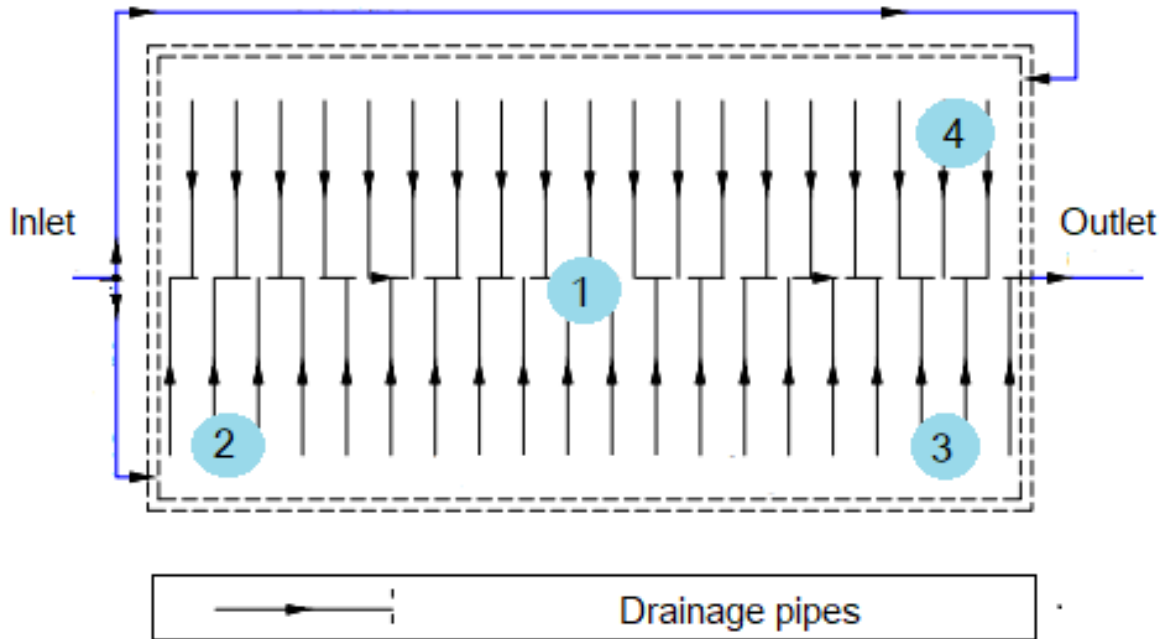
Figure 18: Single ring infiltration test - measuring points

estimated as:

$$G = 0.316\frac{d}{a} + 0.184 \tag{13}$$

with d the depth of insertion of the ring [66]. G can be considered independent of the hydraulic conductivity and soil structure parameter when the ponding depth is larger than 50 mm [65].

Before placing the ring, the mulch layer and IOCS layer were swept out of the way, so the hydraulic conductivity of the filter layer could be tested. As this test only measures at shallow depths, the hydraulic conductivity of the deeper layers could not be assessed. However, as the lowest hydraulic conductivity as well as the occurrence of most of the treatment[24], is expected in the filter layer, a deeper in-situ test was not required.

3.4 PHREEQC modelling

In addition to field data, modelling with PHREEQC (version 3) was used as an approach to get a better insight in the system. This was done using two different type of models: a conceptual model to compare to the results and verify the processes and a transport model to predict the effect of different scenarios on long-term functioning of the biofilter. Both

models will be discussed in more detail in the sections that follow. Before that, PHREEQC will be introduced.

3.4.1 Introduction to PHREEQC

PHREEQC stands for **pH**-**RE**dox-**EQ**uilibrium, while the C indicates that is was written in C++. Meanwhile, kinetic and reactions and one dimensional transport options have been implemented in the program [67]. It was developed by Parkhurst in collaboration with Appelo and can be used used to simulate a variety of reactions and processes in natural waters or in batch- and column-experiments in the laboratory [68].

The program predicts dissolution, precipitation, cation exchange and surface complexation, using mass balances and charge balances. It can do this based on thermodynamic data and other chemical parameters such as aqueous speciation, surface speciation, ion-exchange relationships and rate reactions in geochemistry. These data come from researches over the past years and are included in databases.

Using the keyword SOLUTION, a description of the solution can be entered into the program and EXCHANGE and SURFACE can be used to specify a cation exchange medium or a sorbent respectively.

For this research, the main database PHREEQC.DAT [69] was used, but it did not contain the geochemical data for all heavy metals. Hence, WATEQ4F.dat [61] [70] and minteq.v4.dat were used to complement the data.

3.4.2 Cation Exchange

Ion exchange is the interchange between an ion in solution and another ion in the boundary layer between the solution and a charged surface [71]. Under steady-state chemical conditions, the composition of the exchanger is in equilibrium with the solution. When the water composition changes, the exchanger readjusts to an equilibrium with the new water composition [61]. Ion-exchange is mainly physical and reversible.

The cation exchange capacity (CEC) of a soil
Charged solids with a large specific surface area are most relevant for ion exchange. Clay minerals and organic matter thus contribute to the capacity of a soil to adsorb ions. This cation exchange capacity (CEC) can be expressed in meq/kg [72]. In this research, the CEC of the filter medium was unknown and thus had to be estimated from literature. The CEC of soils is generally given in meq/kg of dry soil and values for dune sand typically range from 0-50 meq/kg [73], of which clay minerals and organic matter are responsible for most of the exchange capacity. Appelo and Postma mention 10 meq/kg as a reasonable value for a sandy aquifer [61]. As the biofilter has been in use and some clay and organic material may have accumulated in the filter over time, the CEC of the biofilter was estimated at 15 meq/kg. The CEC is a parameter that PHREEQC needs in order to calculate the exchanger composition. The input is in meq/L pore water, rather than meq/kg, so the CEC was converted, using a

porosity of 0.39 and a specific weight of 2.65 g/cm^3 for the quartz sand. These values were inserted into Equation 14, where s stands for "per kg solid", q for "per liter pore water", ρ_b for the bulk density of the soil matrix (kg/L) and ϵ_w is the water filled porosity. The CEC comes down to 62 meq/L pore water. In reality, the CEC may deviate and even vary over time as a result of OM and clay concentrations or variations in pH.

$$q = s * \frac{\rho_b}{\epsilon_w}, \tag{14}$$

Calculation of Exchanger Composition
The PHREEQC-database uses the Gaines-Thomas convention to calculate the the composition of the exchanger, by combining the cation exchange selectivity constant for the different ions (Eq. 15 and 16) with the mass balance for the sum of exchangeable cations (Eq. 17). In the equations, I, J, K, ... are the exchangeable cations with charges i,j, k, ... K is the selectivity constant for the relevant ions, and can be found in the PHREEQC database. β is the equivalent fraction of the exchangable ion [61].

$$\frac{1}{i} * I^{i+} + \frac{1}{j} * J - X_j \leftrightarrow \frac{1}{i} * I - X_i + \frac{1}{j} * J^{j+} \tag{15}$$

$$\beta_J = \frac{\beta_I^{j/i} * K_{J \setminus I}^j * [J^{j+}]}{[I^{i+}]^{j/i}} \tag{16}$$

$$\beta_I + \beta_J + \beta_K + ... = 1 \tag{17}$$

3.4.3 Surface Complexation

Variable charge minerals, such as metal oxides, sorb ions from solution without releasing other ions. Hydroxyl groups of these minerals are protonated at low pH and deprotonated at high pH (Eq. 18), thus creating a pH-dependent surface charge. The charge of the soild is counteracted by ions of opposite charge in the diffuse double layer. The protons can be replaced by heavy metals, forming inner-sphere complexes. This type of adsorption involves two effects: a chemical bond between the ion and the surface atoms and an electrostatic effect that depends on the surface charge. Some ions are bound so strongly that they remain fixed on a surface, despite electrostatical repelling charges [72].

PHREEQC uses the double layer adsorption model by Dzombak & Morel [69] to simulate surface complexation on ferrihydrite [61].

$$\equiv MOH_2^+ \leftrightarrow \equiv MOH + H^+ \leftrightarrow \equiv MO^- + 2H^+ \tag{18}$$

In order to model surface complexation in PHREEQC, the medium is simulated by a) the number of sorption sites in mol/L, b) the surface area of hydrous ferric oxides (HFO) in m^2/g

and c) the mass of HFO in grams. Versteeg [50] used experimental values by Genç-Fuhrman et al. [21] to calibrate a model in PHREEQC and find the best fit for parameters a, b, and c. This resulted in $5 * 10^{-5}$ mol/L sorption sites for quartz and $4.835 * 10^{-4}$ mol/L sorption sites for IOCS. Quartz sand showed a best fit with an iron content of 1.4% Fe, whereas the iron content of IOCS is 13.5% [50].The surface area of HFO 600 m^2/g was suggested by [74] and is commonly used [61]. The values found in these previous researches have been used for this model and are summarised in Table 7.

Table 7: Model settings

Parameter	Quartz Sand	IOCS
EXCHANGE		
CEC (eq/L)	0.06	
SURFACE		
number of sites (mol/L)	0.207	2.01
surface area HFO (m2/g)	600	600
mass of HFO (g/L)	93.3	892

3.4.4 Precipitation and Redox Conditions

In addition to ion exchange and surface complexation, PHREEQC calculates the SI of minerals based on ion activities and corrects for aqueous complexes. The database uses the Truesdell-Jones equation for major ions and the Debye-Hückel or Davies equation for minor ions [61]. For SI = 0, the mineral is in equilibrium with the solution, whereas SI > 1 indicates supersaturation and SI < 1 indicates subsaturation, suggesting that precipitation or dissolution is expected for that mineral.

The redox changes in the biofilter were not modelled in detail, but the redox condition of the inlet water was estimated for the solution input, as this can influence the speciation of heavy metals. The exact pe was unknown, but could be estimated based on the concentrations of the known concentrations of two species of a redox couple. The chosen pe was based on the NH_4/NO_3 redox couple. It was calculated by PHREEQC using thermodynamic tables and the pe concept [61], resulting in a pe of 6.52 and 6.71 for the inlet water and initial water respectively.

3.4.5 Conceptual Model

A conceptual model was made to verify the observations in the data. Once it was clear that the replacement of aquifer water initially present in the biofilter by stormwater had a large influence on the observations, a model was made for both waters in equilibrium with the exchange media. Averaged measured inlet concentrations of all measured main ions, nutrients and heavy metals were used to describe the stormwater solution, whereas the intial measurements at the outlet were used to describe the initial water present in the biofilter. Because of the different composition of both waters, the composition of the exchanger and

HFO sites in equilibrium with the waters differs too. This change in exchanger composition was used to predict whether adsorption or desorption is expected when initial water is replaced with aquifer water in the biofilter. This was a quantative analysis, using the mole fraction of ions on the exchanger, rather than the absolute concentrations. The model outcome was then compared to the field data.

3.4.6 Transport Model

In order to predict the lifetime of the biofilter based on saturation of the filter media, PHREEQC was used to simulate advection, adsorption and dispersion. The transport of the contaminants is described by Equation 19, in which c is the solute concentration (mol/L), v is the pore water flow velocity (m/s), D_L is the dispersion coefficient (m^2/s), and R is the retardation factor [61].

$$R\frac{\partial c}{\partial t} = -v\frac{\partial c}{\partial x} + D_L\frac{\partial^2 c}{\partial x^2} \tag{19}$$

In the model, the biofilter is schematised as a vertical column of a number of cells, as is depicted in Figure 19. Each cell consists of a volume of water in the sorption media, initially holding water of a certain composition. When the model starts running, these cells are filled with an inflowing solution, shifting down from cell to cell to simulate advective transport. An explicit finite difference algorithm built into PHREEQC is used for this. The surface complexation and cation exchange data from the database enable PHREEQC to calculate the solid and solution equilibrium. This is repeated for each cell [68]. This way, the cells become saturated from top to bottom as the saturated front moves down. The expected pollutant concentration in the solution after a certain volume of inlet water has passed the filter can be calculated and visualised using a breakthrough curve.

Model Settings
The transport model used the same ion exchange and surface complexation settings as for the conceptual model that were explained in Section 3.4.2 and 3.4.3. Additionally, the model was run without ion exchange and with ion exchange and a stronger CEC. Five cells, of 0.12 m each, were chosen to simulate the 0.6 m filter layer of the Bluebloqs biofilter. This relatively coarse grid is enough to investigate hydrochemical reactions [68]. The column is flushed many times in the simulation, in order to reach breakthrough. More cells are not necessary for this purpose and would result in very long computation times. Flux boundaries were set at the column ends, because the concentration of flow across the boundary is set.

A total of 2000 bed volumes was simulated. The number of shifts is the number of times that water in each cell moves to a neighbouring cell. This number was calculated using the total time of the desired simulation and the time it takes for one pore volume to pass through the filter. With an average volumetric flow rate of 9.71 m^3/h this resulted in 25641 shifts of 2356 seconds. The calculations are specified in the PHREEQC script in Appendix
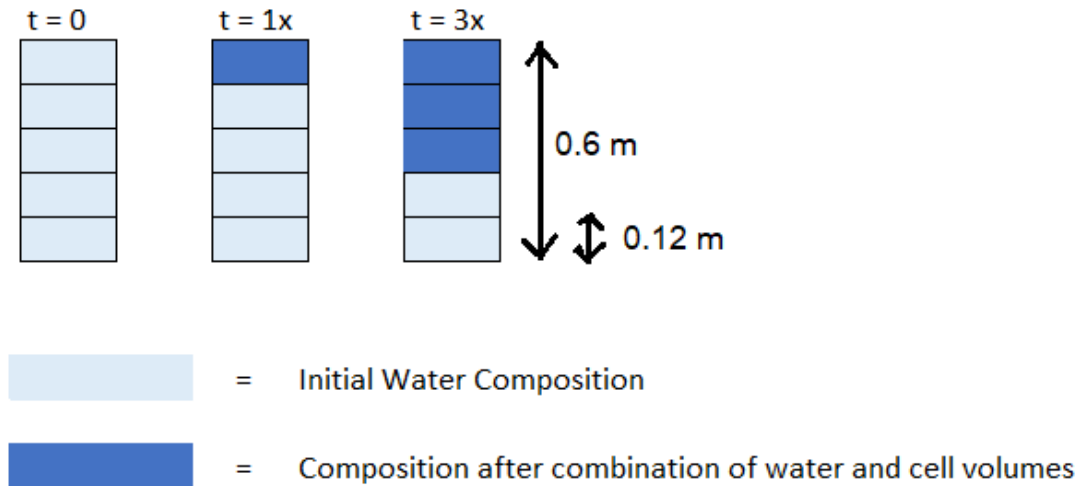
Figure 19: Schematic overview of transport in column

G. This model aimed to simulate the lifetime of the biofilter before breakthrough, starting at the beginning of operation in September 2018.The composition of the initial water in the biofilter at the time is unknown, and was assumed not to contain any heavy metals. The composition of main ions was based on the drinking water composition in Zuid-Holland [75]. The inflowing solution was defined as stormwater only, continuously flowing down the filter for 2000 bed volumes. The pH of the model was fixed at a value of 7.2, the mean and median that was measured at the outlet in the biofilter at Spangen.

Plug Flow vs Preferential Flow
Water distribution and design of the biofilter were found to lead to preferential flow paths in the biofilter. As a result of this, more water flowed through the filter at the inlet corners, whereas less water flowed through the middle of the filter. The effect of this preferential flow paths could be simulated by running three models in parallel, and adjusting the flow accordingly. An overview of this concept is shown in Figure 20. A1, A2 & A3 represent the different areas, and Q1, Q2 & Q3 represent the different flows.
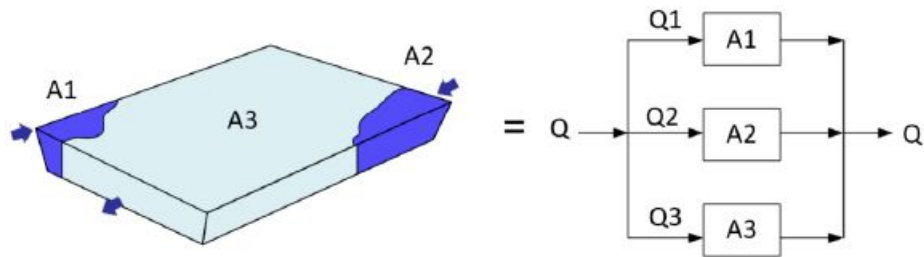
Figure 20: Overview of the biofilter roughly divided into three sections. Section A1 and A2 represent the corners that receive a larger fraction of water. Section A3 represents the middle fraction that receives a smaller water flow. Figure adapted from [3].

This multi pathway approach was used by Jonker (2020) to simulate the effect on pathogen retention in the biofilter, who found the following distribution to best represent the field data: Q1 = Q2 = 40% of total flow, Q3 = 20% of total flow, and A1 = A2 = 10% of the total surface area and A3 = 80% of the total surface area [3]. These values were also used in the current model, simulating metal breakthrough. As heavy metals accumulate over time, validation with the field data was not possible. Different volumes of water dosed over different areas of the biofilter result in different flow rates and total amounts of water passing through the different parts of the filter. The settings for the plug flow and preferential flow model are summarised in Table 8. To obtain the breakthrough of the preferential flow model, the pollutant concentrations from the different parts of the filter were summed up.

Table 8: Model settings for plug flow vs preferential flow

	Area (% of Total)	Volume (% of total)	Linear Velocity (m/h)
		Plug flow	
Total	100	100	0.10
		Preferential Flow	
A1	10	40	0.41
A2	10	40	0.41
A3	80	20	0.03

4 Results & Discussion

This chapter reports and discusses the concentrations of different pollutants found in the inlet and outlet water of the biofilter in Spangen and the processes that could have influenced this. Measurements were done during five events in the period from June - August 2020, on June 9th, June 15th, July 7th, July 14th and August 18th. The duration of events differs and was influenced by how long and how frequently the system paused during a run. The longest continuous event was the one on 06-07-2020 and is therefore used as an example event in some graphs. Similar behaviour was generally found in the other events, of which the data can be found in Appendix B.

4.1 Water Quality

4.1.1 Inlet Water Quality

During the research period, the quality of the water flowing from the buffer to the biofilter was measured. The water quality of the inlet water is reported in table 9, as well as the quality that was found in previous research on the same site between 27-09-2018 and 01-07-2019 [1]. Most of the concentrations measured in the current research correspond well with values that were found earlier. However, concentrations of Mn, NO_3^- and PO_4^{3-} are higher than observed in the previous research, while the DO is lower. Some measured concentrations also vary from what is expected for typical Dutch stormwater runoff. These typical values can be found in Appendix C. For some parameters, Dutch literature was not found, so typical values of international stormwater are cited in the text instead.

Table 9: Inlet water Quality Spangen. n = 20

| | UWB Spangen - Current Study | | | | UBW Spangen [1] | Phreatic groundwater [1] |
	mean	median	min	max		30-10-2018
Heavy Metals (ug/L)						
Cr	0.5	0.5	0.3	0.8	-	-
Ni	2.2	2.0	1.7	4.5	<5	-
Cu	1.2	0.61	0.25	7.7	<5	-
Zn	47	32.4	17.3	235	26-220	-
Pb	0.4	0.3	0.1	1.0	<5	-
Cd	0.0	0.0	0.0	0.0	<1	-
As	2.4	2.4	1.2	4.8	<4	-
Fe	778	735	250	1480	530-3500	16000
Mn	840	857	600	1071	190-690	1800
Co	0.3	0.2	0.2	0.9	<2	-
Nutrients (mg/L)						
NO3	2.9	3.0	2.4	5.4	<0.22 - 1.28	0.06
NO2	0.1	0.0	0.0	0.7	-	-
NH4	1.7	1.7	1.1	2.3	0.63 - 2.9	14.2
PO4	7.1	7.1	4.9	8.6	<0.15 -1.04	3.4
SO4	14	14	9.4	25.3	<30 - 61	<30
Physico-Chemical Parameters						
EC (uS/cm)	770.3	779.7	661	1034	516-1064	1385
DO (mg/L)	0.1	0.0	0.0	1.1	1.17 - 3.85	0.29
pH (-)	7.1	7.1	7.0	7.4	6.5 - 7.5	6.7

EC values in the inlet water at Spangen were measured between 661 and 1034 $\mu S/cm$ and were reported to be between 516 and 1064 $\mu S/cm$ by Zuurbier and van Dooren [1]. Typical EC values in stormwater runoff are expected to be <300 $\mu S/cm$ [76, 77]. The reason for these high EC values is leakage of phreatic groundwater (10 - 20 m^3/d) into the buffer [1], which can at the same time explain the high values for Fe and Mn [78] and low values for Cu and Pb. The EC of the phreatic groundwater was last reported in October 2018 as 1385 $\mu S/cm$ [1].

DO values measured in this research were generally <0.1 mg/L, not only lower than was measured in earlier research [1], but also lower than is typical for stormwater runoff [79, 80, 76]. During the research or Zuurbier and van Dooren [1], the event frequency had not been set to once a week. Hence, events occurred more frequently during their research, with less idle time in between, as was illustrated in Section 2.3. In the current research, the time in between events was usually at least six days long, during which the inlet water was stored in the retention buffer. The underground retention basin separates the water it contains from the atmosphere, so that no oxygen can get into the water through diffusion from the atmosphere or photosynthesis, the two main sources of dissolved oxygen [81]. The

only incoming source of oxygen is thus the collected stormwater. Microbes use this oxygen for repspiration when a carbon source is present, resulting in suboxic or anoxic conditions in the buffer [82] Due to unreliable TOC-analysis results, the concentrations of the carbon source are not known, but Boogaard et al. [6] reported average Dutch BOD stormwater values of 5.7 mg/L. BOD is generally expressed as oxygen consumption in five days at 20 °C. During the research period, the water usually stayed in the retention buffer for more than five days in between events. Additionally the buffer was never emptied completely (see Figure 9 and 10), so that part of the water remained in the buffer even longer, making microbial respiration a likely explanation for the observed oxygen depletion. Nitrification also consumes oxygen and could contribute to high nitrate concentrations found in the stormwater. NH_4^+ concentrations in the phreatic groundwater are high and leakage of this water into the buffer could result in oxygen consumption and nitrate production.

The neutral pH of the inlet water is slightly higher than expected for rainwater in the Netherlands [83], but is not atypical for stormwater runoff [76], suggesting that the pH was buffered while running off. Another explanation could be that denitrification occurred in the retention buffer under the suboxic conditions in the buffer, during which H^+ is consumed. However, this is counterindicative of the relatively high NO_3^- concentrations.

Not only NO_3^-, but also PO_4^{3-} concentrations are a lot higher than typical Dutch stormwater concentrations and their concentrations reported earlier by Zuurbier & van Dooren [1]. Phosphate concentrations were measured on the IC match with the concentrations measured on the DA and the total P measured on the ICP-MS. The remarkably high concentrations are thus not a result of an analysis error. The reason for this elevation remains unclear. Phosphate concentrations in the phreatic groundwater are not as high as the concentrations found in the stormwater. A difference in the sampling method may explain difference between concentrations found earlier on the same site [54] and concentrations found in this research. During earlier research, the system was not always running, resulting in samples containing water from the pipes instead of from the buffer. In the current research, this was avoided by making sure the system was always running during sampling rounds. Additionally, part of the Spangen drainage area was not yet connected to the stormwater sewer when the research by Zuurbier & van Dooren [1] was carried out. An expansion of the area can impact the nutrient concentrations in the inlet water. However, these variations could only explain deviations between the current research and earlier research on the same site. It does not give an insight in why the measured nutrient concentrations are much higher than those of typical Dutch stormwater runoff.

Nevertheless, stormwater quality can vary as a result of environmental factors such as temperature and rainfall frequency and intensity. This also leads to seasonal variations in nutrient concentrations: total-N and total-P concentrations are typically higher in spring [84]. In the month preceding the sampling rounds, it hardly rained. Long dry periods can lead to nutrient buildup [85]. These nutrients are consequently flushed into the buffer with the next rain events. In the case of phosphate, the highest concentrations were seen on the first sampling day and reduce with every following event, supporting this theory.

The sampling rounds were carried out in spring and summer, so the seasonal effect may contribute to higher concentrations. Additionally, abundant birds in this time of the year could contribute to additional N and P through their faeces [86].

All in all, the high concentrations of nitrate and phosphate can be the result of many mechanisms and more research into the origins of these nutrients on this site is necessary to provide a final conclusion. Even so, the high concentrations are important to note, as nitrate can play an important role in nitrification and denitrification reactions in the biofilter [87], whereas phosphate can influence the (de)sorption of heavy metals on variable charge minerals [88]. This will be further discussed in Section 4.3.4.

Particulate and Dissolved Metals
Metals occur in the water in dissolved and particulate form. This influences their mobility and toxicity, but can also give more insight in the inlet water in Spangen and the effect of storage in the retention buffer. Figure 21a shows the percentage of metals bound to particles found in the inlet water in this study in a box-whisker plot. The values can be compared to values commonly found in Dutch in two different studies in Figure 21b and 21c. Some of the whiskers in the Spangen data lie below 0%, meaning that the dissolved fraction was higher than the total fraction of the metal. This is not possible and is due to an inaccuracy in the analysis. In reality this means that the dissolved and total concentrations lie very close together, indicating that all of the metal present is in dissolved form.
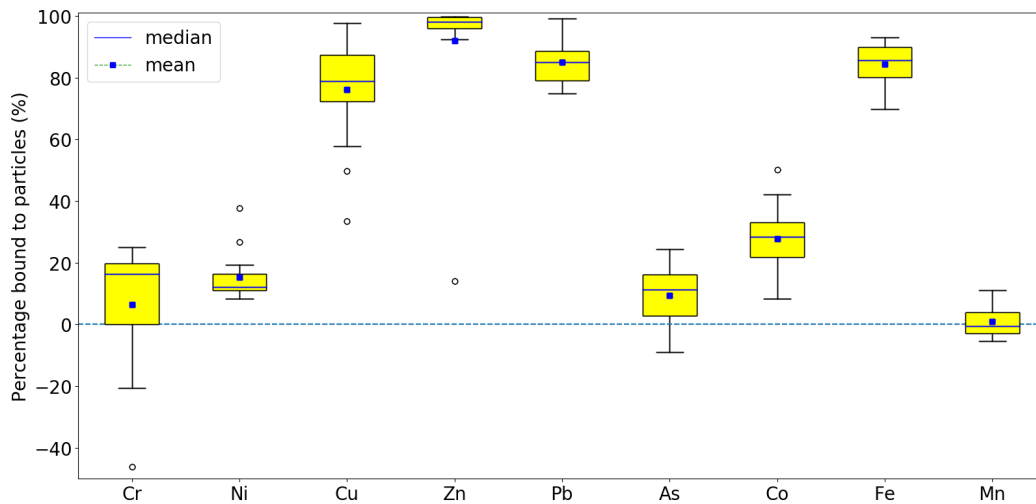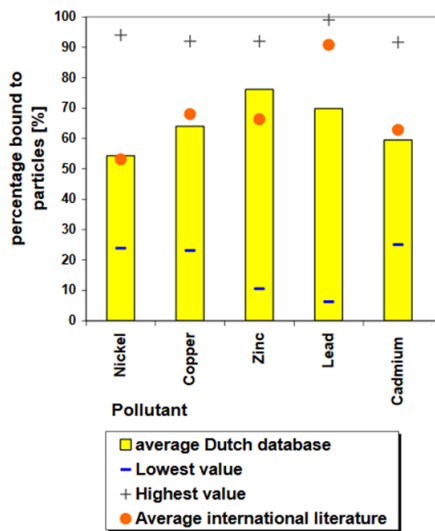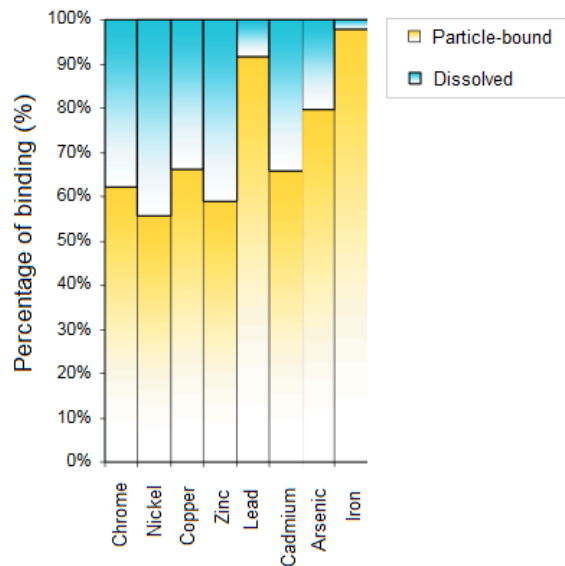
Figure 21: (a) Percentage of bounds metals in inlet water measured during events at Spangen. (b) Average percentage of bound metals in stormwater runoff from literature [6]. (c) Average percentage bound metals in Dutch stormwater runoff from literature [7] .

Cu, Zn, Pb and Fe were found mainly in particulate form in the inlet water in Spangen. For Pb and Fe this corresponds well to typical values. The bound fraction of Cu and Zn is on the high end of the typical range. Both metals could be adsorbed to iron(III) precipitates,

whereas Cu is also strongly associated with organic matter, and could be complexed to suspended OM [36, 89]. Nevertheless, no strong correlation between iron oxides and heavy metal concentrations was found, using suspended Fe concentrations as an approximation for Fe(III) oxides (see Appendix E). If the redox potential is low enough, Cu^{2+} could be reduced to the insoluble Cu^0 [90], but the presence of nitrate suggests that this is not the case.

Cr, Ni, As, on the other hand, show a lower bound fraction than was expected from literature. Cr likely occurs mainly as Cr(III) in the suboxic conditions in the biofilter. Its aqueous concentration is mainly controlled by dissolution and precipitation reactions and its solubility is low [91]. Because the concentration of Cr in the inlet water is very low, the concentrations do not exceed the solubility, resulting in a large dissolved fraction. The relatively high EC in the retention buffer, as a result of phreatic groundwater leakage, comes with a relatively high concentrtion of Cl^-. An increase in Cl^- concentrations can increase the formation of nickel chloride [92], a soluble nickel compound, that can contribute to the high fraction of dissolved nickel in the inlet water. Arsenic may be present mainly in its reduced form as arsenite in the suboxic conditions in the retention buffer. In this form it is more toxic and bioavailable than arsenate [88], which would be expected in oxic stormwater runoff. Hence this may explain the high dissolved fraction of As.

The neutral pH of the water in the retention buffer is comparable to pH generally found in stormwater [93] and is not expected to contribute much to dissolved fractions of any metal deviating from average stormwater values [94]

4.1.2 Outlet Water Quality

Table 10 shows the pollutant concentrations that were found at the outlet, as well as the concentrations found be Zuurbier & van Dooren [1]. The variations between minimum and maximum concentration are larger than in the inlet water, because the water that flows out of the biofilter is a combination of water from the buffer and of aquifer water from the irrigation cycles as was discussed in Section 2.4. These mixing fractions will be explained in more detail in Section 4.2. Most concentrations are in the same range as were found by Zuurbier & van Dooren [1], but the concentrations of NO_3^- and PO_4^{3-} are significantly higher, as well as the EC.

Table 10: Outlet Water Quality Spangen. n = 19

	UWB Spangen - Current Study				UWB Spangen [1]
	mean	median	min	max	
Heavy Metals (ug/L)					
Cr	0.4	0.3	0.2	0.7	-
Ni	4.2	3.9	2.7	6.8	<5 - 11
Cu	1.5	1.3	1.0	2.4	<5
Zn	35.2	31.3	24.8	58.5	<20 - 84
Pb	0.4	0.3	0.1	0.8	<5
Cd	0.0	0.0	0.0	0.0	<1
As	3.7	3.8	2.9	4.6	<4 - 6.5
Fe	101	50.5	17.2	350	34-1500
Mn	237	78.0	6.9	1012	28-430
Co	0.5	0.5	0.2	1.1	<2
Nutrients (mg/L)					
NO3	7.4	4.8	3.0	28.2	<0.22 - 4.9
NO2	0.1	0.0	0.0	0.5	-
NH4	1.2	1.2	0.3	2.1	0.09 - 1.26
PO4	2.2	2.2	0.5	3.7	<0.15 - 0.46
SO4	12.4	12.3	7.7	20.3	<30 - 58
Physico-Chemical Parameters					
EC (uS/cm)	1113	952	820	1863	103 - 1086
DO (mg/L)	1.0	0.5	0.0	3.7	1.25 - 6.89
pH (-)	7.2	7.2	6.9	7.4	6.6-7.5

The outlet concentrations are compared to the inlet concentrations in Table 11. In the case of phosphate, the higher outlet concentrations are likely the result of higher phosphate levels in the inlet water as was discussed in Section 4.1.1, whereas the nitrate values are higher than in the inlet water. Elevated concentrations of several metals also occur. This is the case for Ni, Cu, As and Co. Note that the concentrations at the outlet contain a mix of stormwater from the buffer and initial water from the aquifer. A direct comparison with the inlet concentrations is thus not possible. This problem will be addressed in the next section.

Table 11: Mean values of inlet and outlet water quality during the period of research.

	n = 20 mean inlet	n = 19 mean outlet	Target Value [2]
Heavy Metals (ug/L)			
Cr	0.5	0.3	2.5*
Ni	2.2	3.9	20**
Cu	1.2	1.3	1.3*
Zn	47	31.3	65**
Pb	0.4	0.3	7.4**
Cd	0.0	0.0	0.35**
As	2.4	3.8	18.7**
Fe	778	50.5	10***
Mn	840	78.0	-
Co	0.3	0.5	0.7*
Nutrients (mg/L)			
NO3	2.9	4.8	50**
NO2	0.1	0.0	-
NH4	1.7	1.2	3.2*
PO4	7.1	2.2	21.2**
SO4	14	12.3	-
Physico-Chemical Parameters			
EC (uS/cm)	770.3	1113	-
DO (mg/L)	0.13	1.0	-
pH (-)	7.14	7.18	-

*Wet Circulaire Bodemsanering voor diep grondwater (>10 m-mv) **Permit ***Operational

Comparison to the target vales in Table 11 shows that none of the mean concentrations exceed the target concentrations, with the exception of Fe, which concerns an operational target value, rather than a legal limit. Nevertheless the maximum concentrations found do in some cases (Cu, Co) exceed the target values. In other cases the concentrations remain below the target concentration. Nevertheless, pollutant concentrations are meant to decrease, rather than increase in the biofilter. The possible causes for this release will be discussed later in this chapter. The irrigation of the biofilter with aquifer water and the water flow in the biofilter are in important factor to take into account, as the outlet water consists partly of inlet water and partly of aquifer water.

4.2   Water Flow in the Biofilter

The irrigation of the biofilter with water from the aquifer was introduced in Section 2.4. In case of a weekly feed event from the feed buffer, like in the research period, this means

that the biofilter is filled with water from the aquifer before the feed event. This water has different properties than the stormwater in the retention buffer, as can be seen for the EC in Table 12. The transition from initial water to feed water and thus high to low EC during the feed event is shown in Figure 22.

Table 12: Initial and feed water EC for the events that are shown

Event Date	Initial EC ($\mu s/cm$)	Final EC ($\mu s/cm$)	Mean inlet EC ($\mu s/cm$)	Std Dev inlet EC ($\mu s/cm$)
9/06/2020	1200	851	807 (n = 12)	15.6
15/06/2020	1700	968	848 (n = 29)	55.8
6/07/2020	1860	829	808 (n = 37)	19.9
14/07/2020	1730	820	732 (n = 22)	17.1
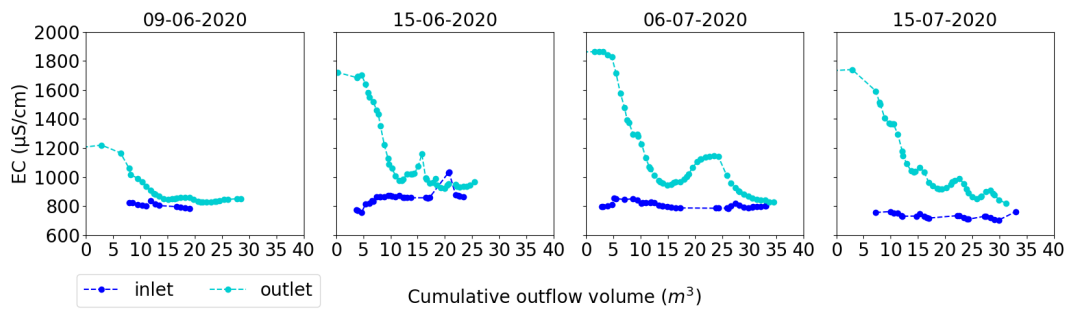
Figure 22: EC comparison for four different feed events

The initial EC value at the outlet is higher than that of the inlet, because the EC of the aquifer water is higher than that of stormwater. Groundwater influences contribute to this high EC in the aquifer, this will be discussed in section 4.5. Towards the end of the event, the EC at the biofilter outlet approaches the lower EC value of the stormwater. The gradual transition from a high to a lower EC suggests mixing of the two waters, rather than a plug flow that was expected in the biofilter. This becomes clear when looking at figure 23 in which ideal plug flow behaviour and completely mixed flow are plotted in the same graph as the actual measured EC.
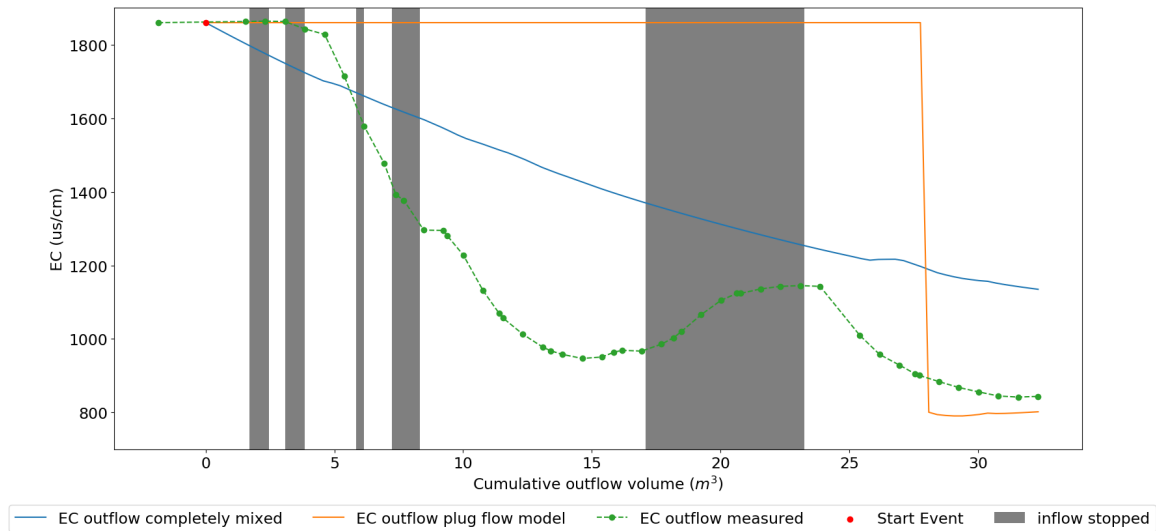
Figure 23: Comparing measured EC (06-07-2020) to plug flow and completely mixed flow

The actual measurements show combined behaviour. The first few cubic metres follow the plug flow trend, after which mixing of the two types of water starts. The curve is, however, much steeper than a completely a mixed flow. This can be explained by preferential flow and short-circuiting. The deposition of water on only small area of the biofilter likely contributes to the development of preferential flow paths for the water to flow through. Another factor is the location of the outlet close to one of the inlets, as was visible in Figure 18, providing an easier flow-path. This implies that the majority of the feed water passes through only a small volume of the biofilter, basically reducing its effective volume. The inflow of feed water pauses regularly, as was explained in Section 2.3. While the inflow stops, the outflow continues in order to lower the water level in the biofilter. These moments of paused inflow allow the water that is not in the short-circuit pathways to flow towards the outlet. These volumes still contain the initial water with a high EC, explaining the rise in measured EC while the inflow was paused. Short-circuiting results in low retention times for most of the treated water, because large volumes of water pass through a small biofilter volume, while only small volumes of water pass through the larger volume.

4.2.1 Hydraulic Conductivity

Visual inspection and analysis of the electrical conductivity already revealed preferential flow paths in the biofilter. Hydraulic conductivity tests were conducted to get a better insight into the hydraulic functioning of the biofilter.

Constant Head Test
The biofilter in Spangen consists of three layers of quartz sand: the filter layer, the transition layer and the drainage layer. The porosity and hydraulic conductivity of these different

41

sands were measured in the lab using a constant head test. Both the porosity and hydraulic conductivity increase with increasing grain size (see Table 13). The table also includes the standard deviation σ and the relative standard deviation (RSD). The hydraulic conductivity is about a tenfold higher than the hydraulic conductivity that is recommended for biofilters, which is generally 100-300 mm/h, to ensure a large enough treatment capacity without compromising on support for plant growth and surface area for adsorption [24].

Table 13: Hydraulic conductivity of the sands used in the filter, transition and drainage layer of the investigated Spangen biofilter. n = 3

	Grain Size		
	0.4 - 0.8 mm	0.8-1.25 mm	1.2 - 2.0 mm
Biofilter application	Filter Sand	Transition Layer	Drainage Layer
Layer thickess in biofilter (m)	0.6	0.2	0.3
Porosity (-)	0.38	0.39	0.41
Hydraulic Conductivity (mm/h)	3592	14745	15613
Hydraulic Conductivity σ (mm/h)	46	1099	1036
Relative Standard Deviation (%)	1.3	7.5	6.6

In-situ Hydraulic Conductivity

The single-ring infiltration test was used to determine the hydraulic conductivity of the filter layer in the field. It becomes clear that the hydraulic conductivity is heterogeneous over the filter with the highest values in the middle, followed by the corner of the filter that is not flooded during an event (see Table 14). The hydraulic conductivity on these locations is larger than was indicated by the lab test. The corner near the inlet and outlet of the system have a hydraulic conductivity that is lower than measured in the lab test, with the value of the corner near the inlet, which is always flooded during events, being the lowest.

Table 14: In-situ saturated hydraulic conductivity at various points spatially distributed over the biofilter. n= 1

Sample Point	Location	Kfs (mm/h)
1	Middle of biofilter	9743
2	"Dry corner" not reached by inlet water during event	5513
3	Corner where inlet water flows onto biofilter	990
4	Corner near biofilter outlet	3038

Heterogeneity is to be expected in a field scale biofilter, because it is affected by many factors, including compaction, clogging and vegetation. The differences that were found in the BB in Spangen are very large. Although seemingly contradictory at first, the low hydraulic conductivity near the inlet and outlet support the theory of short circuiting. As more feed water follows the short-circuit flow paths, it brings in more suspended and dissolved solids. Removal of these pollutants from the water results in clogging of the biofilter and thus a lower hydraulic conductivity where most of the water passed through. Despite this, the

hydraulic conductivity in these corners was still more than a threefold higher than the recommended hydraulic conductivity for biofilters [24], so that the water was still able to pass through the biofilter easily.

Metal Accumulation in the Biofilter

4.2.2 Mixing Fractions

Short-circuiting does not only result in short retention times, it also results in different fractions of initial water and feed water at the outlet. These fractions make it challenging to analyse the removal of heavy metals in the system. Hence, the EC could be used as a conservative tracer to estimate the expected concentrations of metals and nutrients if mixing was the only mechanism occurring in the biofilter. This method is explained in Section 3.2 and is applied in Section 4.3. Figure 24 shows the measured inlet and outlet EC and the fraction of inlet water based on this. Initially, all the water consists of aquifer water, so there is no inlet water coming out at the outlet. After the system starts running, the fraction of inlet water increases gradually, already before the water volume initially present in the biofilter ($28\ m^3$) has flown out. The grey areas represent the times when the inflow paused. During these pauses of inflow, initial water that was still present outside of the preferential flow paths has the opportunity to flow to the outlet. Thereby decreasing the fraction of inlet water at the outlet as can be seen from the increased EC. Back-calculating the outlet EC based on an estimation of the inlet EC and the mixing fractions gives a perfect fit with the measured EC, because that is what the estimation is based on. The same mixing fractions can be used to predict the concentrations of contaminants if mixing is the only mechanism taking place. If the measured data fit well with the estimated curve, then mixing is the only process that has an effect on the concentration of the element. If the measured data lies below the mixing curve, removal is likely, whereas measured data above the mixing curve indicates release.

43
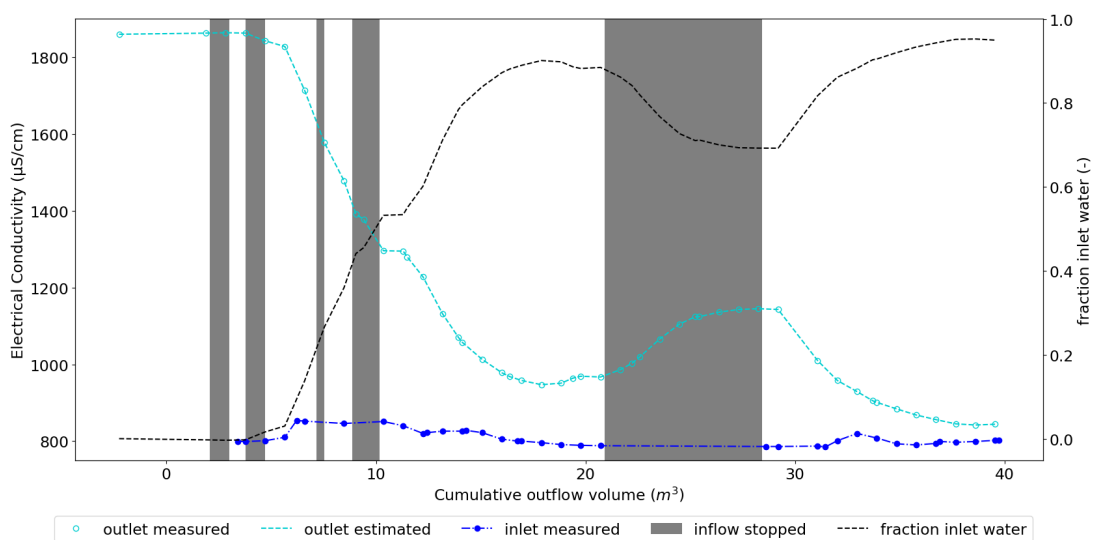
Figure 24: The measured EC at the inlet and outlet plotted together with the estimated EC based on the fraction of inlet water.

4.3 Water Quality Changes in the Biofilter

4.3.1 Background Ionic Composition

The main background ions in the water were measured during the five feed events. Their concentrations are shown in Figure 25. The macro chemistry of the inlet water is relatively stable throughout the run, with bicarbonate (HCO_3^-) the most prominent anion, followed by chloride (Cl^-). Calcium (Ca^{2+}), sodium (Na^+) and magnesium (Mg^{2+}) are the cations present in the highest concentrations. In the outlet water, the EC starts high as a result of the irrigation cycles with aquifer water that contains elevated levels of Cl^- and Na^+, and to a lesser extend Ca^{2+} and Mg^{2+}. The EC decreases during the event as the initial water mixes with water from the inlet. The EC that was estimated from the equivalent ions present in the water corresponds well to the measured EC for the inlet water, but a little bit less well for the outlet water, especially when the cations were used to estimate the EC. This can also be seen when looking at the Charge Balance Error (CBE). The error is acceptable for all inlet samples (Table 15), but is too high for most of the outlet samples. A reason for these deviations could be that high Na^+ concentrations can have an effect on the accuracy of the ICP-MS, used to measure the cation concentrations. Concentrations of prominent cations such as Na^+ or Ca^{2+} may be overestimated.

Table 15: Charge Balance Error (CBE) describes the accuracy of the macro-chemical analysis of inlet water from feed event on 06-07-2020

Runtime (min)	Sum Anions (meq/L)	Sum Cations (meq/L)	CBE (%)	EC measured ($\mu S/cm$)
13	8.07	8.05	-0.12	799
36	8.54	8.80	1.51	851
93	7.74	7.80	0.36	786
121	7.94	8.08	0.88	808

Table 16: Charge Balance Error (CBE) describees the accuracy of macro-chemical analysis of outlet water from feed event on 06-07-2020

Runtime (min)	Sum Anions (meq/L)	Sum Cations (meq/L)	CBE (%)	EC measured ($\mu S/cm$)
15	17.75	20.85	8.01	1863
35	13.20	15.08	6.63	1392
92	11.62	12.22	2.54	1124
121	8.75	10.88	10.83	901
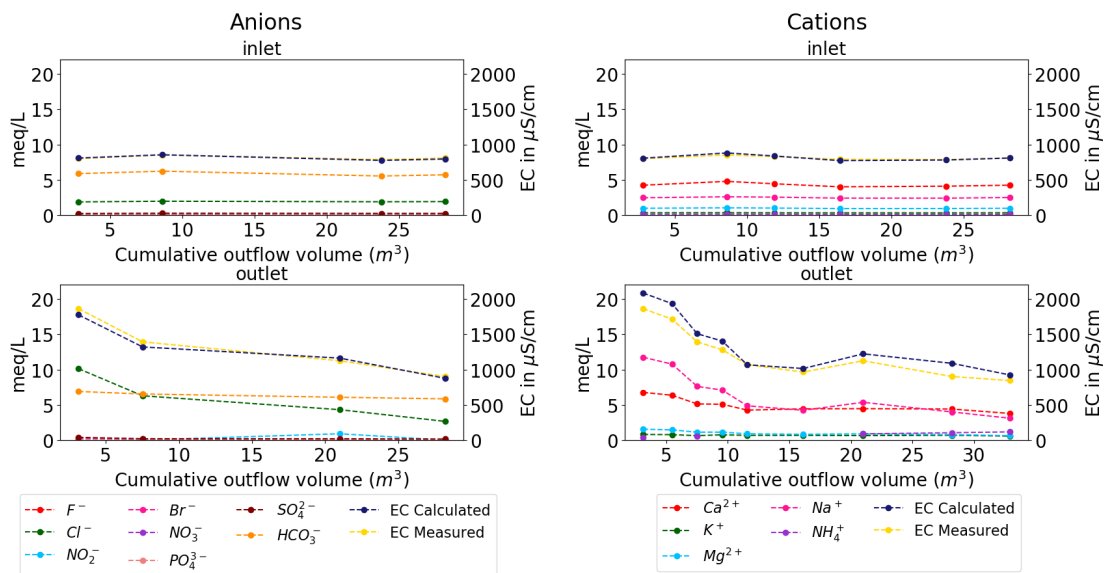
Figure 25: Macro chemistry of inlet and outlet water on 06-07-2020

4.3.2 Major ions

In order to analyse what is happening to the major ions in the biofilter, the measured values at the inlet and outlet were plotted in one graph with the fraction of inlet water and the estimated concentrations of the ion based on it. Na^+, K^+, Mg^{2+} and Cl^- are assumed to behave conservatively, meaning that they are not (much) affected by changes in temperature,

pH and pressure [95] and do not take part in chemical reactions. Figure 26 shows that the measured concentrations for Na^+, K^+ and Cl^- follow the "mixing only" estimations quite well, indicating that mixing is indeed the only process that has a major effect on them. In contrast, the measured values for Ca^{2+} and SO_4^{2-}, their measured values lie lower than the "mixing only" line, suggesting that another process contributes to the removal of these ions. In the case of Mg on the other hand, the measured concentrations are slightly elevated. The processes that may influence these observations for Ca^{2+} and Mg^{2+} will be discussed in this section, while SO_4^{2-} will be discussed in Section 4.3.4.
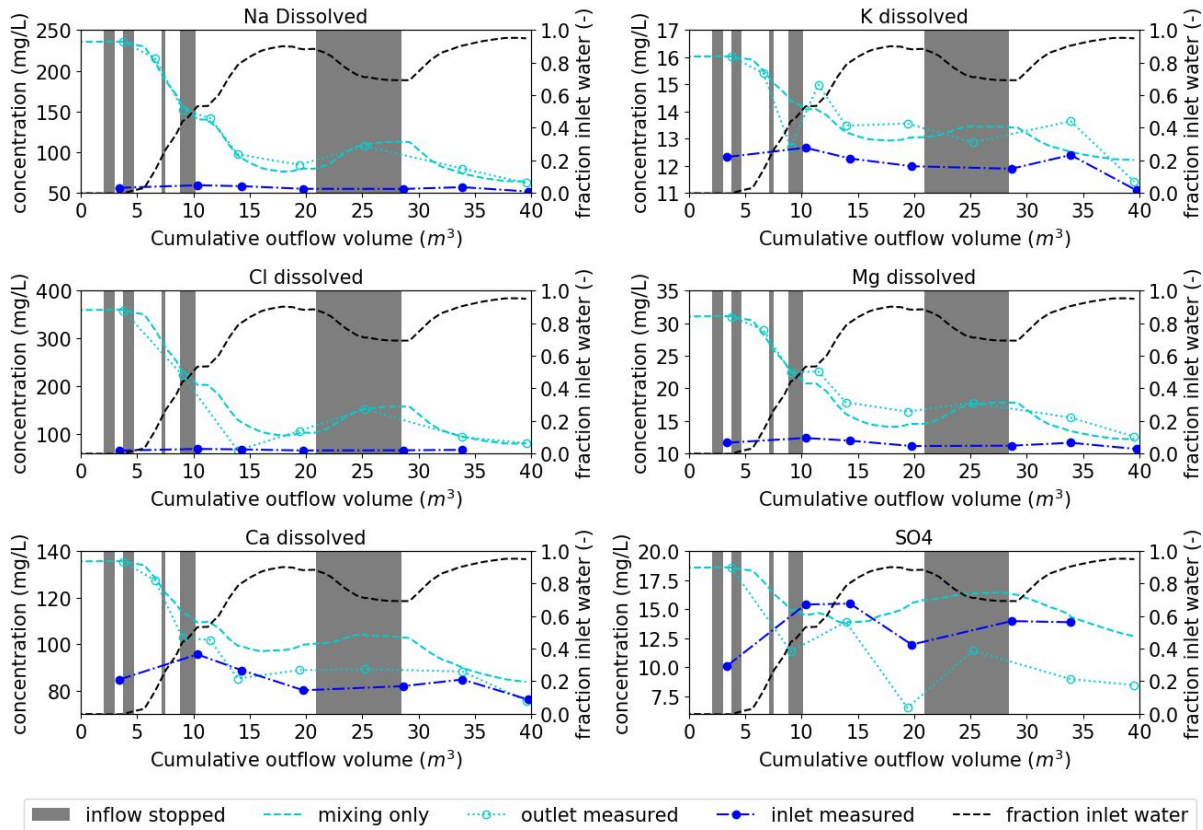
Figure 26: A selection of major ions from which conservative behaviour was expected. Their measured concentrations at the inlet and outlet, on 06-07-2020, are plotted in the same graph as their estimated concentrations based on mixing fractions.

Calcium

Section 4.2 explained that the salinity of the water in the biofilter decreases during an event. A change in salinity can trigger cation exchange reactions to take place. During this exchange, Na^+, that was adsorbed to biofilter media can be replaced by Ca^{2+} from the inlet water following equation 20 in which X represents the filter media [61].

$$Ca^{2+} + 2Na - X \longrightarrow Ca - X_2 + 2Na^+ \tag{20}$$

In this case, an increase in Na^+ would be expected, but it is not seen. Even so, Na^+ could still be released in absolute concentrations that are to small to perceive. Alternatively, when Na^+ is present in the clay in relatively low concentrations, it is possible that Ca^{2+} will exchange for Mg^{2+} instead [96], resulting in an increased Mg^{2+} concentration, which appears to occur. Other possible processes that can influence Ca removal include surface complexation reactions and precipitation as calcite or gypsum. However, at these low concentrations precipitation seems unlikely. This is confirmed by an SI calculation using PHREEQC. Calcite is in equilibrium in both the initial and inlet water (SI = 0.16 and 0.02 respectively), whereas the SI for gypsum is negative for both waters.

Lastly, the deviation between estimated values and measured values of Ca^{2+} may be the result of lower accuracy in the analysis, as a result of high Na^+ concentrations. The difference between measured and estimated Ca^{2+} concentration is small and Figure 27 shows that the reduction in concentration is not seen during all events.
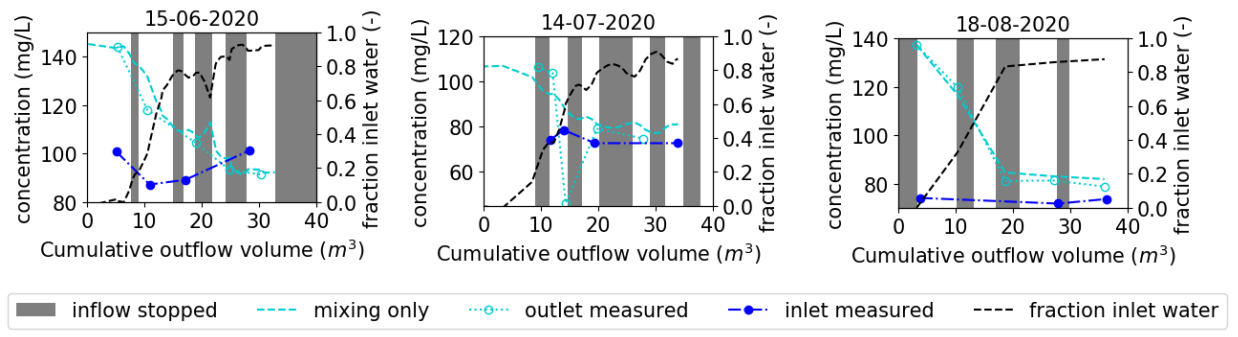
Figure 27: Calcium concentrations compared for three different feed events. The measured data points at the outlet coincide well with the estimated mixing only line.

Alkalinity
In most natural waters, the total alkalinity is also generally conservative [97]. Figure 28 shows that this is also the case in the biofilter. The measured data points at the outlet coincide well with the estimated mixing only line, indicating that mixing is the only process affecting this parameter. This confirms that strong precipitation or dissolution of calcite, is unlikely [98].
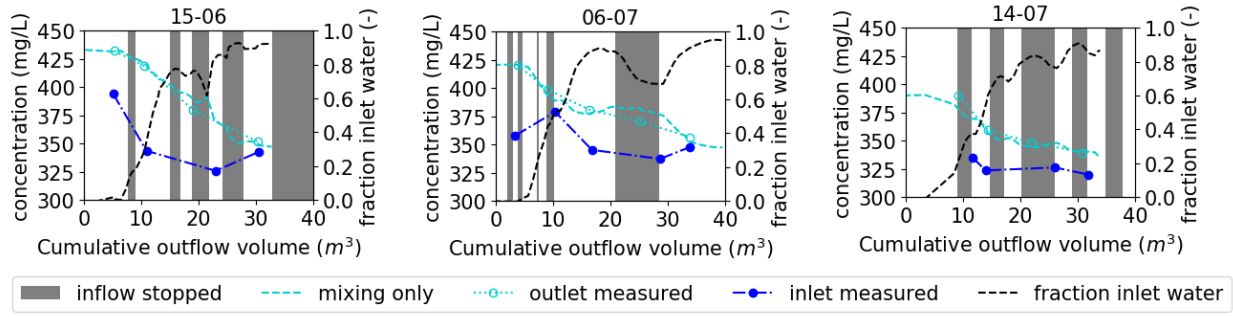
Figure 28: Total alkalinity (as HCO_3^-) comparison for three different feed events. The measured data points at the outlet coincide well with the estimated mixing only line.

4.3.3 Physico-chemical Parameters

As nutrients and metals are generally not conservative, it is important to analyse the physico-chemical parameters that affect them, before moving on to the analysis of the behaviour of nutrients and metals in the biofilter. The inlet water, outlet water and water extracted from the aquifer were all analysed for pH, EC, DO, temperature, turbidity and total alkalinity during the five feed events. The mixing of the aquifer water with the inlet water was already discussed with regards to the EC and alkalinity in Section 4.2 and 4.3.2 respectively, but it is also visible for DO and temperature. The pH on the other hand is relatively stable and the values in the inlet and outlet water are too close together to show a clear effect of the mixing. Turbidity varies in the inlet water, but is constantly well removed, so that also there the mixing effect is not noticeable. All these parameters are described in more detail in this section. It is important to note that, although concentrations for these physicochemical paramters were measured, the mechanisms that govern them were not. This section aims to hypothesise the observed concentrations, but more research is necessary to confirm these theories.

Temperature
Comparing the temperature during events on different days, a trend is visible: the temperature at the outlet first drops slightly, before rising to the temperature of the inlet water (see Figure 29). A temperature gradient in the biofilter is probably the cause of this. The water near the top is influenced more by the temperature of the atmosphere, than water deeper down. As measurements were taking place in the morning, a colder night temperature caused the water near the surface to be cooler than the water deeper down. When the event starts, the temperature at the outlet will first drop slightly when the water from near the surface arrives. After that, the temperature rises as a result of mixing with warmer water from the retention buffer. The temperature of both inlet and outlet water have increased with each following event as the air temperatures were getting warmer.
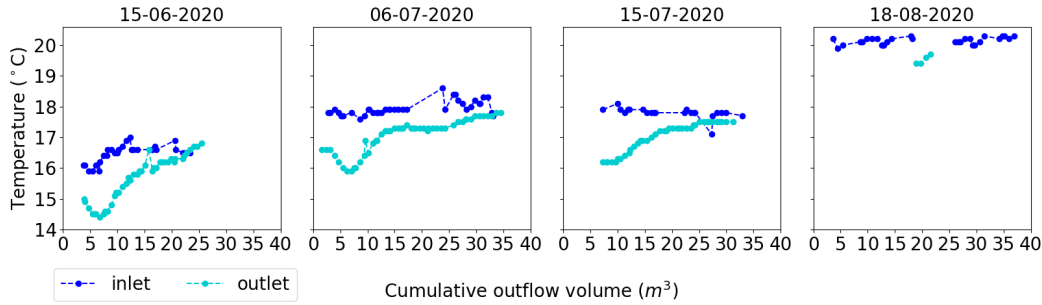
Figure 29: Temperature comparison for four different feed events

Dissolved Oxygen

The DO shows a similar trend as the temperature, but inverted, as can be seen in Figure 30. The concentrations of dissolved oxygen in the inlet water are constantly very low, whereas the dissolved oxygen concentrations at the outlet start higher and rise slightly, before dropping to the values of the inlet water. This is likely caused by an oxygen gradient in the biofilter. Near the water surface, oxygen can diffuse into the standing water [99] to be further transported down into the saturated zone by advection [100]. It is possible that parts of the filter remain oxic as a result of the preferential flow explained in Section 4.2. Vegetation can aid aeration by providing micro-pathways for oxygen transport and diffusing oxygen from their root system into the surrounding media [101]. Varying root oxygen release rates have been reported for various macrophytes in different researches and conditions, ranging between 0.02 g/m^2/d and 38.4 g/m^2/d [102]. Rates for the specific plants used in this biofilter were not found. However it is known that wetland plants can release oxygen into the soil. This aeration effect can influence soil chemistry and create an aerobic rhizosphere [103].

Oxygen concentrations near the surface are thus expected to be higher than deeper in the biofilter, causing a slight peak in dissolved oxygen when the water from the surface reaches the outlet. After that, the concentration of dissolved oxygen decreases as a result of mixing with the anoxic water from the buffer. This means that during the start of the feed event, oxygen-containing water is injected into the aquifer. The water that is extracted from well 1, still contains some oxygen as is can be see in Table 17. When this water is used to irrigate the biofilter, it already contains some oxygen, before oxygen from the atmosphere has diffused into the water.

Figure 30 also shows that the peak concentration of dissolved oxygen in the outlet water lowers for each following event. This could be related to the rising temperatures and salt concentrations as were discussed earlier. Oxygen solubility decreases with increasing temperatures [104, 105] and increasing salt concentrations [105]. Additionally, microbial activity generally increases with increasing temperatures [106]. The lower oxygen peaks on the warmer days could be a result of increased microbial respiration.

49
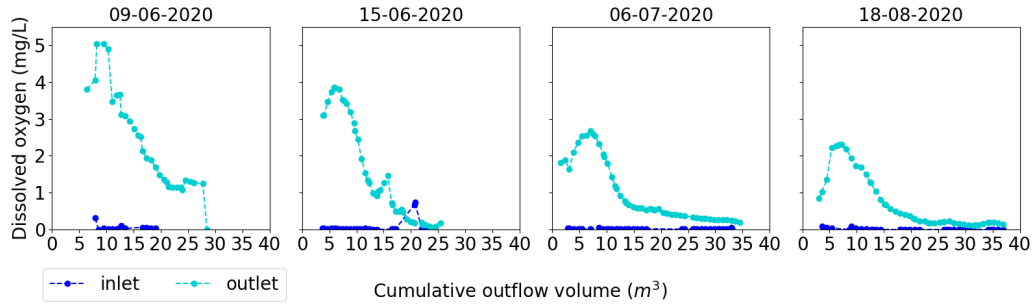
Figure 30: Dissolved Oxygen comparison for four different feed events

Table 17: Concentrations of initial DO before feed event, average DO of inlet water and DO in water extracted from well 1.

Event Date	Initial DO (mg/L)	Mean feed water DO (mg/L)	DO in extracted water from well 1 (mg/L)
9/06/2020	3.8	0.05 (n = 12)	1.11
15/06/2020	3.1	0.70 (n = 29)	0.70
6/07/2020	1.8	0.16 (n = 37)	1.17
18/08/2020	0.8	0.01 (n=33)	1.56

Turbidity

The turbidity varied a lot, not only over the different feed events, but also within the separate events (see Figure 31). However, on average the values were not that different for most events. Except for the event that was measured on 18-08 and shows a much lower turbidity in the inlet water, possibly because more antecedent rain had previously washed away sediment. In all cases, the turbidity of the outlet water was low, showing that particulate material is removed well, regardless of varying inlet concentrations. This is in accordance with literature, where turbidity removals of over 95% have been reported [107].
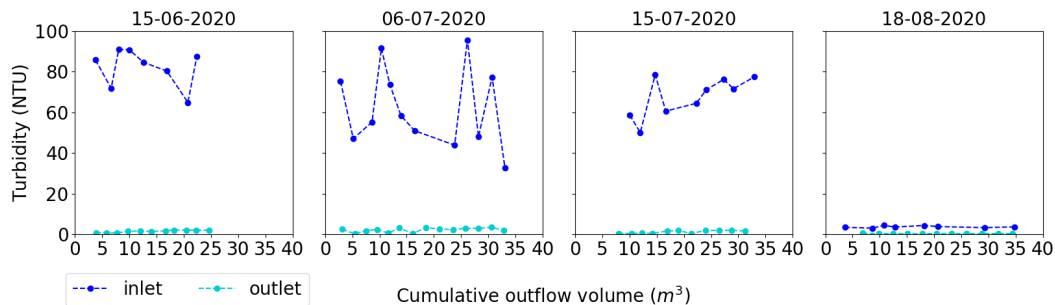
Figure 31: Turbidity comparison for four different feed events

As a higher turbidity indicates more suspended solids that heavy metals could potentially sorb to, a relation between turbidity and heavy metal concentrations might be expected.

50

Earlier research on stormwater in Australia found a correlation between Pb, Fe and Al and TSS [108]. No such correlation was found for any of the heavy metals in this research. The linear regression plots can be found in Appendix E.

pH

Although the pH is relatively stable for all events, some differences can be observed in Figure 32. The pH at the outlet is sometimes higher (09-06, 06-07 and 14-07) than at the inlet, while at other times the opposite is true (15-06 and 18-08). The sudden drop in pH at the outlet on 18-08 is likely to be a measuring error. Although nitrification and denitrification can affect the pH, other evidence that these reactions take place in the biofilter is lacking. This will be shown in Section 4.3.4. Specific adsorption or desorption can also have an effect on the pH [20], but clear factors indicating why the pH at the outlet was higher during some events and lower during others were not observed. Although the outlet pH remains quite steady throughout the run, the data seem to show a rise in pH during the start of the run, this is especially visible on 15-06. As the initial water consists of water from the aquifer, the low initial pH could indicate oxidation of sulphur compounds, ammonium, or iron in the aquifer or in the biofilter when it is not running. The reaction equations of these processes can be found in Appendix D, the production of H^+ reduces the pH. Oxidation in the aquifer could be the result of water relatively rich in oxygen being injected into the aquifer [83]. For all measurements, the pH of the systems remains between 5.5 - 7.5,which is the desired range for biofilters in order to support plant growth [24]. The measured values are on the high side of this range, which is an advantage for metal adsorption. A low pH favours metal dissolution and heavy metals need to compete with H^+ ions for sorption sites. As pH increases, more sorption sites become available [108].
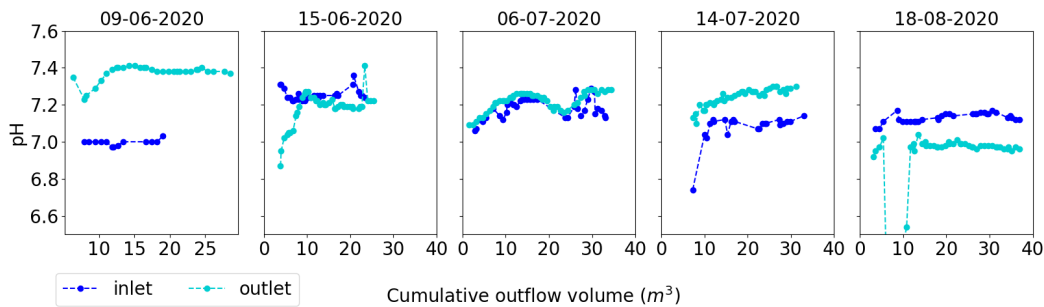
Figure 32: pH comparison for four different feed events

4.3.4 Nutrients

Using the mixing fractions again, the expected concentrations of nutrients in the case of mixing only could be estimated. These were plotted together with the measured data at the inlet and outlet. The results of 06-07-2020 are shown in Figure 33.
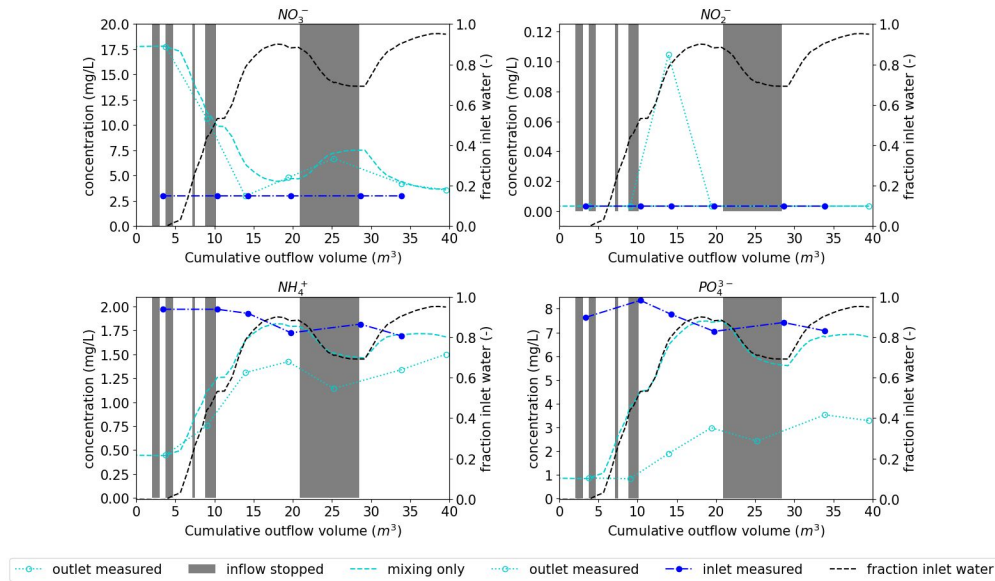
Figure 33: The measured concentration of nutrients at the inlet and outlet on 06-07-2020, plotted together with the estimation for mixing only. The difference between the "mixing only" concentration and the measured concentration shows removal or release of the nutrient.

Nitrogen Conversion in the Biofilter

Like the conservative ions in Section 4.3.2, the measurements at the outlet for NO_3^- do not deviate much from its expected concentrations based on mixing only, suggesting that no other processes influence NO_3^-. NO_2^- does not appear to be present in both the inlet and the outlet water, with the exception of one peak at the outlet. The concentration of NO_2^- was probably under the detection limit of the IC for most of the measurements, except that peak. These very low concentrations are expected, because nitrite is an intermediate in the nitrification and dentirification reactions and is only stable at very low concentrations [72]. In contrast, the measured values of NH_4^+ and PO_4^{3-} are lower than the concentrations based on mixing, indicating that removal takes place in the biofilter. Under aerobic circumstances the removal of NH_4^+ could indicate that nitrification occurs, converting NH_4^+ into NO_2^- and consequently into NO_3^-. However, concentrations of NO_2^- are too low to be detected, whereas NO_3^- does not show clear removal or release. One could argue that the slight peak in NO_2^- that coincides with what appears to be a slight dip in NO_3^- in Figure 33 could indicate that reduction of NO_3^- is taking place. However, this same dip is also visible in the Cl^- concentration when looking back at Figure 26. As Cl^- is more conservative than EC [63], this apparent deviation in NO_3^- and Cl^- is probably a slight deviation in EC instead, as was mentioned in Section 3.2. There is thus no indication that nitrification or denitrification occurs in the biofilter. Still NH_4^+ is removed. Because the concentration of NH_4^+ is much lower than that of NO_3^-, it is possible that nitrification occurs on such a small scale that the increase in NO_3^- is not clearly visible. Alternatively, NH_4^+ removal could be

52

the result of another process. As the retention time in the biofilter is short and nitrification is a slow process [87], it is not surprising that no indication of nitrification during an event was found. Additionally, the low oxygen concentrations during part of the run do not favour nitrification processes. Note that the initial NO_3^- concentration is much higher than the inlet concentrations, but is also higher than concentrations that were measured in the aquifer that was used for irrigation, in which the NO_3^- concentrations are lower than in the inlet water [1]. Possible causes of this are discussed in Section 4.5.

Other processes possibly responsible for the removal of NH_4^+ are plant uptake or adsorption. However, plant uptake is estimated at roughly 10% and plant requirements are thought to be met for the most part by existing nitrogen pools, rather than incoming sources. Its significance for nitrogen uptake is still debated [87]. Adsorption of NH_4^+, on the other hand, can be significant through cation exchange with the filter medium[72, 109]. Additionally, ammonia can form complexes with heavy metals. These complexes have been shown to be adsorbed successfully by IOCS [110], resulting in simultaneous removal of NH_4^+ and heavy metals.

The Fate of Phosphate
PO_4^{3-} can also potentially be removed by different processes in the biofilter. Although biological processes such as plant uptake and microbial assimilation play a role in the removal, earlier research has shown that the most significant processes are geochemical: adsorption, and precipitation as cation-P complexes [111]. The kinetics of precipitation reactions are rather slow and a hydraulic retention time of several days is needed [112]. As this retention time is not reached in the biofilter, adsorption is likely the primary mechanism to explain the removal of PO_4^{3-} during the event. The adsorption mechanism is rather complex and consists of several steps, of which the first step is a electrostatic ion-exchange reaction with outer-sphere hydroxyl complexes. This step occurs within minutes and is highly reversible. The PO_4^{3-} that is sorbed rapidly during events can be relocated to less reversible inner-sphere complexes in between events, by a slower adsorption reaction [112], freeing up rapid-reversible sites for the next event. The specific adsorption of PO_4^{3-} may have a negative effect on adsorption of metal cations also forming inner-sphere complexes and inhibiting the same sites as has been observed by others for Cd and Cu [113]. However, the specific adsorption of PO_4^{3-} also increases the surface negative charges, thereby possibly enhancing outer-sphere adsorption of heavy metals [88]. PO_4^{3-} adsorbs well to IOCS [114] and has a high affinity for ferric iron. Although plant uptake of PO_4^{3-} is limited, the vegetation may play an important role in P-retention, oxidising sorbed ferrous iron to ferric iron with oxygen from their roots [112].

The Fate of Sulphate
Sulphate was already briefly discussed and shown to be removed in the biofilter in Section 4.3.2. This paragraph will go deeper into processes that can affect sulphate. Removal was seen in all events and could be the result of biological reduction or sorption processes. Surface complexation of the SO_4^{2-} anion is strongest at low pH and decreases towards neutral pH such as in the biofilter. Additionally, SO_4^{2-} competes with PO_4^{3-} for the same adsorption

sites [115, 116], making adsorption an unlikely mechanism for SO_4^{2-} removal.

Under aerobic conditions, oxygen is used as an electron acceptor, but when anoxic conditions occur, this role will be taken over by other elements. Electron acceptors with a higher redox potential will be reduced first, sequentially: O_2, NO_3^-, Mn^{4+}, Fe^{3+}, SO_4^{2-} and methanogenesis [61]. This means that nitrate and ferric iron will be reduced, before reduction of sulphate occurs. In this research, sulphate removal was observed in the presence of nitrate, making sulphate reduction an unlikely explanation for this removal too. Moreover, earlier in this section it was shown that a strong reduction of nitrate does not occur. A DNA analysis by Vita Marquenie [117] tested two cores of the Spangen biofilter for microbial presence and found a very limited presence of sulphate reducing bacteria, The deepest sample core was taken from a depth of 50 cm, so a strongly reducing zone in the deepest layer of the filter or elsewhere in the filter is not ruled out. Because some parts of the filter are by-passed by most of the water, sulfate reduction under anoxic condition may take place in parts of the filter. However, the actual removal mechanism behind sulphate removal remains unclear and more research is needed to investigate the process behind sulphate removal in the biofilter.

4.3.5 Metals

Many of the main ions and nutrients either showed mixing only behaviour or removal from the biofilter. Some slight release of Mg was seen, possibly as the result of ion-exchange, but the relative release was only small. In case of heavy metals, this is different. In Section 4.1.2 it was already seen that the average total concentration of Ni, Cu, As and Co was higher at the outlet than at the inlet. The high outflow values are partly the result of mixing with higher initial concentrations in the biofilter as a result of irrigation with aquifer water. Mixing fractions were used on the dissolved concentrations of these metals to see if this was the only process affecting the outlet concentrations. The focus was on dissolved metals for various reasons. First of all, the EC that was used as a tracer is based on dissolved ions, and hence the method can only be used to estimate the concentration of other ions in solution. Secondly, the particulate metals are expected to be removed quite well by filtration in the top layer on the biofilter [87, 35]. This is supported by the great decrease in turbidity that was found in this research (Section 4.3.3) and the fraction of particle-bound and dissolved metals that is shown in Figure 34. The inlet values are the same as were shown in Figure 21a, but are compared to the outlet values in this section. The dissolved fraction of most metals is higher in the outlet water than in the inlet water. This suggests that a lot of the particle-bound metals are either removed or desorbed in the biofilter. Lastly, dissolved metals are generally more mobile, more bioavailable and more toxic to the environment than their particulate counterparts [35], making their removal more pressing.
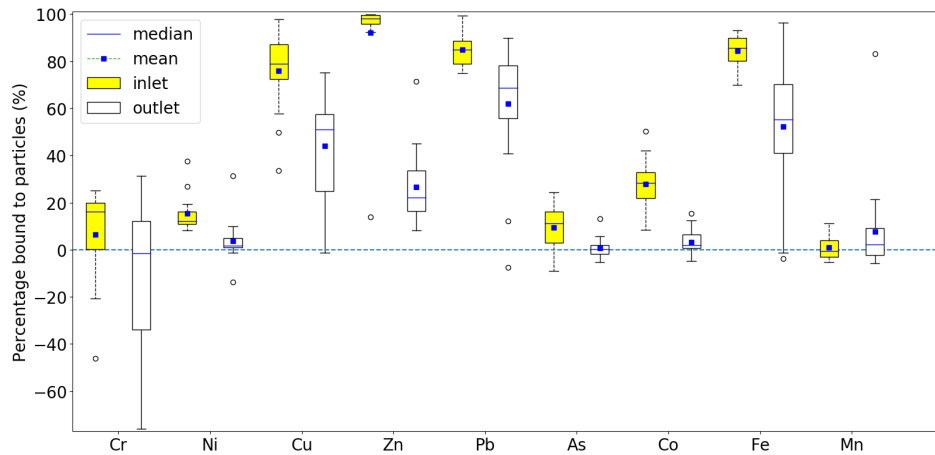
Figure 34: Comparing the percentage of metals bound to particles at the inlet and outlet of the Spangen biofilter

Metal Release in the Biofilter

Figure 35 shows that Ni, Cu, Zn, As, & Co measured concentrations are higher than the concentrations expected based on mixing only. This suggests that these metals are released in the biofilter. Note that for all of these metals, the initial concentration is higher than the inlet concentration. Upon inflow of water with lower concentrations, the initially retained metals could be released into the solution to find a new equilibrium, leading to a net desorption. This effect could be enhanced by the presence of other ions in the inlet water, that compete for the same adsorption sites. Phosphate has been shown to suppress the adsorption of certain metals, such as Cu and Cd, by occupying the same inner-sphere sites [88]. Zn ions can be easily exchanged when competing with other metals [118].
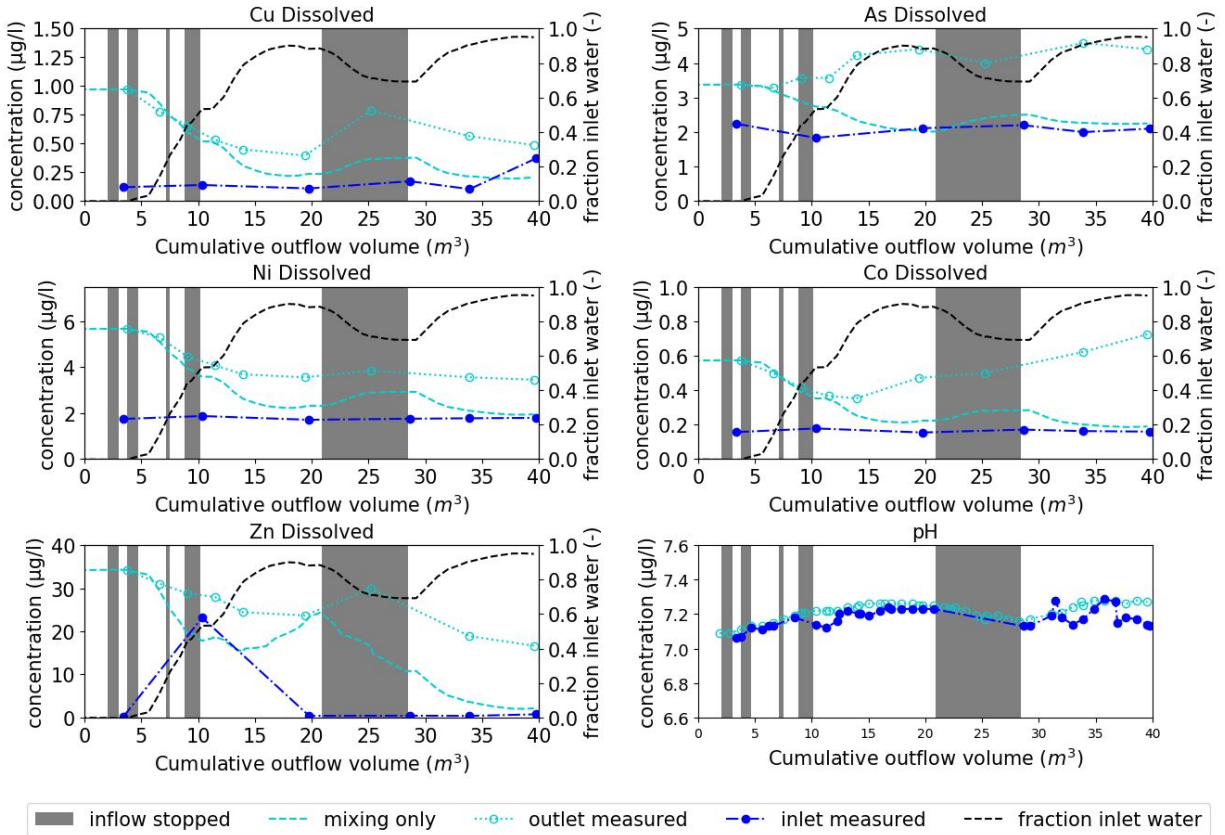
Figure 35: The measured concentrations, on 06-07-2020, of metals that are released in the biofilter, plotted together with their estimated concentration based on mixing only.

Although pH is one of the most important parameters influencing metal adsorption [119], the slight changes in pH during the event do not seem to have a great impact on the metal retardation. The trend for each metal is similar during each event, regardless of the slightly different pH situation in the different events. The oxygen-containing water in the biofilter is replaced with suboxic water from the buffer. This leads to a lower redox potential and reduction of iron oxides in the biofilter could be expected, thereby releasing adsorbed heavy metals [94]. On a first thought, this would work well with the observation that the release of the metals seems to start only after several cubic metres of water have passed. This coincides with the anoxic conditions in the biofilter. However, in that case a release of Fe would also be expected. The next paragraph will show that Fe gets removed, rather than released, showing that desorption as a result of iron oxide reduction does not occur. Desorption as a result of a change in water composition and competition with other ions is therefore more likely. That some metals start to be released later than others depends on their affinity for the filter material, and concentrations of the metal and other competing ions involved.

Heavy Metal Removal in the Biofilter

Figure 36 shows that the measured Fe, Mn and Cr concentrations lie below their estimated concentrations based on mixing fractions. This indicates that these metals are removed in the biofilter. As opposed to the metals that were released in the biofilter, the inlet concentrations of these three metals were higher than the initial concentrations, causing net sorption. It is clear that Fe is strongly removed, thus ruling confirming that iron oxide reduction as a result of the change in redox conditions is not likely.
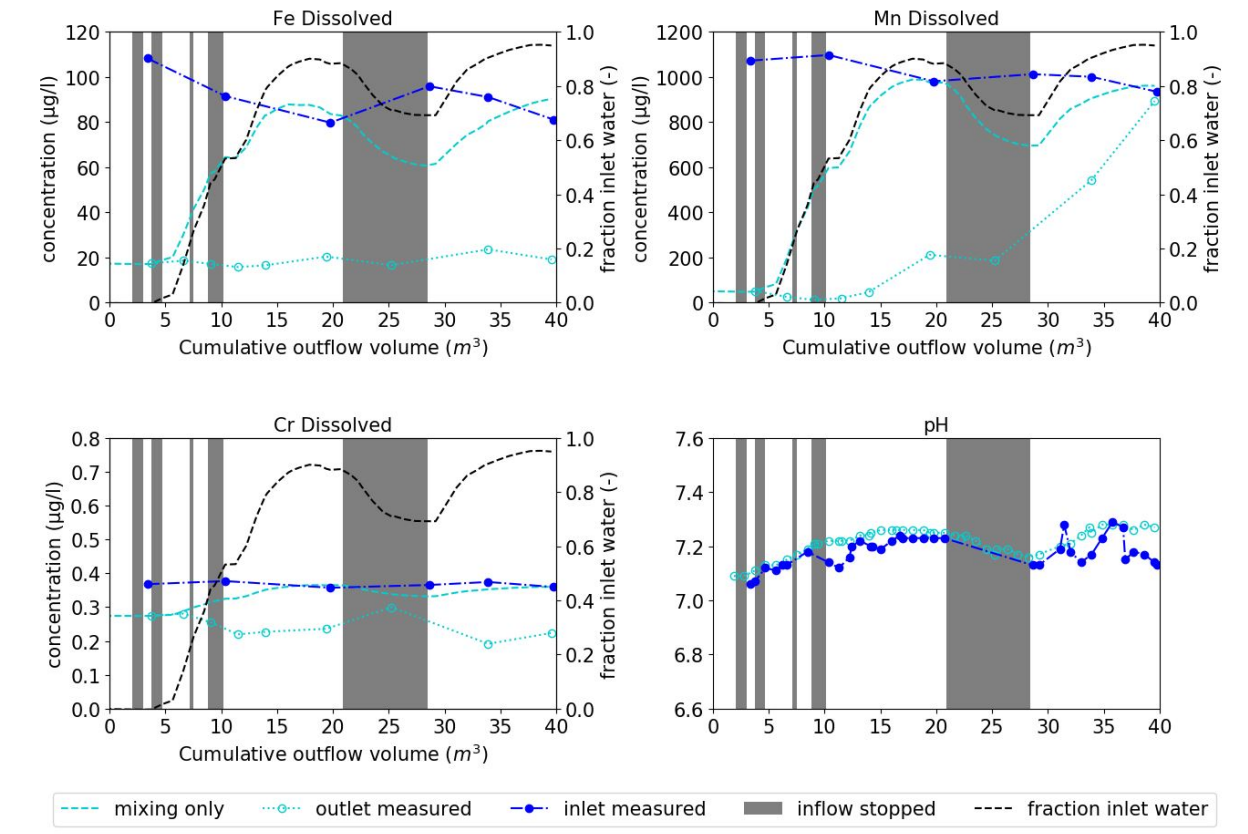
Figure 36: The measured concentrations, on 06-07-2020, of metals that are removed in the biofilter, plotted together with their estimated concentration based on mixing only.

The removal of Fe and Cr remains steady throughout the full run. Dissolved Fe is assumed to be Fe^{2+}, which can adsorb to the filter media [114] by means of surface complexation. The same is true for Cr, whether as Cr^{3+} or Cr^{6+}. Mn is well removed at the start of the event, but removal gets less efficient over time. The concentration of dissolved Mn is much higher than the concentration of the other two metals. The high concentrations saturate the easily accesible sorption sites during the time the first cubic metres of water flowed through the biofilter, leading to slower adsorption rates. Alternatively, Buamah et al [120] suggests that a locally lower pH change may result in a lower adsorption capacity. This pH change in the pores of the IOCS could be caused by the adsorption of Mn, in which H^+ is released.

57

Lead

The results of Pb varied per event as can be seen from Figure 37. On 15-06-2020, removal seemed to occur. However, on 06-07-2020 and 14-07-2020, no clear release or removal is seen. Because the concentrations of Pb were a lot below 1 $\mu g/L$, the accuracy of the ICP-MS may impact the measured data. Based on the surface complexation constant for Pb [69] and selectivity sequences [119], show that Pb has a high affinity for HFO.
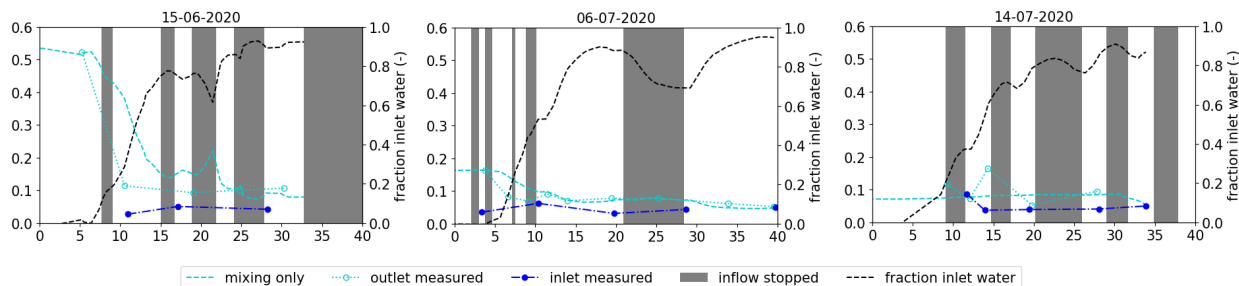
Figure 37: The measured concentrations of Pb at the inlet and outlet of various events, plotted together with its estimated concentration based on mixing only

4.4 PRHEEQC Conceptual Model

An equilibrium model in PHREEQC can give an insight into whether sorption or desorption is expected, when the water composition in the biofilter changes from initial water to inlet water. In order to do this, the initial water was simulated in PHREEQC, in equilibrium with the filter media and the same was done for the inlet water. The difference in the sorbed fraction for each ion in the two different water types, can give an indication of whether sorption or desorption is expected. As ion exchange and surface complexation reactions are generally very rapid [121], an equilibrium model can give a decent approximation. The model is explained in more detail in Section 3.4. Because the CEC used was a rough estimate, mole fractions are used to indicate relative removal or release, rather than estimating the absolute amount of moles that was sorbed. This gives an indication of whether sorption or desorption is expected, without quantifying to what extent. The relative differences show by how much the sorbed fraction of each ion increased or decreased. Because it concerns fractions, rather than absolute amounts, this is independent of the CEC.

Cation Exchange

Table 18 shows the mole fraction of several ions that were adsorbed to the filter media by means of ion exchange. The composition of the exchangeable ions on the media depends on their concentrations in the solution and their affinity for the medium [122]. The cations that take up the largest fraction of ion exchange sites are the main ions Ca^{2+}, Mg^{2+}, Na^+ & K^+ in both the initial water and the inlet water. However, the fraction of Ca^{2+} that is adsorbed to the exchanger increases in contact with inlet water, whereas the fractions of Mg^{2+} and Na^+ decrease and K^+ stays more or less the same. This corresponds to the

observations in Section 4.3.2, except that a release of Na^+ was not observed. The fraction of NH_4^+ that is adsorbed by ion exchange is a lot smaller than that of the main ions, but so is its concentration in solution. The relative increase of the sorbed fraction when in equilibrium with the inlet water is significant and confirms that cation exchange contributes to the removal of NH_4^+ in the biofilter that was observed in Section 4.3.2. Several heavy metals show removal or release as a result of ion exchange. Removal is observed in the case of Fe and Mn, whereas Zn & Cu show release. Also in the case of heavy metals do the results correspond to the results that were found in Section 4.3.5. However, even though ion exchange can contribute to removal of heavy metals from solution, most sorption is the result of surface complexation [72].

Table 18: Mole fraction of ions adsorbed to media by ion exchange and expected (de)sorption based on cation exchange in a PHREEQC equilibrium model

| | Cation Exchange | | |
	Initial Water mole fraction	Inlet Water mole fraction	Relative Difference
CaX2	6.78E-01	8.04E-01	18.7%
MgX2	1.63E-01	1.14E-01	-29.9%
NaX	1.30E-01	4.23E-02	-67.4%
KX	2.60E-02	2.69E-02	3.67%
SrX2	1.92E-03	1.97E-03	2.73%
NH4X	1.26E-03	7.09E-03	463%
BaX2	1.26E-04	2.20E-04	74.3%
MnX2	7.00E-05	2.55E-03	3.54E+03%
ZnX2	5.94E-05	1.46E-06	-97.5%
LiX	1.59E-05	1.29E-05	-18.7%
HX	1.14E-05	1.69E-05	47.8%
FeX2	4.58E-07	1.89E-04	4.11E+04%
CuX2	1.47E-07	4.45E-08	-69.8%
PbX2	8.71E-09	3.68E-09	-57.8%
AlX3	1.87E-09	2.35E-08	1.15E+03%

Sorption	Desorption

Surface Complexation

Just like for cation exchange, Table 19 shows whether sorption or desorption can be expected when the water composition changes from initial water to inlet water, resulting in a shift in equilibrium. Some ions that were mentioned with respect to cation exchange occur again in Table 19, because both processes play a role in their removal or release. From the main cations, Mg^{2+} and Ca^{2+} are also influenced by surface complexation. In the case of Mg^{2+} both processes result in release into the solution, but Ca^{2+} removal as a result of ion exchange is counteracted by a release as a result of surface complexation. This could explain

why removal of Ca^{2+} was not observed in all events in Section 4.3.2.

Table 19: Mole fraction of ions adsorbed to media by surface complexation and expected (de)sorption based on surface complexation in a PHREEQC equilibrium model

	Surface Complexation		
	Initial Water mole fraction	Inlet Water mole fraction	Relative difference
CO3	7.02E-01	5.40E-01	-23.0%
OH	2.11E-01	2.48E-01	17.6%
PO4	5.67E-02	1.94E-01	243%
Mg	1.86E-02	9.46E-03	-49.2%
Ca	2.75E-03	2.34E-03	-14.7%
Cu	2.66E-03	5.92E-04	-77.8%
As	2.42E-03	1.37E-04	-94.3%
Zn	1.74E-03	3.14E-05	-98.2%
O	1.38E-03	3.90E-04	-71.8%
Mn	1.21E-04	3.22E-03	2.56E+03%
SO4	8.61E-05	1.85E-05	-78.5%
F	7.50E-05	4.67E-05	-37.7%
Se	6.05E-05	1.04E-05	-82.8%
Pb	2.80E-05	8.67E-06	-69.1%
Ni	1.36E-05	5.21E-06	-61.7%
B	6.81E-06	2.50E-06	-63.3%
Co	3.88E-06	1.87E-06	-51.8%
Fe	3.27E-06	5.61E-04	1.71E+04%
Sr	1.12E-06	8.30E-07	-26.19%
Ba	1.77E-08	2.22E-08	25.3%
Cr	4.10E-11	8.48E-11	107%

Sorption	Desorption

Note that PO_4^{3-} occupies a large fraction of the available sorption sites and that this fraction increases significantly when initial water is replaced with inlet water. This confirms the hypothesis that specific adsorption plays a large role in the removal of PO_4^{3-} in the biofilter. Moreover, most heavy metals desorb as a result of surface complexation. Cu and Zn, that showed desorption as a result of cation exchange, also show desorption as a result of surface complexation, along with As, Ni & Co. Desorption was also seen in the measured concentrations described in section 4.3.5. In that same section, Fe, Mn and Cr were shown to be removed from solution, corresponding to the expected sorption based on the conceptual model.

Sulphate is expected to desorb, based on the conceptual model, but sulphate removal was seen based on the measurements. This model can thus not be used to predict sulphate

behaviour and processes other than adsorption may play a role in its removal.

The redox conditions were challenging to simulate, because the exact pe is unknown and the system was not in equilibrium. As was explained in Section 3.4, the pe resulting from the N-couple was 6.62 in the initial water and 6.44 at the inlet. However, the lack of oxygen and the smell of sulphur could indicate that the redox conditions in the inlet were lower in reality. The model was also run with a negative pe (-3.11) for the inlet water, while the pe for the initial water remained at 6.71. Even though the fractions shifted a bit, the expected (de)sorption remained the same for all elements, except Cr. However the PHREEQC database, based on data from Dzombak & Morel, and Ball & Nordstrom [123], only contains surface complexation constants for Cr^{6+}, whereas most Cr is expected to be present as Cr^{3+}. As adsorption onto Fe and Mn oxides is also expected for Cr^{3+} [20, 124], more literature or experimental research is needed to improve the conceptual model for Cr.

The pH in the system is relatively stable, and changes in redox conditions do not have a large effect on the model. This means that previously sorbed metals mainly show desorption as a result of competition for sorption sites. Changes in water composition and high phosphate concentrations in the inlet water play a large role in this.

Based on this conceptual model the inverse would be expected to happen when the filter medium is in equilibrium with the inlet water, and water from the aquifer is fed to the filter. This means that during the first irrigation round after the stormwater event, PO_4^{3-}, Mn, Fe and Cr would be expected to leach, whereas Cu, As, Zn, Ni, Pb & Co would be expected to be retained by adsorption. Additional measurements during the first irrigation round are needed to support this hypothesis.

4.5   The Influence of Groundwater and Processes in the Aquifer

The effect of mixing of two types of water could be estimated by mixing fractions as was done in the previous sections. However, this does not yet explain the initial concentration of various ions in the biofilter. Some of these may not be explained by processes that occur in the biofilter, but are a result of processes in the aquifer or contribution from external sources. The high initial salinity and NO_3^- concentration that were mentioned in Section 4.2 and 4.3.4 will be discussed in this section, as well as a possible source of high concentrations for certain heavy metals in the aquifer.

4.5.1   Salinisation

As the biofilter is irrigated with water from well 1, the initial conditions in the biofilter are expected to represent the water in the aquifer after treatment in the biofilter. The water around the well should mainly consist of infiltrated stormwater, but as a result of the long dry period and irrigation with aquifer water, the extracted water is mixed with groundwater. This is visible by looking at the EC in Figure 38 where peaks and increasing salinities from the end of April indicate salinisation of the wells and the infiltrated water as a result of

irrigation with the high salinity water. The water at well 1 has a lower salinity than at well 2, because freshwater has a lower density than brackish water, causing a gradient from freshwater at the top of the aquifer to water with a high salinity in the deeper layers. Well 1 is shallower than well 2, explaining the lower salinity at well 1. For this reason, water is meant to be infiltrated in well 2 and extracted in well 1. Nevertheless, it seemed that during the research period, water was extracted from the deeper well 2 and used for irrigation, based on observations and reports from the operator. This can cause high salinities in the water that is used to irrigate the biofilter. The salinity in the water that is infiltrated into the aquifer is at times even higher than the water extracted at well 2, possibly as a result of evaporation. The fluctuations in EC are caused by alternating inflows of stormwater with a lower EC and aquifer water with a higher EC. High salinities have been shown to negatively impact metal removal in biofiltraton systems by increasing metal solubility. Sodium ions can compete with heavy metals for sorption sites, whereas chloride ions may bind to heavy metal ions and prevent them from sorbing to the filter media [38].
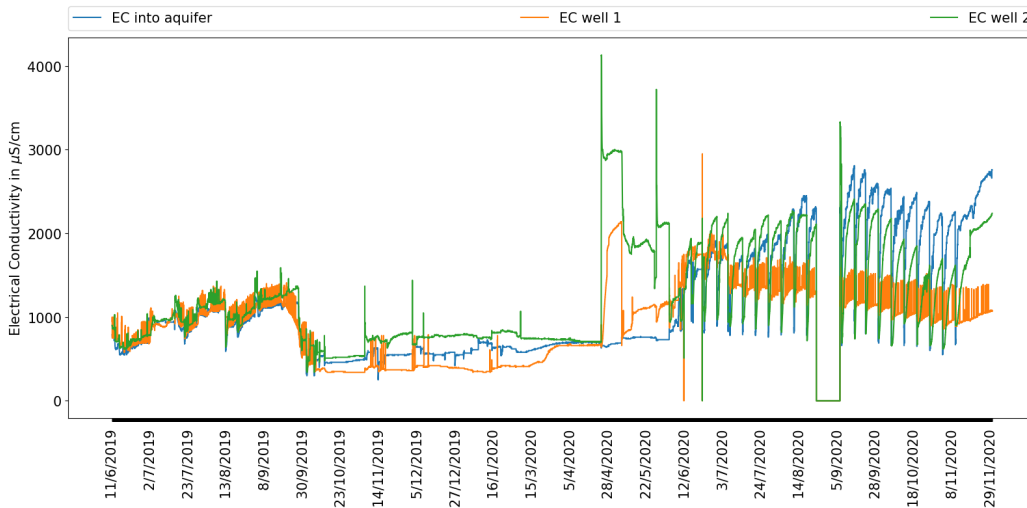
Figure 38: Salinisation at the wells and infiltration water

This salinisation shows the influence of groundwater on the extracted water that is used for irrigation. Other parameters in the aquifer are thus also influenced by the groundwater quality. Table 20 shows the concentrations that were measured at the outlet at the beginning of the run on 06-07-2020, as well as the stormwater values on the same day, and the concentrations in the groundwater that were measured at the monitoring wells by Zuurbier & van Dooren [1] a year earlier. This is the latest information available on the groundwater quality. The concentrations of the main ions Ca^{2+}, K^+, Mg^{2+}, Na^+ and Cl^-, measured in outlet initially give a representation of the water in the aquifer. The concentrations of the main ions found in this water are clearly elevated compared to stormwater values and are

instead within the range of the groundwater concentrations. This shows that the groundwater has a large influence on the water quality in the aquifer and thus on the water that is extracted from it. Pollutants from the groundwater are added to the biofilter during the irrigation rounds, as becomes visible from the initial concentrations at the outlet.

Table 20: Initial biofilter concentrations compared to stormwater and groundwater concentrations. "m-GL" stands for metres below ground level.

	Current Research (06-07-2020)		Zuurbier en van Dooren (01-07-2019) [1]			
	Initial Concentration Outlet	Average Stormwater (n=6)	17-19 m-GL	20-21 m- GL	23-24 m-GL	26-27 m-GL
EC (us/cm)	1860	808 (n = 37)	1002	1035	2090	5630
Ca (mg/L)	135	84.5	81	77	80	250
Fe (mg/L)	0.017	0.091	1.9	1.5	1.3	11
K (mg/L)	16	12.1	5.3	8.2	7.8	14
Mg (mg/L)	31	11.5	15	14	32	78
Mn (ug/L)	51	1025	270	390	470	680
Na (mg/L)	235	56.1	99	110	180	840
NH4 (mg/L N)	0.35	1.4	1.0	2.7	5.0	18
PO4 (mg/L P)	0.29	2.46	<0.05	0.14	0.44	<0.05
NO3 (mg/L N)	4.01	0.7	<0.05	<0.05	<0.05	<0.05
HCO3 (mg/L)	421	353.5	300	290	260	720
Cl (mg/L)	359	67.1	140	150	180	1400
SO4 (mg/L)	18.56	13.5	10	12	17	<1
DO (mg/L)	1.81	0.02 (n = 37)	1.11	0.76	0.43	0.34

4.5.2 Initial Nitrogen Concentrations

More interesting are the concentrations of NO_3^- and NH_4^+ as shown in Figure 39. The concentration of NO_3^- initially present in the biofilter is much higher than the concentration in stormwater or in groundwater. This means that the high nitrate concentration that is seen in every event must be the result of another process or is added to the system from an external source. An external source that could contribute to high NO_3^- is the faeces of birds and pets that may end up in the filter [86] or orgaganic N from plants that is converted to inorganic N. However, what is striking is that the initial NH_4^+ concentration is very low; much lower than that of the stormwater or the groundwater. Although adsorption may have contributed partly to this removal, the very low NH_4^+ concentrations and high NO_3^- concentrations seem to suggest that NH_4^+ was converted to NO_3^-. This nitrification could occur in the biofilter during periods when the system is not fed with water. Alternatively the process could take place in the aquifer, when water that contains oxygen is infiltrated into the suboxic groundwater. The first few cubic metres of water that are infiltrated into the groundwater are relatively rich in oxygen and during irrigation rounds, the system does not run as long as during an event, meaning that only the relatively oxygen-rich water is infiltrated into the aquifer. Nitrate concentrations in the groundwater are very low, so most of the nitrate present at the outlet initially would be a result of nitrification processes. This means that approximately 0.29 mmol/L N is converted from $NH_4 - N$ to $NO_3 - N$. This corresponds with ammonium concentrations found in the groundwater and the low ammonium concentrations that were measured in the initial outlet water (see Table 20).
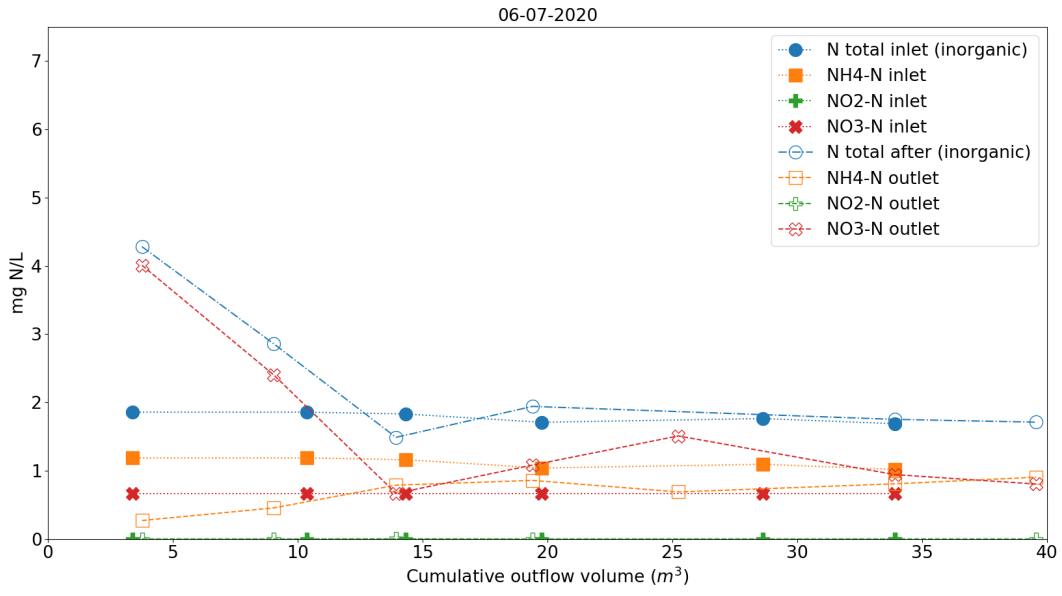
(a)
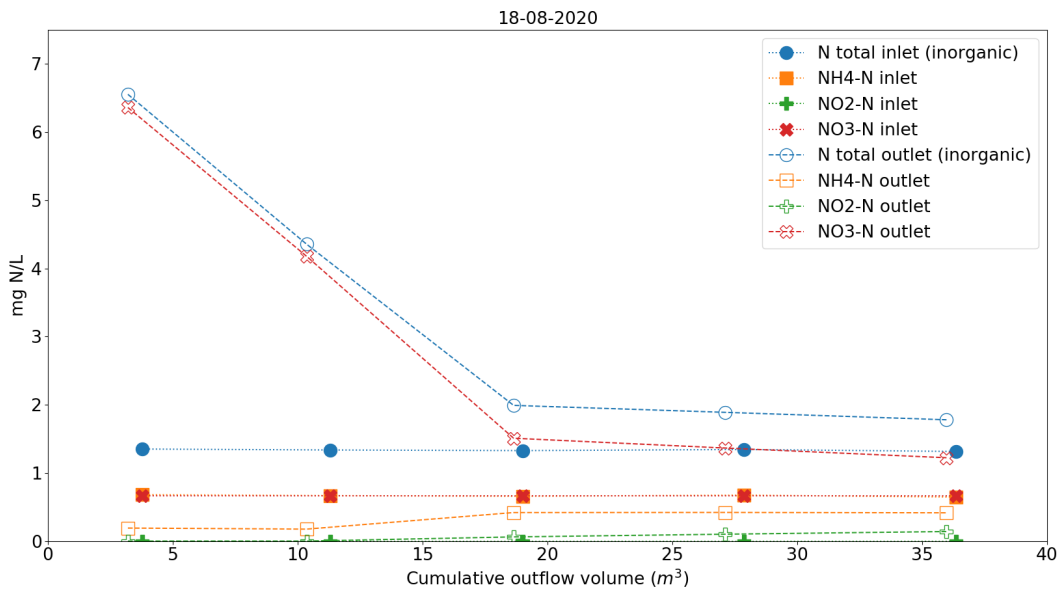
(b)

Figure 39: Comparison of nitrogen concentrations at the inlet and outlet during events on two different days

4.5.3 Pyrite Oxidation

Infiltrating relatively oxygen- water into a relatively oxygen-poor environment could oxidise not only ammonium to nitrate, but can also oxidise other compounds, such as iron sulphides [83]. Iron sulphides like pyrite can occur in sedimentary aquifer material and often contain heavy metals, Ni and Co in particular [125]. When pyrite is oxidised by oxygen or nitrate, these metals are released into solution and sulphate is produced. The initial concentration of sulphate in the water seems to be slightly elevated compared to both stormwater and groundwater in the area, as can be seen in Table 20. The measured heavy metal concentrations in the groundwater of Spangen were not published, but initial heavy metal concentrations are compared to stormwater in Spangen and average groundwater concentrations in the Netherlands in Table 21. Ni is one of the metals that has an initial concentration that is much higher than the average stormwater concentration and average background concentration in Dutch groundwater.

Table 21: Initial biofilter heavy metal concentrations compared to stormwater concentrations in Spangen and average background groundwater concentrations in groundwater (>10 m) in the Netherlands

	Current Research (06-07-2020)		Ministerie van Infrastructuur en Milieu [126]
	Initial Measured	Average Stormwater (n = 6)	Netherlands background
As ($\mu g/L$)	3.37	2.1	7
Ba $\mu g/L$)	67.63	61.5	200
Cd ($\mu g/L$)	0	0.0	0.06
Cr $\mu g/L$)	0.27	0.4	2.4
Co ($\mu g/L$)	0.57	0.16	0.6
Cu $\mu g/L$)	0.97	0.17	1.3
Pb ($\mu g/L$)	0.16	0.04	1.6
Ni $\mu g/L$)	5.66	1.8	2.1
Zn ($\mu g/L$)	34.18	4.35	24

These observations show that oxidation of nitrate and pyrite in the aquifer is a possible explanation for concentrations of nitrate and several heavy metals that exceed both stormwater and expected groundwater concentrations. Further research is necessary to confirm this theory.

4.6 PHREEQC Transport Model

The PHREEQC transport model could was used to predict the concentration of several metals at the outlet of the biofilter, throughout its lifetime. The average water quality at the inlet was used to describe the water that flows into the biofilter over time, simulating 2000 bed volumes. Irrigation cycles were not simulated and the pH was fixed at 7.2. Dissolved concentrations of pollutants were used, rather than total concentrations as was done by Versteeg (2020) [50]. Additionally, the effect of preferential flow was incorporated in this model, by modelling the biofilter as three columns. Two of these had a surface area of 10% of the

total surface area each, through each of which 40% of the inlet water was flowing. The third column had a surface area of 80% of the total surface area, through which 20% of the water was flowing. The columns with a small surface area were used to simulate the wet corners, and the column with a large surface area was used to simulate the relatively dry part in the middle of the biofilter. The breakthrough curves in Figure 40 describe plug flow (left) and preferential flow (right) in the biofilter in Spangen. For both cases, Ni & Co show complete breakthrough in a very early stage. Although complete breakthrough is slightly delayed in the preferential flow model, the 0.8 fraction broke through even sooner. This behaviour can be explained, because the corners A1 and A2 were saturated sooner, whereas the middle part A3 had to treat less water and thus less contaminants, resulting in slower breakthrough. As the water of the three parts is mixed in the effluent, the complete breakthrough is delayed, until this occurs in the middle part. Nevertheless, this means that the majority of the water by-passes treatment, way before complete breakthrough occurs. Breakthrough of a 0.8 fraction of the inlet concentration of Zn occurred after 1085 bed volumes (BV) in a plug flow situation, but after only 395 BV when preferential flow occurred. Cu and Pb also start to break through after approximately 200 BV in the latter situation. This shows the effect of the current design and operation on the lifetime of the biofilter with regards to metal retention. On 06-07-2020, the day on which the longest continuous event was measured, 330 BV had passed. The model was run including and excluding ion exchange, but the effect of this change was not noticeable.
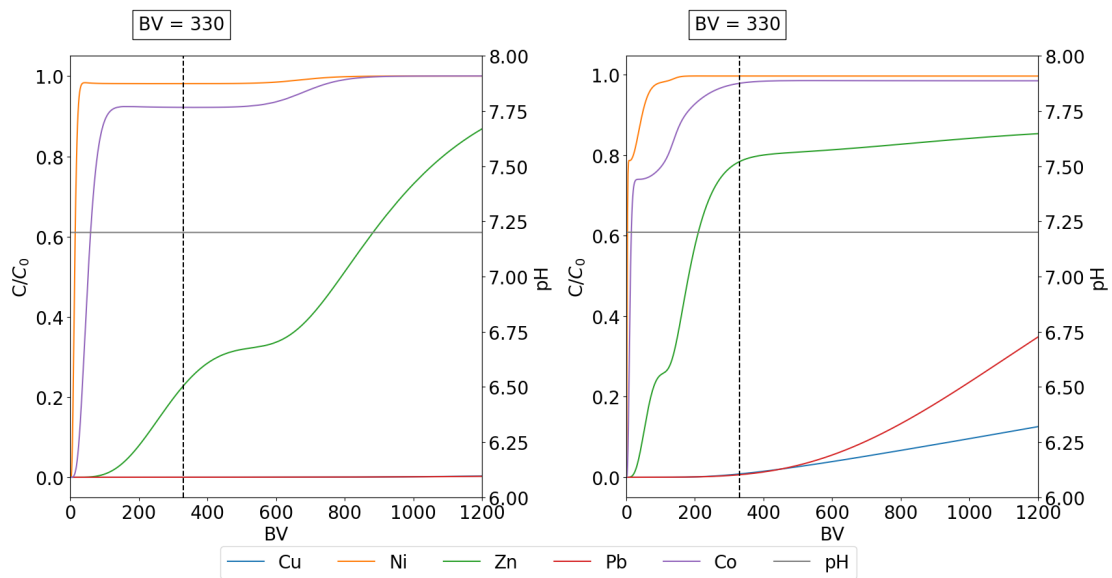
Figure 40: A breakthrough curve of the metals in the biofilter under plug flow conditions (left) and under short-circuiting conditions, assuming 80% of the inlet water flows through 20% of the biofilter. The last 20% flows through the other 80% (right)

Sensitivity Analysis

In order to see how sensitive the model is with regards to several parameters, a sensitivity analysis was carried out. Figure 41 shows the results of these variations on the breakthrough curve for zinc. A variation in the concentration of Zn itself hardly influences the moment when breakthrough occurs. Variations in pH, PO_4^{3-} and alkalinity however, influence the breakthrough curve to a rather large extend. It is known from literature that pH is one of the most important parameters influencing metal adsorption [119]. Figure 41 shows that breakthrough occurs much faster at lower pH, as is expected for positively charged metals such as Zn. The influence of alkalinity is also expected, as at higher alkalinity, more CO_3^- can occupy inner-sphere sorption sites. Less expected, but also of large influence on the breakthrough of Zn, is the concentration of PO_4^{3-}. In contrast with experimental observations, lower PO_4^{3-} concentrations correspond with faster breakthrough in the model. As PO_4^{3-} and most HMs have opposite charges, their interaction can be complex. Phosphate can decrease the adsorption of HMs by occupying inner-sphere sorption sites and by formation of complexes in solution, that can also lower the free ion activity of the metal ion. Nevertheless, phosphate could also increase HM sorption by forming complexes that have a higher affinity to the filter material than the HM itself. In addition to this, adsorption of PO_4^{3-} can increase surface negative charges [88]. Not all of these effects may be incorporated in the PHREEQC database and more research is needed to investigate exactly how phosphate influences the surface charge and interacts with heavy metals.

Figure 41: Breakthrough curves of Zn under varying concentrations of Zn, pH, PO4 and alkalinity

4.7 Design & Operational Implications and Optimisation

4.7.1 Implications

Hydraulic Conductivity & Short Circuiting
During this research it was found that the hydraulic conductivity at Spangen was very high, resulting in low hydraulic re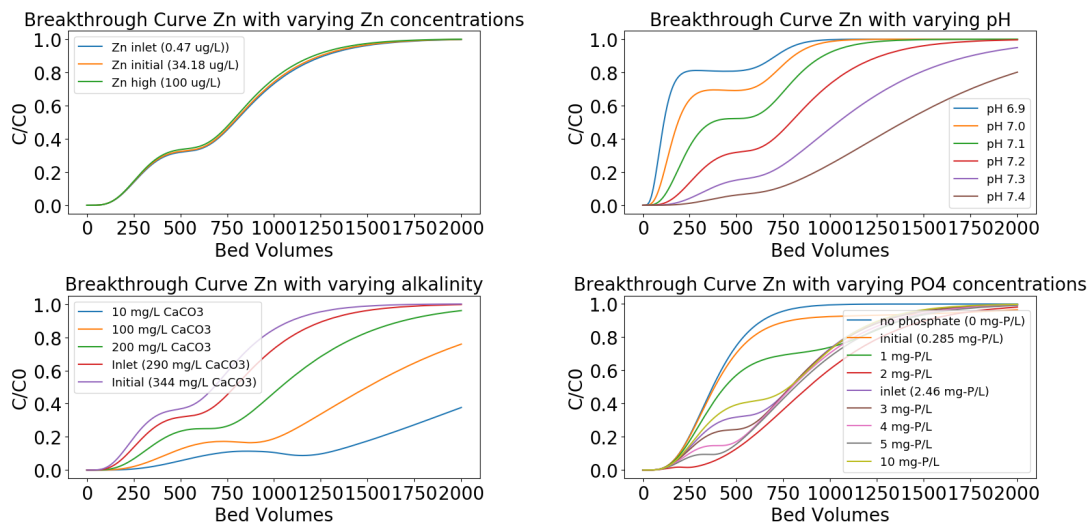tention times in the system. In addition to this, the construction of the outlet in very close proximity to the inlet results in short-circuiting and preferential flow, reducing the hydraulic retention time even further. Although both surface complexation and ion exchange are rapid processes that occur at microsecond timescale [121], longer contact times with the medium are needed for metals to be able to diffuse into the pores of lesser accessible adsorption sites [127]. In addition to this, metals accumulate more in the preferential paths [45], resulting in earlier breakthrough. Preferential flow and short-circuiting is even further promoted by heterogeneous distribution of water onto the filter and the lack of a ponding zone.

Irrigation with Aquifer Water
From the system analysis, it was concluded that water from the aquifer is used to irrigate the biofilter three times a day, replacing the stormwater initially present in the submerged zone. This has a large effect on metal retention and accumulation.

First of all, recirculating water from the aquifer also recirculates metals, adding more metals to the biofilter, leading to faster accumulation and breakthrough and thus a shorter biofilter lifetime. Secondly, the water in the aquifer has a different quality then stormwater. When the water initially present in the aquifer is replaced with stormwater, which contains lower concentrations of certain metals, desorption is facilitated by a decrease in the free metal activity in solution [88, 128, 129]. Lastly, the irrigation water from the aquifer does not only bring additional metals, but also salts, leading to salinisation in the biofilter. High salt concentrations may lead to higher dissolved fractions for several metals, resulting in poorer removal [35, 38]. Although observations were limited to what happens when aquifer water is replaced by stormwater, the reverse is expected when stormwater is replaced by aquifer water. That means that the heavy metals that desorbed during stormwater events, will sorb during irrigation rounds, whereas metals that sorbed during a stormwater event are expected to desorb during irrigation. This prediction corresponds with the conceptual PHREEQC model.

pH and Dissolved Oxygen
The pH in both the buffer and the biofilter is relatively constant around neutral for all events. Although pH is one of the most important parameters influencing metal adsorption [119], the small fluctuations are not expected to have a large influence on the results of this research.

Suboxic conditions prevailed in the buffer tank, whereas dissolved oxygen concentrations in the biofilter varied. The highest measured concentrations in the biofilter ranged between 2 and 5 mg/L in the events, but the oxygen concentrations reduced to 0 mg/L once the water

in the aquifer was replaced by water from the buffer. No clear effect as the result of this has been observed, but it is expected that previously sorbed metals will remobilise if reducing conditions in the biofilter persist long enough to reduce iron oxides [94, 20]. On the contrary, high initial values of NO_3^- and Ni could indicate that oxidation of NH_4^+ and metal sulphides in the aquifer contributes to release of these pollutants in the aquifer.

4.7.2 System Optimisation

In order to address some problems that were mentioned in the previous section, improvements in both design and operation are suggested.

Hydraulic Conductivity
The current filter media consist of medium-coarse sand with grain size between 0.4 - 0.8 mm. A well-graded sand with an appropriate particle size distribution is recommended for biofiltration systems. The medium should be sand-based, but should contain all particle size ranges from 0.05 mm to 3.4 mm, in different fractions [24]. Lowering the hydraulic conductivity in the filter can be done by incorporating smaller soil particles. The addition of clay and silt particles has the additional benefit of creating a larger specific surface area for adsorption of dissolved pollutants [24]. Alternatively, the flow could be regulated like in sand filters, for example by regulating the pressure with a pressure compensated flow control valve or an adjustable raised outlet.

Preferential Flow and Short-Circuiting
Maximising the distance between inlet and outlet is going to contribute reduce short-circuiting and improve hydraulic efficiency [24, 130, 131]. Additionally, designing the inlet to distribute water more evenly over the biofilter surface will also help to prevent short-circuiting, while ensuring that the full volume of the biofilter is used. This can be achieved by allowing the water to pond on the biofilter surface, simultaneously enabling more contact between the inlet water and IOCS, which will also have a positive effect on metal removal [55, 132, 133].

Other ways to improve homogeneous distribution of inlet water is to introduce evenly spaced perforated pipes or trenches [134], or using rotary or fixed nozzle distribution systems such as is one in trickling filters [135, 129]

Recirculation of Aquifer Water
Irrigating the biofilter with aquifer water is not recommended. In order to overcome a foul smell, water standing in the biofilter for too long, or the biofilter drying out, the biofilter could be irrigated more frequently, with small water volumes from the buffer. Doing this will also contribute to shorter retention times in the buffer and may have an effect on the oxygen conditions in the buffer.

Monitoring Water Quality and Treatment Performance
Evaluation of the water quality and treatment performance of the biofilter needs to be improved. Outlet samples taken at the start of the run can give insight into the treatment performance when the system is not running. To compare inlet water quality to outlet qual-

ity during a run, the system should be running. An inlet sample can be taken at the start of the run, but all initial standing water needs to be allowed to flush out before sampling at the outlet.

4.7.3 Limitations

During the study, some limitations were encountered. These limitations and their effects are discussed in this chapter.

To begin with, the system hydraulics and operation were not as expected, making it difficult to test the actual removal performance. Water from different sources was added to the filter. In combination with preferential flow and short-circuit paths in the filter, this resulted in mixed water samples at the outlet. This was overcome by predicting the mixing only concentrations using EC as a tracer. Nevertheless, these estimations have an impact on the accuracy of the results. Estimations based on Cl^- would be more accurate, but a lack of datapoints made EC a more useful tracer. An important note is that the composition of water in the aquifer was unknown. Although pH and dissolved oxygen were monitored in this research, their effect on metal removal in this system remained unclear and may have been overshadowed by the effect of unexpected hydraulic conditions and recirculation of aquifer water.

In addition to this, the DOC analysis failed unfortunately (see Section 3.1.3 for details), so that the effect of this parameter could not be analysed.

Furthermore, the in-situ hydraulic conductivity measurement should ideally have been carried out one month after the start of operation and again two years after operation, in order to see how the hydraulic conductivity is affected by pollutant retention. This was not possible, as the system had already been in operation for almost two years when the research started. Repeating the experiment in the future may still give an insight in the changes over time. Additional limitations of the test are the possibility of soil compaction when the ring was driven into the ground, or preferential flow along the sides of the ring [136]. In addition to this, the high hydraulic conductivity of the filter in combination with manual timing and pouring of the water impacted the accuracy of the measurement. The measurement was only carried out once for each measuring point, because of time constraints. A ring infiltration test only measures the hydraulic conductivity in the top layer of the filter. A deep ring test needs to be carried out to get more insight into the hydraulic conductivity in deeper layers of the filter.

Moreover, collected data belong to five events in spring and summer. The collected data is thus limited in terms of quantity and effects of certain environmental conditions that can change with the season.

Environmental factors, but also the operations of this biofilter make the results site-specific. Nevertheless, the effect of large changes in inlet water quality on metal retention and the effect of short-circuiting on metal breakthrough are also applicable to other biofiltration

systems.

Lastly, the PHREEQC model was simplified by using a fixed pH and homogeneous redox conditions. In reality, these conditions are more complex, so the model can only predict breakthrough to a certain extent.

5 Conclusions & Recommendations

5.1 Conclusions

This research aimed to investigate the performance of the Bluebloqs biofilter in Spangen with a main focus on heavy metal removal.

The first research question evaluated the removal of heavy metals in the biofilter. Analysis of the chemical water quality and treatment performance has shown that mean heavy metal and nutrient concentrations in the outlet of the biofilter do not exceed infiltration regulations. In case of Cu and Co, maximum concentrations do exceed infiltration regulations. Fe continuously exceeds the operational limit, with the risk of well clogging. Although infiltration regulations are generally met, this does not mean that the biofilter performs optimally. Moreover, mean heavy metal and nutrient concentrations in the stormwater already complied with regulations before treatment, with the exception of SO_4^{2-} and PO_4^{3-}.

For Ni, Cu, As, & Co total and dissolved concentrations were higher after treatment than before. In case of Zn, the total concentration decreased after treatment, but the dissolved concentration increased. The increased concentrations are partially explained by irrigation of the biofilter with water from the aquifer. This water contained higher concentrations of these metals, that were directly added to the system, resulting in mixed outlet samples consisting of stormwater and aquifer water. Using mixing fractions to account for the effect of mixing, showed that for all metals mentioned in this paragraph, desorption occured. The remobilisation of these heavy metals is likely a result of a decrease in the metal concentration in the solution phase when stormwater from the buffer was introduced. This leads to lower free metal activity and desorption of surface-bound material. Additionally, high PO_4^{3-}, Fe & Mn concentrations were found in the stormwater. These pollutants were removed well and are expected to inhibit sorption sites available for heavy metals. Additionally, the high salinity of the aquifer water may contribute to a higher dissolved metal fraction. The observed desorption of Ni, Cu, As, Co & Zn and adsorption of Fe, Mn & PO_4^{3-} are confirmed by a conceptual model in PHREEQC. Based on these results it can be concluded that the extent to which heavy metals are removed in the biofilter is not sufficient.

The second research question aimed to identify factors in the design and operation of the system that negatively impact heavy metal removal. The biofilter at Spangen was found to be designed and operated in a way that lead to preferential flows and short hydraulic retention times. Factors that contributed to this were the construction of the outlet near the inlet, the high hydraulic conductivity of the filter and the heterogeneous distribution of water over the filter surface. As a result of this, only a small volume of the filter is effectively used to treat the majority of the water. More accumulation of metal takes place in these preferential paths, leading to faster breakthrough. This is supported by a hydraulic conductivity that is a factor ten higher in the inlet corner, compared to the middle of the biofilter.

The third research question explored how the system could be optimised. To answer this

question, solutions for the factors mentioned above were evaluated. A design that maximises the space between inlet and outlet of the system is recommended. In addition, the inlet should be designed in such a way that water is distributed evenly over the entire filter. Ideally water is left to pond on the filter, before infiltrating into the filter media, but other solutions can include evenly spaced perforated pipes or trenches or a rotary distribution system. A lower hydraullic conductivity can be achieved by incorporating smaller particles in the filter media or regulating the pressure with an adjustable raised outlet or a pressure compensated flow control valve. Finally irrigation with aquifer water is advised against.

5.2 Recommendations

The sensitivity analysis of the breakthrough curve shows a positive effect of phosphate on zinc retention. This does not agree with experimental data suggesting a negative impact of phosphate on heavy metal removal. This may be related to the way surface charge is calculated in PHREEQC. Future research could investigate this using a batch experiment and a model.

Furthermore, the removal process for sulphate remained unclear. Further research to investigate the presence of sulphate-related microbes and the spatial distribution of oxygen in the biofilter is needed to draw conclusions about the removal of sulphate in the biofilter.

Another parameter that would be interesting to measure in order to build on the conclusions from this research is the concentration of total and dissolved organic matter. Metal-OM complexes can have an effect on the retention and possible leaching of metals, especially for Cu [137]

Hatt et all (2011) recommended adding materials with a high CEC to delay breakthrough of metals [47]. This effect was not seen in the PHREEQC model, but would be good to confirm with experimental data.

Previous studies suggested that accumulation of metals in the filter media may exceed health and environmental guidelines, before breakthrough of metals occurs [45, 47]. A risk assessment of this accumulation to public health and surrounding ecosystems is thus recommended.

Several lab and column studies [38, 44, 138] suggested that lower temperatures and snowmelt can have a negative effect on performance of biofilters. Monitoring the system not only in spring and summer, but year round, can give more information on field-scale.

Bibliography

[1] K.G. Zuurbier and T.C.G.W. van Dooren. Urban Waterbuffer. Technical Report December, KWR, 2019.

[2] Koen Zuurbier, Bert De Doelder, Wilrik Kok, Boris Van Breukelen, Allied Waters, and Field Factors. Preventing pluvial flooding and water shortages by integrating local aquifer storage and recovery in urban areas. *ISMAR10 Symposium*, pages 1–9, 2019.

[3] T M Jonker. Fate of Escherichia coli , Enterococci and Campylobacter in the Bluebloqs Biofilter. 2020.

[4] KNMI. Netherlands Seismic and Acoustic Network. Royal Netherlands Meteorological Institute (KNMI), Other/Seismic Network, 1993. 10.21944/e970fd34-23b9-3411-b366-e4f72877d2c5.

[5] Delft University of Technology. Lecture notes in soil mechanics, 2019 - 2020.

[6] Floris Boogaard, Frans van de Ven, Jeroen Langeveld, and Nick van de Giesen. Stormwater Quality Characteristics in (Dutch) Urban Areas and Performance of Settlement Basins. *Challenges*, 5(1):112–122, 2014.

[7] T. van Mosseveld, P.M.N. Schipper, and F.C. Boogaard. KWALITEITSASPECTEN INFILTREREN STEDELIJK WATER BETER BEKEKEN. Technical report, STOWA, Utrecht, 2005.

[8] LS Clesceri, AE Greenberg, and AD Eaton. Standard methods for the examination of water and wastewater apha. *AWWA, WEF, Monrovia, USA*, 1998.

[9] Ministerie van Infrastructuur en Waterstaat. Infiltratiebesluit bodembescherming, 2009.
https://wetten.overheid.nl/BWBR0005957/2009-12-22.

[10] Sara Hughes, Eric K Chu, and Susan G Mason. Climate change in cities. *Innovations in Multi-Level Governance. Cham: Springer International Publishing (The Urban Book Series)*, 2018.

[11] Robert I McDonald, Katherine Weber, Julie Padowski, Martina Flörke, Christof Schneider, Pamela A Green, Thomas Gleeson, Stephanie Eckman, Bernhard Lehner, Deborah Balk, et al. Water on an urban planet: Urbanization and the reach of urban water infrastructure. *Global Environmental Change*, 27:96–105, 2014.

[12] Fabio Recanatesi, Andrea Petroselli, Maria Nicolina Ripa, and Antonio Leone. Assessment of stormwater runoff management practices and bmps under soil sealing: a study case in a peri-urban watershed of the metropolitan area of rome (italy). *Journal of environmental management*, 201:6–18, 2017.

[13] Gilles Erkens, Tom Bucx, Rien Dam, Ger De Lange, and John Lambert. Sinking coastal cities. *Proceedings of the International Association of Hydrological Sciences*, 372:189, 2015.

[14] Adrian D Werner, Mark Bakker, Vincent EA Post, Alexander Vandenbohede, Chunhui Lu, Behzad Ataie-Ashtiani, Craig T Simmons, and David Andrew Barry. Seawater intrusion processes, investigation and management: recent advances and future challenges. *Advances in water resources*, 51:3–26, 2013.

[15] PJ Dillon, Paul Pavelic, Declan Page, Helen Beringen, and John Ward. Managed aquifer recharge. *An introduction waterlines report series*, 13, 2009.

[16] Elise Bekele, Declan Page, Joanne Vanderzalm, Anna Kaksonen, and Dennis Gonzalez. Water recycling via aquifers for sustainable urban water quality management: Current status, challenges and opportunities. *Water*, 10(4):457, 2018.

[17] Declan Page, Elise Bekele, Joanne Vanderzalm, and Jatinder Sidhu. Managed aquifer recharge (mar) in sustainable urban water management. *Water*, 10(3):239, 2018.

[18] Laila C Søberg, Ryan Winston, Maria Viklander, and Godecke-Tobias Blecken. Dissolved metal adsorption capacities and fractionation in filter materials for use in stormwater bioretention facilities. *Water research X*, 4:100032, 2019.

[19] Hülya Genç-Fuhrman, Peter S Mikkelsen, and Anna Ledin. Simultaneous removal of as, cd, cr, cu, ni and zn from stormwater: Experimental comparison of 11 different sorbents. *Water research*, 41(3):591–602, 2007.

[20] Heike B. Bradl. Adsorption of heavy metal ions on soils and soils constituents. *Journal of Colloid and Interface Science*, 277(1):1–18, 2004.

[21] Hülya Genç-Fuhrman, Peter S. Mikkelsen, and Anna Ledin. Simultaneous removal of As, Cd, Cr, Cu, Ni and Zn from stormwater: Experimental comparison of 11 different sorbents. *Water Research*, 41(3):591–602, 2007.

[22] Peter Dillon. Future management of aquifer recharge. *Hydrogeology journal*, 13(1):313–316, 2005.

[23] Laila C. Søberg, Maria Viklander, and Godecke Tobias Blecken. The influence of temperature and salt on metal and sediment removal in stormwater biofilters. *Water Science and Technology*, 69(11):2295–2304, 2014.

[24] Emily Payne, Belinda Hatt, Ana Deletic, Meredith Dobbie, David McCarthy, and Gayani Charasena. *Adoption Guidelines for Stormwater Biofiltration Systems Cities as Water Supply Catchments*. 2015.

[25] TKI Urban Water Buffer. Urban waterbuffer, April 2020.

[26] K Bratieres, T D Fletcher, A Deletic, L Alcazar, and S Le Coustumer. Removal of nutrients , heavy metals and pathogens by stormwater biofilters. *11th International Conference on Urban Drainage, Edinburgh*, (January):1–10, 2008.

[27] Xueli Sun and Allen P. Davis. Heavy metal fates in laboratory bioretention systems. *Chemosphere*, 66(9):1601–1609, 2007.

[28] Allen P. Davis, Mohammad Shokouhian, Himanshu Sharma, and Christie Minami. Laboratory Study of Biological Retention for Urban Stormwater Management. *Water Environment Research*, 73(1):5–14, 2001.

[29] Allen P. Davis, Mohammad Shokouhian, Himanshu Sharma, Christie Minami, and Derek Winogradoff. Water Quality Improvement through Bioretention: Lead, Copper, and Zinc Removal. *Water Environment Research*, 75(1):73–82, 2003.

[30] Jianlong Wang, Yuanling Zhao, Liqiong Yang, Nannan Tu, Guangpeng Xi, and Xing Fang. Removal of heavy metals from urban stormwater runoff using bioretention media mix. *Water (Switzerland)*, 9(11), 2017.

[31] Belinda E. Hatt, Tim D. Fletcher, and Ana Deletic. Hydraulic and pollutant removal performance of fine media stormwater filtration systems. *Environmental Science and Technology*, 42(7):2535–2541, 2008.

[32] Belinda E. Hatt, Tim D. Fletcher, and Ana Deletic. Hydrologic and pollutant removal performance of stormwater biofiltration systems at the field scale. *Journal of Hydrology*, 365(3-4):310–321, 2009.

[33] Vladimir Novotny. *Water quality: diffuse pollution and watershed management*. John Wiley & Sons, 2002.

[34] Christopher M. Dean, John J. Sansalone, Frank K. Cartledge, and John H. Pardue. Influence of Hydrology on Rainfall-Runoff Metal Element Speciation. *Journal of Environmental Engineering*, 131(4):632–642, 2005.

[35] Katharina Lange, Heléne Österlund, Maria Viklander, and Godecke Tobias Blecken. Metal speciation in stormwater bioretention: Removal of particulate, colloidal and truly dissolved metals. *Science of the Total Environment*, 724, 2020.

[36] Tone M. Muthanna, Maria Viklander, Nina Gjesdahl, and Sveinn T. Thorolfsson. Heavy metal removal in cold climate bioretention. *Water, Air, and Soil Pollution*, 183(1-4):391–402, 2007.

[37] Laila C. Søberg, Maria Viklander, and Godecke Tobias Blecken. Do salt and low temperature impair metal treatment in stormwater bioretention cells with or without a submerged zone? *Science of the Total Environment*, 579:1588–1599, 2017.

[38] Hannah Kratky, Zhan Li, Yijun Chen, Chengjin Wang, Xiangfei Li, and Tong Yu. A critical literature review of bioretention research for stormwater management in cold climate and future research recommendations. *Frontiers of Environmental Science and Engineering*, 11(4):1–15, 2017.

[39] Marla Maniquiz-Redillas and Lee Hyung Kim. Fractionation of heavy metals in runoff and discharge of a stormwater management system and its implications for treatment. *Journal of Environmental Sciences (China)*, 26(6):1214–1222, 2014.

[40] Laila C. Søberg, Maria Viklander, and Godecke Tobias Blecken. Do salt and low temperature impair metal treatment in stormwater bioretention cells with or without a submerged zone? *Science of the Total Environment*, 579:1588–1599, 2017.

[41] Sam A. Trowsdale and Robyn Simcock. Urban stormwater treatment using bioretention. *Journal of Hydrology*, 397(3-4):167–174, 2011.

[42] Belinda E. Hatt, Ana Deletic, and Tim D. Fletcher. Stormwater reuse: Designing biofiltration systems for reliable treatment. *Water Science and Technology*, 55(4):201–209, 2007.

[43] Godecke Tobias Blecken, Yaron Zinger, Ana Deletić, Tim D. Fletcher, and Maria Viklander. Influence of intermittent wetting and drying conditions on heavy metal removal by stormwater biofilters. *Water Research*, 43(18):4590–4598, 2009.

[44] Tone Merete Muthanna, Maria Viklander, Godecke Blecken, and Sveinn T. Thorolfsson. Snowmelt pollutant removal in bioretention areas. *Water Research*, 41(18):4061–4072, 2007.

[45] Björn Kluge, Arvid Markert, Michael Facklam, Harald Sommer, Mathias Kaiser, Matthias Pallasch, and Gerd Wessolek. Metal accumulation and hydraulic performance of bioretention systems after long-term operation. *Journal of Soils and Sediments*, 18(2):431–441, 2018.

[46] Wenjun Feng, Belinda E. Hatt, David T. McCarthy, Tim D. Fletcher, and Ana Deletic. Biofilters for stormwater harvesting: Understanding the treatment performance of key metals that pose a risk for water use. *Environmental Science and Technology*, 46(9):5100–5108, 2012.

[47] B. E. Hatt, A. Steinel, A. Deletic, and T. D. Fletcher. Retention of heavy metals by stormwater filtration systems: Breakthrough analysis. *Water Science and Technology*, 64(9):1913–1919, 2011.

[48] Laila C. Søberg, Ryan Winston, Maria Viklander, and Godecke Tobias Blecken. Dissolved metal adsorption capacities and fractionation in filter materials for use in stormwater bioretention facilities. *Water Research X*, 4:100032, 2019.

[49] Terry Lucke, Carsten Dierkes, and Floris Boogaard. Investigation into the long-term stormwater pollution removal efficiency of bioretention systems. *Water Science and Technology*, 76(8):2133–2139, 2017.

[50] Pim Versteeg. *Assessing adsorption of heavy metals from urban stormwater runoff in the Bluebloqs biofiltration system*. PhD thesis, 2020.

[51] Bevolkng (gebied/buurt).

[52] Fränkische. Rigofill st. Product Brochure.

[53] Fränkische. Sedipoint sedimentation shaft. Product Brochure.

[54] K.G. (KWR) Zuurbier and T.C.G.W. (KWR) van Dooren. Rapport_Impact_Waterkwaliteit_Urban Waterbuffer. Technical Report December, 2019.

[55] C. H. Lai and C. Y. Chen. Removal of metal ions and humic acid from water by iron-coated filter media. *Chemosphere*, 44(5):1177–1184, 2001.

[56] Cristina Saladrich Català. *Field Factors ANALYSIS OF BLUEBLOQS BIOFILTER BB1 . 0*. PhD thesis, 2019.

[57] KWR Water Research Institute. Overzicht_data.xlsx, 2020.

[58] Merve Zeyrek, Kadriye Ertekin, Sibel Kacmaz, Cemil Seyis, and Sedat Inan. An ion chromatography method for the determination of major anions in geothermal water samples. *Geostandards and Geoanalytical Research*, 34(1):67–77, 2010.

[59] Lenntech Water treatment & purification. Water analysis accuracy tester.

[60] Brian A Pellerin, Wilfred M Wollheim, Xiahong Feng, and Charles J Vörösmarty. The application of electrical conductivity as a tracer for hydrograph separation in urban catchments. *Hydrological Processes: An International Journal*, 22(12):1810–1818, 2008.

[61] C. A.J. Appelo and D. Postma. Geochemistry, groundwater and pollution. *Geochemistry, groundwater and pollution*, 2005.

[62] Karina Cano-Paoli, Gabriele Chiogna, and Alberto Bellin. Convenient use of electrical conductivity measurements to investigate hydrological processes in alpine headwaters. *Science of the Total Environment*, 685:37–49, 2019.

[63] Micòl Mastrocicco, Henning Prommer, Luisa Pasti, Stefano Palpacelli, and Nicolò Colombani. Evaluation of saline tracer performance during electrical conductivity groundwater monitoring. *Journal of contaminant hydrology*, 123(3-4):157–166, 2011.

[64] Sébastien Le Coustumer, Tim D. Fletcher, Ana Deletic, Sylvie Barraud, and Justin F. Lewis. Hydraulic performance of biofilter systems for stormwater management: Influences of design and operation. *Journal of Hydrology*, 376(1-2):16–23, 2009.

[65] Sébastien Le Coustumer, Tim D Fletcher, Ana Deletic, and Matthew Potter. Hydraulic performance of biofilter systems for stormwater management : lessons from a field study. *Evolution*, 2008.

[66] Belinda Hatt and Sebastien Le Coustumer. In Situ Measurement of Hydraulic Conductivity. (April):1–7, 2008.

[67] David L Parkhurst and C. A.J. Appelo. Introduction.

[68] David L Parkhurst and CAJ Appelo. Description of input and examples for phreeqc version 3: a computer program for speciation, batch-reaction, one-dimensional transport, and inverse geochemical calculations. Technical report, US Geological Survey, 2013.

[69] David A Dzombak and Francois MM Morel. *Surface complexation modeling: hydrous ferric oxide*. John Wiley & Sons, 1990.

[70] D Kirk Nordstrom and Donald G Archer. Critical evaluation of the thermodynamic properties and geochemical relationships for selected arsenic species. *GSA Abstracts with Programs, Paper*, (131-5), 2002.

[71] Donald L. Sparks. Ion exchange processes. In *Ion Exchangers*, pages 187–205. 2003.

[72] C Anthony J Appelo and Dieke Postma. *Geochemistry, groundwater and pollution*. CRC press, 2004.

[73] NSW Government. Cation exchange capacity, Sep 1993.

[74] James A Davis, Robert O James, and James O Leckie. Surface ionization and complexation at the oxide/water interface: I. computation of electrical double layer properties in simple electrolytes. *Journal of colloid and interface science*, 63(3):480–499, 1978.

[75] Het Water Laboratorium. VWA Raport. Technical report, Het Water Laboratorium, 2021.

[76] Roberta Hofman-Caris, Cheryl Bertelkamp, Luuk de Waal, Tessa van den Brand, Jan Hofman, René van der Aa, and Jan Peter van der Hoek. Rainwater harvesting for drinking water production: a sustainable and cost-effective solution in the netherlands? *Water*, 11(3):511, 2019.

[77] Wolfgang Gernjak, J Lampard, and Janet Tang. Characterisation of chemical hazards in stormwater. *Cities as Water Supply Catchments–Risk and Health: Understanding Stormwater Quality Hazards. Co-operative Research Centre for Water Sensitive Cities, Technical Report C*, 1:2–1, 2017.

[78] Jason R Masoner, Dana W Kolpin, Isabelle M Cozzarelli, Larry B Barber, David S Burden, William T Foreman, Kenneth J Forshay, Edward T Furlong, Justin F Groves, Michelle L Hladik, et al. Urban stormwater: An overlooked pathway of extensive mixed contaminants to surface and groundwaters in the united states. *Environmental science & technology*, 53(17):10070–10081, 2019.

[79] EPA. Preliminary data summary of urban storm waterbest management practices, 1999. data retrieved from EPA, `https://www3.epa.gov/npdes/pubs/usw_b.pdf`.

[80] T Datry, Florian Malard, and Janine Gibert. Dynamics of solutes and dissolved oxygen in shallow urban groundwater below a stormwater infiltration basin. *Science of the Total Environment*, 329(1-3):215–229, 2004.

[81] Wilko Verweij, J Van der Wiele, I Van Moorselaar, and E Van der Grinten. Impact of climate change on water quality in the netherlands. *RIVM rapport 607800007*, 2010.

[82] Jason Berberich, Tao Li, and Endalkachew Sahle-Demessie. Biosensors for monitoring water pollutants: A case study with arsenic in groundwater. In *Separation Science and Technology*, volume 11, pages 285–328. Elsevier, 2019.

[83] M.P.C.P. Paulissen, R C Nijboer, and P.F.M. Verdonschot. Grondwater in perspectief. page 71, 2007.

[84] Joseph S Smith, Ryan J Winston, R Andrew Tirpak, David M Wituszynski, Kathryn M Boening, and Jay F Martin. The seasonality of nutrients and sediment in residential stormwater runoff: Implications for nutrient-sensitive waters. *Journal of Environmental Management*, 276:111248, 2020.

[85] Yun-Ya Yang and Mary G Lusk. Nutrients in urban stormwater runoff: Current state of the science and potential mitigation options. *Current Pollution Reports*, 4(2):112–127, 2018.

[86] Alexandra Müller, Heléne Österlund, Jiri Marsalek, and Maria Viklander. The pollution conveyed by urban runoff: a review of sources. *Science of the Total Environment*, 709:136125, 2020.

[87] Emily G.I. Payne, Tim D. Fletcher, Perran L.M. Cook, Ana Deletic, and Belinda E. Hatt. Processes and drivers of nitrogen removal in stormwater biofiltration. *Critical Reviews in Environmental Science and Technology*, 44(7):796–846, 2014.

[88] Antonio G. Caporale and Antonio Violante. Chemical Processes Affecting the Mobility of Heavy Metals and Metalloids in Soil Environments. *Current Pollution Reports*, 2(1):15–27, 2016.

[89] M. McBride, S. Sauvé, and W. Hendershot. Solubility control of Cu, Zn, Cd and Pb in contaminated soils. *European Journal of Soil Science*, 48(2):337–346, 1997.

[90] R Rangsivek and MR Jekel. Removal of dissolved metals by zero-valent iron (zvi): Kinetics, equilibria, processes and implications for stormwater runoff treatment. *Water Research*, 39(17):4153–4163, 2005.

[91] D. Rai, L.E. Eary, and J.M. Zachara. Environmental chemistry of chromium. *The Science of the Total Environment*, 86(1):155–23, 1989.

[92] Gretchen K. Bielmyer, Carri Decarlo, Cameron Morris, and Thomas Carrigan. The influence of salinity on acute nickel toxicity to the two euryhaline fish species, Fundulus heteroclitus and Kryptolebias marmoratus. *Environmental Toxicology and Chemistry*, 32(6):1354–1359, 2013.

[93] Roberta Hofman-Caris, Cheryl Bertelkamp, Luuk de Waal, Tessa van den Brand, Jan Hofman, René van der Aa, and Jan Peter van der Hoek. Rainwater harvesting for drinkingwater production: A sustainable and cost-effective solution in The Netherlands? *Water (Switzerland)*, 11(3), 2019.

[94] M. C. Chuan, G. Y. Shu, and J. C. Liu. Solubility of heavy metals in a contaminated soil: Effects of redox potential and pH. *Water, Air, and Soil Pollution*, 90(3-4):543–556, 1996.

[95] James I Drever et al. *The geochemistry of natural waters*, volume 437. Prentice hall Englewood Cliffs, 1988.

[96] Regina M Capuano and Cole R Jones. Cation exchange in groundwater-chemical evolution and prediction of paleo-groundwater flow: A natural-system study. *Water Resources Research*, 56(8):e2019WR026318, 2020.

[97] *Adsorptive Removal of Heavy Metals from Groundwater by Iron Oxide based adsorbents*.

[98] Dieter A. Wolf-Gladrow, Richard E. Zeebe, Christine Klaas, Arne Körtzinger, and Andrew G. Dickson. Total alkalinity: The explicit conservative expression and its application to biogeochemical processes. *Marine Chemistry*, 106(1-2 SPEC. ISS.):287–300, 2007.

[99] Jaime Nivala, Scott Wallace, Tom Headley, Kinfe Kassa, Hans Brix, Manfred van Afferden, and Roland Müller. Oxygen transfer and consumption in subsurface flow treatment wetlands. *Ecological Engineering*, 61:544–554, 2013.

[100] Ray Dexter. Redox processes. *IB Chemistry Revision Guide*, pages 106–120, 2019.

[101] Laila C Søberg. Bioretention for stormwater quality treatment: Effects of design features and ambient conditions.

[102] Faiza Rehman, Arshid Pervez, Bahadar Nawab Khattak, and Rafiq Ahmad. Constructed wetlands: perspectives of the oxygen released in the rhizosphere of macrophytes. *CLEAN–Soil, Air, Water*, 45(1), 2017.

[103] Raphael Mainiero and Marian Kazda. Effects of carex rostrata on soil oxygen in relation to soil moisture. *Plant and Soil*, 270(1):311–320, 2005.

[104] Aleksandra Walczyńska and Łukasz Sobczyk. The underestimated role of temperature–oxygen relationship in large-scale studies on size-to-temperature response. *Ecology and Evolution*, 7(18):7434–7441, 2017.

[105] Robert G Wetzel. *Limnology: lake and river ecosystems*. gulf professional publishing, 2001.

[106] U. Skiba. Denitrification. In Sven Erik Jørgensen and Brian D. Fath, editors, *Encyclopedia of Ecology*, pages 866–871. Academic Press, Oxford, 2008.

[107] Juan Wu, Xiaoyan Cao, Jing Zhao, Yanran Dai, Naxin Cui, Zhu Li, and Shuiping Cheng. Performance of biofilter with a saturated zone for urban stormwater runoff pollution control: Influence of vegetation type and saturation time. *Ecological Engineering*, 105(August 2017):355–361, 2017.

[108] Lars Herngren, Ashantha Goonetilleke, and Godwin A. Ayoko. Understanding heavy metal and suspended solids relationships in urban stormwater using simulated rainfall. *Journal of Environmental Management*, 76(2):149–158, 2005.

[109] Xiaolu Chen, Edward Peltier, Belinda S.M. Sturm, and C. Bryan Young. Nitrogen removal and nitrifying and denitrifying bacteria quantification in a stormwater bioretention system. *Water Research*, 47(4):1691–1700, 2013.

[110] Mark M. Benjamin, Ronald S. Sletten, Robert P. Bailey, and Thomas Bennett. Sorption and filtration of metals using iron-oxide-coated sand. *Water Research*, 30(11):2609–2620, 1996.

[111] Jiake Li and Allen P. Davis. A unified look at phosphorus treatment using bioretention. *Water Research*, 90:141–155, 2016.

[112] William C. Lucas and Margaret Greenway. Nutrient Retention in Vegetated and Non-vegetated Bioretention Mesocosms. *Journal of Irrigation and Drainage Engineering*, 134(5):613–623, 2008.

[113] Wei Li, Shuzhen Zhang, Wei Jiang, and Xiao quan Shan. Effect of phosphate on the adsorption of Cu and Cd on natural hematite. *Chemosphere*, 63(8):1235–1241, 2006.

[114] S K Sharma. Adsorptive iron removal from groundwater. *Intemational Institute for Infrastructural, Hydraulic and Environmental Engineering*, Master the:39–41, 2001.

[115] EJ Kamprath, WL Nelson, and JW Fitts. The effect of ph, sulfate and phosphate concentrations on the adsorption of sulfate by soils. *Soil Science Society of America Journal*, 20(4):463–466, 1956.

[116] Massimo Pigna, Alejandra A Jara, ML Mora, and Antonio Violante. Effect of ph, phosphate and/or malate on sulfate sorption on andisols. *Journal of Soil Science and Plant Nutrition*, 7:662–673, 2007.

[117] Vita Marquenie. personal communication.

[118] Bruna Fonseca, Hugo Figueiredo, Joana Rodrigues, A Queiroz, and Teresa Tavares. Mobility of cr, pb, cd, cu and zn in a loamy sand soil: A comparative study. *Geoderma*, 164(3-4):232–237, 2011.

[119] Donald L. Sparks. Sorption Phenomena on Soils. *Environmental Soil Chemistry*, pages 133–186, 2003.

[120] R. Buamah, B. Petrusevski, and J. C. Schippers. Adsorptive removal of manganese(II) from the aqueous phase using iron oxide coated sand. *Journal of Water Supply: Research and Technology - AQUA*, 57(1):1–11, 2008.

[121] Donald L. Sparks. Kinetics of Soil Chemical Processes. *Environmental Soil Chemistry*, pages 207–244, 2003.

[122] Julia Gebert. Lecture notes "soil properties and processes iii: Complexation, redox process", 2020.

[123] James W Ball and D Kirk Nordstrom. User's manual for wateo4f, wtth revised thermodynamic data base and test cases for calculating speciation of major, trace, and redox elements in natural waters. 1991.

[124] Girish Choppala, Nanthi Bolan, Megharaj Mallavarapu, and Zuliang Chen. Sorption and mobility of chromium species in a range of soil types. *19th World Congress of Soil Science, Soil Solutions for a Changing World*, (August):239–242, 2010.

[125] Georg J. Houben, Maria A. Sitnikova, and Vincent E.A. Post. Terrestrial sedimentary pyrites as a potential source of trace metal release to groundwater – A case study from the Emsland, Germany. *Applied Geochemistry*, 76:99–111, 2017.

[126] Ministerie van Infrastructuur en Milieu. Circulaire bodemsanering per 1 juli 2013, Jun 2013.

[127] GW Bruemmer, J Gerth, and KG Tiller. Reaction kinetics of the adsorption and desorption of nickel, zinc and cadmium by goethite. i. adsorption and diffusion of metals. *Journal of Soil Science*, 39(1):37–52, 1988.

[128] Yan Gao, Amy T Kan, and Mason B Tomson. Critical evaluation of desorption phenomena of heavy metals from natural sediments. *Environmental science & technology*, 37(24):5566–5573, 2003.

[129] Leonard Metcalf, Harrison P Eddy, and Georg Tchobanoglous. *Wastewater engineering: treatment, disposal, and reuse*, volume 4. McGraw-Hill New York, 1991.

[130] CQ Guo, B Dong, JJ Liu, and FP Liu. The best indicator of hydraulic short-circuiting and mixing of constructed wetlands. *Water Practice and Technology*, 10(3):505–516, 2015.

[131] JC Agunwamba. Effect of the location of the inlet and outlet structures on short-circuiting: Experimental investigation. *Water environment research*, 78(6):580–589, 2006.

[132] Valentine Uwamariya. Adsorptive removal of heavy metals from groundwater by iron oxide based adsorbents. 2013.

[133] Sutha Khaodhiar, Mohammad F. Azizian, Khemarath Osathaphan, and Peter O. Nelson. Copper, chromium, and arsenic adsorption and equilibrium modeling in an iron-oxide-coated sand, background electrolyte system. *Water, Air, and Soil Pollution*, 119(1-4):105–120, 2000.

[134] Linda Olsson. Effect of design and dosing regime on the treatment performance of vertical flow constructed wetlands, 2011.

[135] Torsten Wik. Trickling filters and biofilm reactor modelling. *Reviews in Environmental Science and Biotechnology*, 2(2):193–212, 2003.

[136] WD Reynolds, BT Bowman, RR Brunke, CF Drury, and CS Tan. Comparison of tension infiltrometer, pressure infiltrometer, and soil core estimates of saturated hydraulic conductivity. *Soil Science Society of America Journal*, 64(2):478–484, 2000.

[137] Kristin Karlsson, Godecke-Tobias Blecken, Björn Öhlander, and Maria Viklander. Environmental Risk Assessment of Sediments Deposited in Stormwater Treatment Facilities: Trace Metal Fractionation and Its Implication for Sediment Management. *Journal of Environmental Engineering*, 142(11):04016057, 2016.

[138] Godecke Tobias Blecken, Jiri Marsalek, and Maria Viklander. Laboratory study of stormwater biofiltration in low temperatures: Total and dissolved metal removals and fates. *Water, Air, and Soil Pollution*, 219(1-4):303–317, 2011.

[139] STOWA/Stichting RIONED. Database kwaliteit afstromend hemelwater, 2020. data retrieved from STOWA, https://www.stowa.nl/sites/default/files/assets/PUBLICATIES/Publicaties\%202020/2020-05\%20STOWA\%202020-05\%20Kwaliteit\%20van\%20afstromend\%20hemelwater\%20in\%20Nederland.pdf.

[140] F Boogaard, Gerdrik Bruins, and Ronald Wentink. *Wadi's: aanbevelingen voor ontwerp, aanleg en beheer: gebaseerd op zes jaar onderzoek van de wadi's in Enschede gecombineerd met overige binnen-en buitenlandse ervaringen*. Stichting Rioned, 2006.

Appendices

A   Regulations

Regulations 22-12-2009

Table 22: Dutch Infiltration Regulations [9]

Substance	unit	threshold (*dissolved*)[1]
MACRO PARAMETERS		
pH	–	–[2]
Suspended Solids	mg/l	$0{,}5^3$
calcium (Ca ++)	mg/l	–[2]
chloride (CI-)	mg/l	$200^{2,3}$
bicarobonate (HCO3-)	mg/l	–[2]
sodium (Na+)	mg/l	$120^{2,3}$
ammonium (NH4+)	mg/l-N	
nitrate (NO3-)	mg/l-N	$5{,}6^{2,3}$
total-phosphate (PO42-tot)	mg/l-P	0,4
sulphate (SO42-)	mg/l	150^2
fluoride (F-)	mg/l	1
cyanides total (CN (tot))	µg/l	10
HEAVY METALS		
arsenic (As)	µg/l	10
barium (Ba)	µg/l	200^3
cadmium (Cd)	µg/l	0,4
cobalt (Co)	µg/l	20
chrome (Cr)	µg/l	2
copper (Cu)	µg/l	15
mercury (Hg)	µg/l	0,05
nickel (Ni)	µg/l	15
lead (Pb)	µg/l	15
zinc (Zn)	µg/l	65

1) The threshold for suspended solids concerns the non-dissolved material.

2) Area of concern for issuing permits related to the local situation.

3) During a period of 70 days per year, these values may exceed the aforementioned values, as long as they do not exceed the following limits: suspended solids 2 mg/l; Cl^- 300 mg/l; Na^+ 180 mg/l; NO_3 2-11,2 mgN/l; Ba 300 µg/l.

B   Water Quality

B.1   physico-chemical parameters
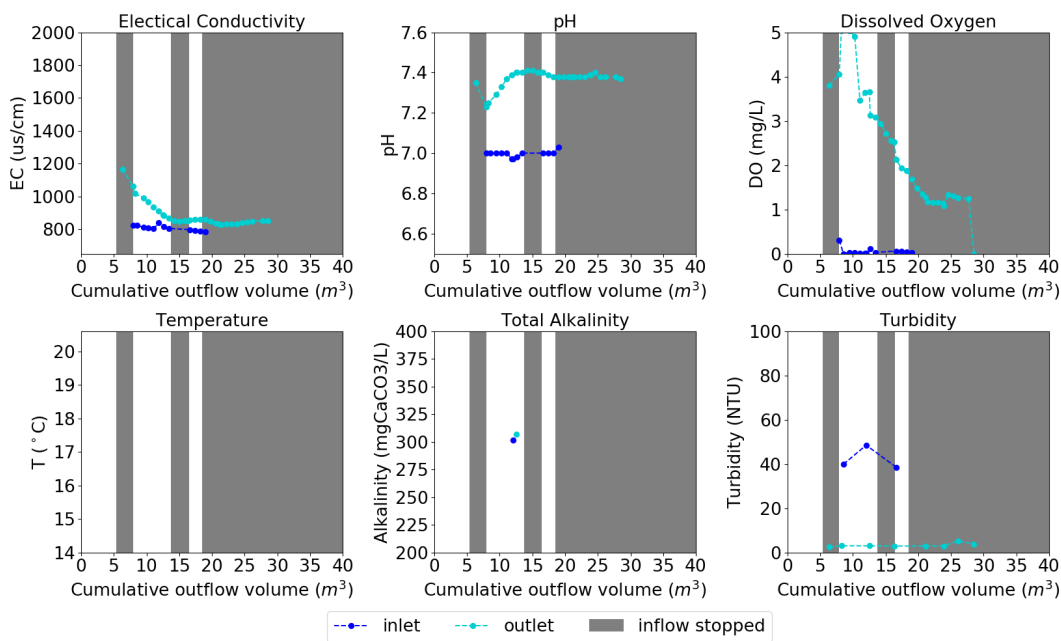
Figure 42: Physico-chemical parameters measured at Bluebloqs biofilter Spartaplein on 09-06-2020
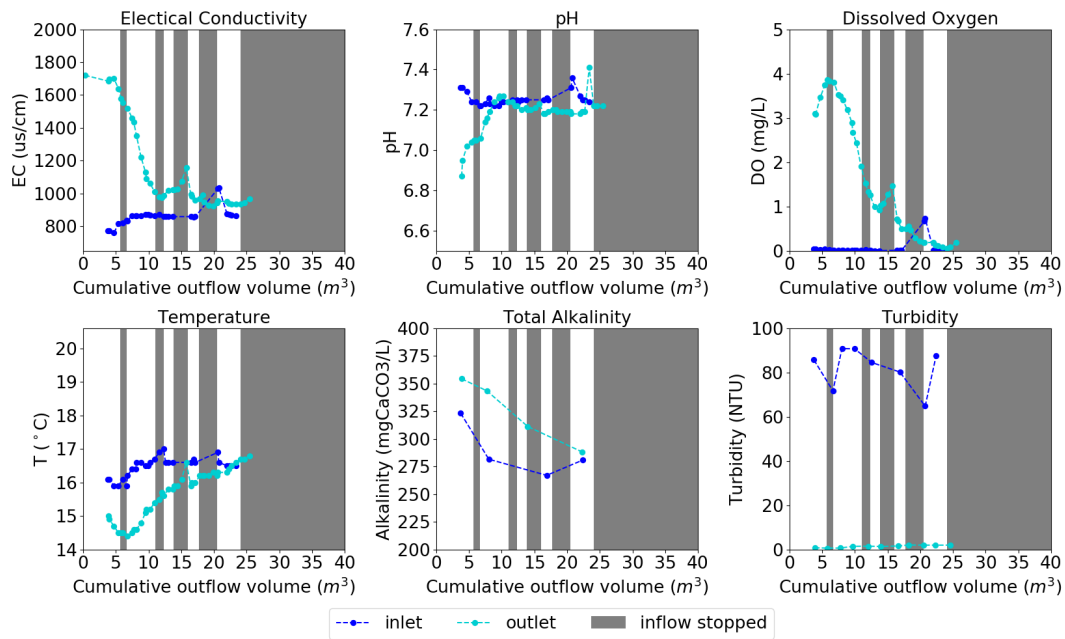
Figure 43: Physico-chemical parameters measured at Bluebloqs biofilter Spartaplein on 15-06-2020
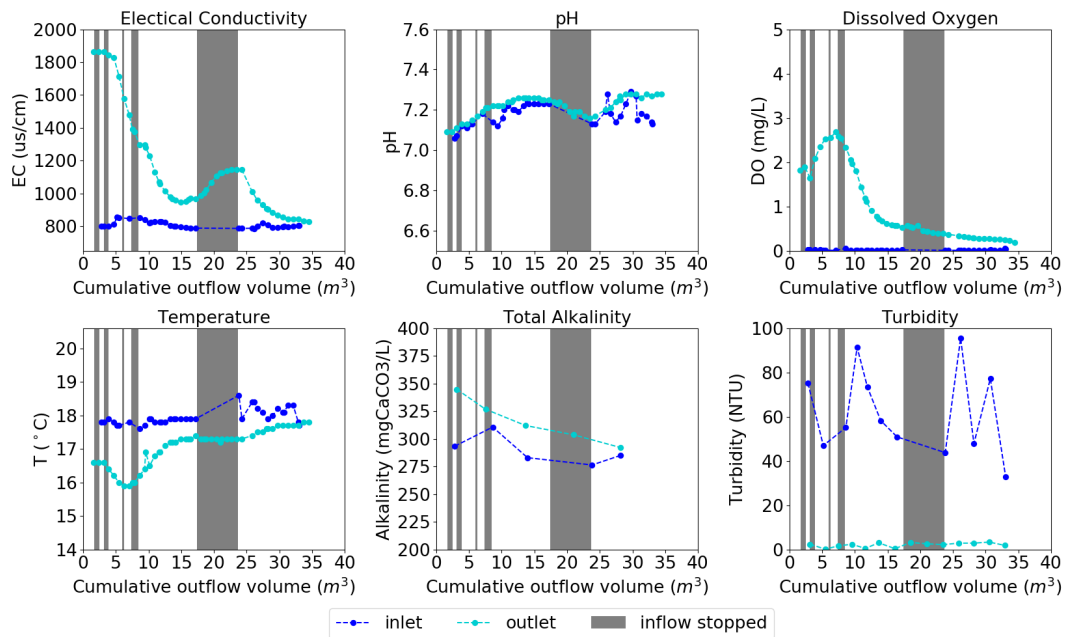
Figure 44: Physico-chemical parameters measured at Bluebloqs biofilter Spartaplein on 06-07-2020
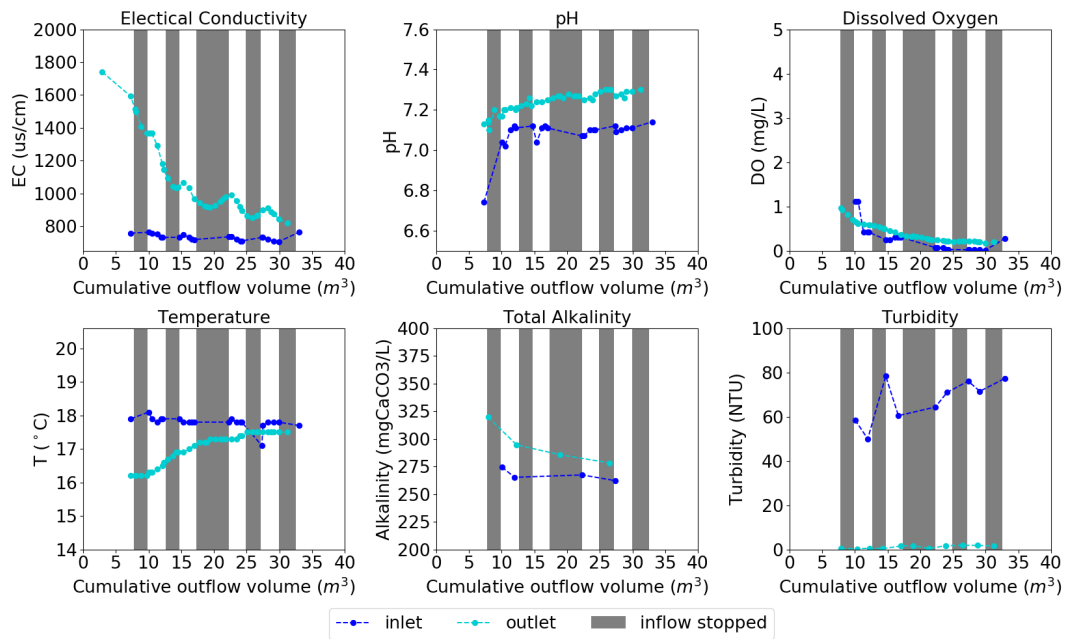
Figure 45: Physico-chemical parameters measured at Bluebloqs biofilter Spartaplein on 14-07-2020
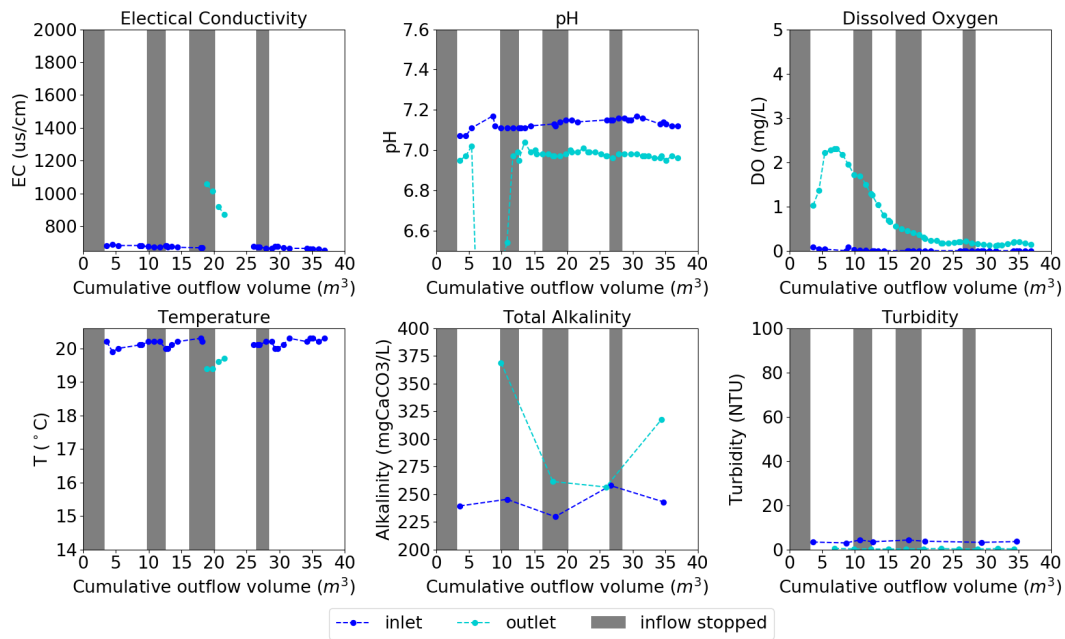
Figure 46: Physico-chemical parameters measured at Bluebloqs biofilter Spartaplein on 18-08-2020

B.2   Main Ions

B.2.1   Mixing Fractions
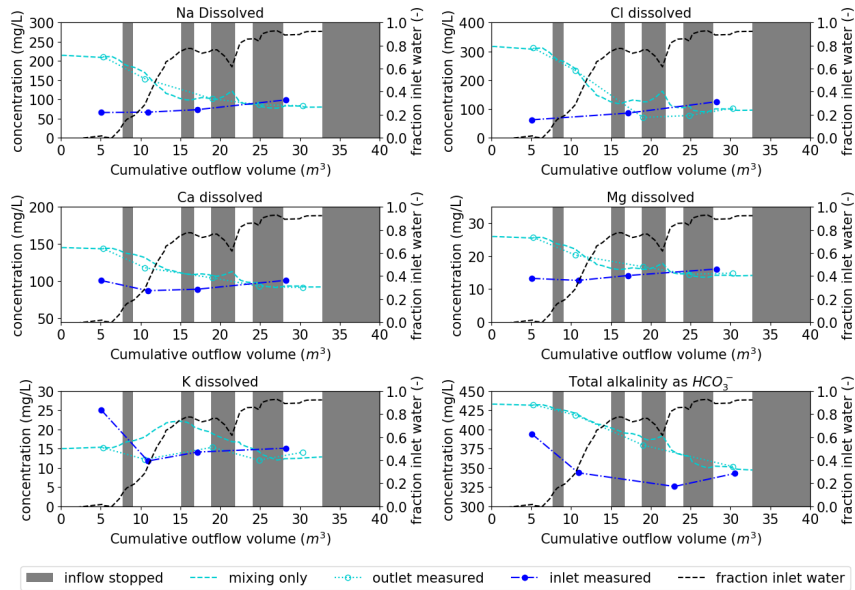
Figure 47: Measured alkalinity and concentrations of Na, Cl, Mg, and K, on 15-06-2020, plotted together with their estimated concentration based on mixing only.
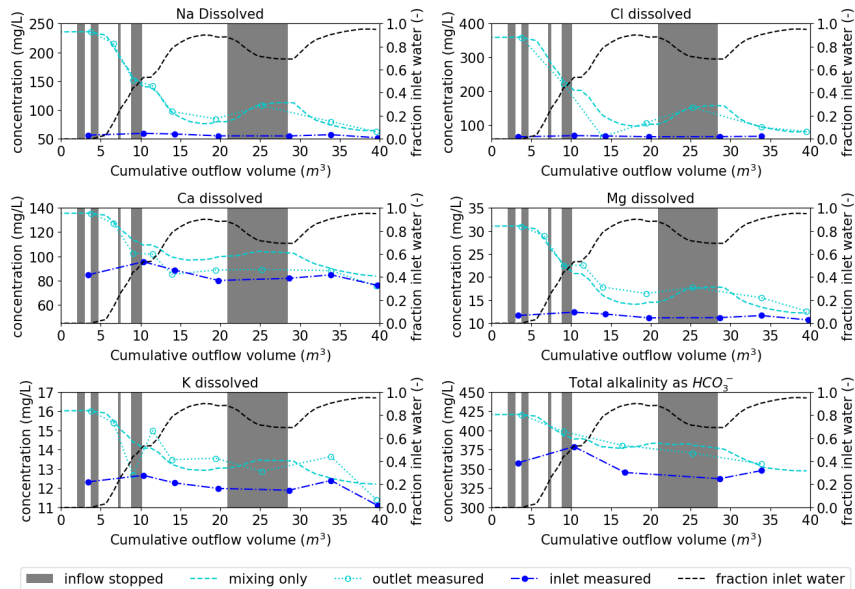
Figure 48: Measured alkalinity and concentrations of Na, Cl, Mg, and K, on 06-07-2020, plotted together with their estimated concentration based on mixing only.
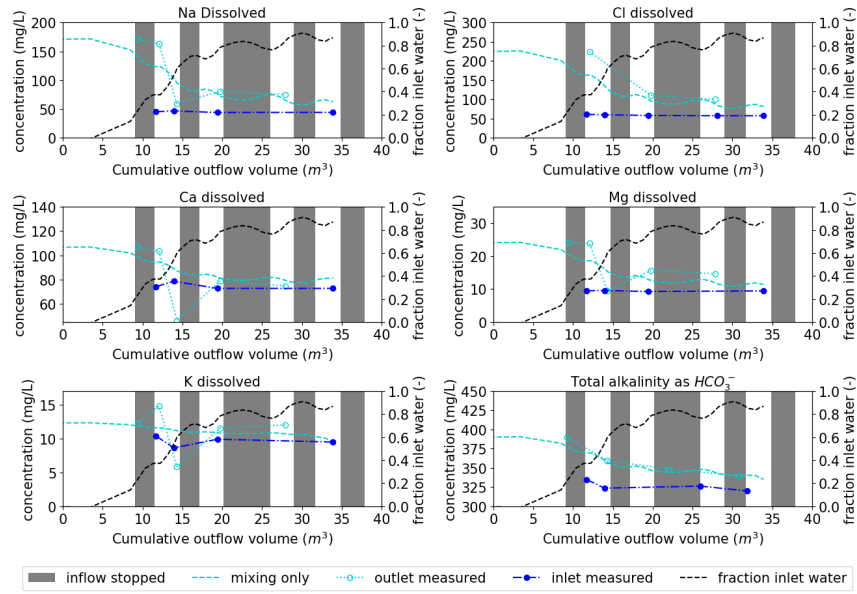
Figure 49: Measured alkalinity and concentrations of Na, Cl, Mg, and K, on 14-07-2020, plotted together with their estimated concentration based on mixing only.
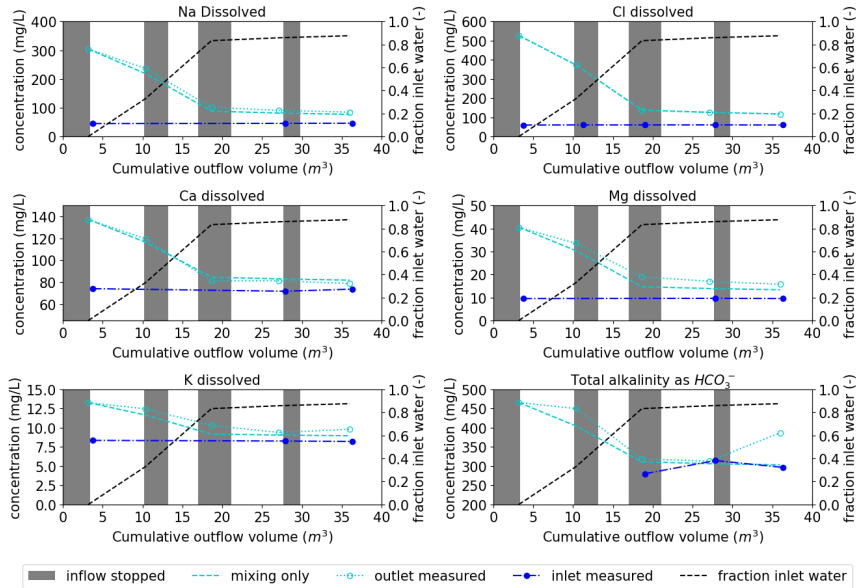
Figure 50: Measured alkalinity and concentrations of Na, Cl, Mg, and K, on 18-08-2020, plotted together with their estimated concentration based on mixing only.

B.3 Nutrients

B.3.1 Mixing Fractions
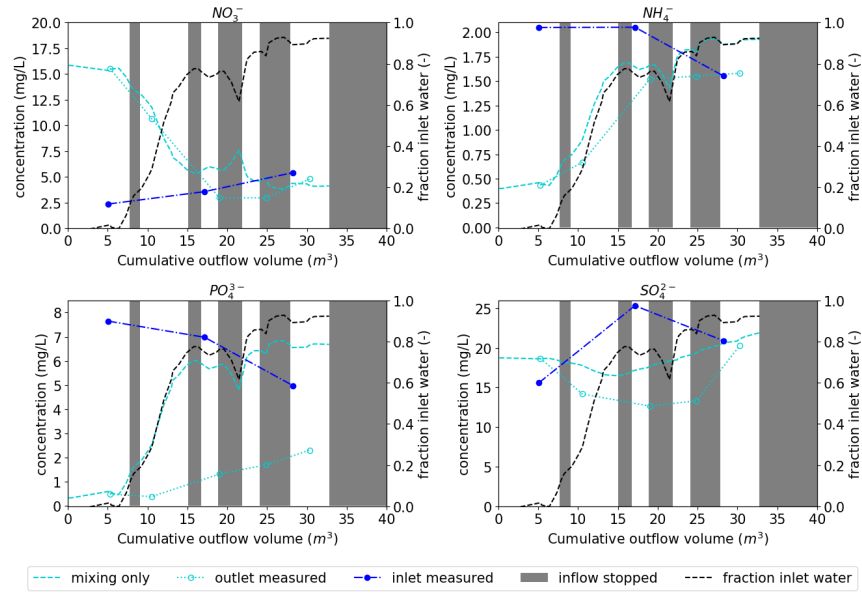
Figure 51: Measured nutrient concentrations on 15-06-2020, plotted together with their estimated concentration based on mixing only.
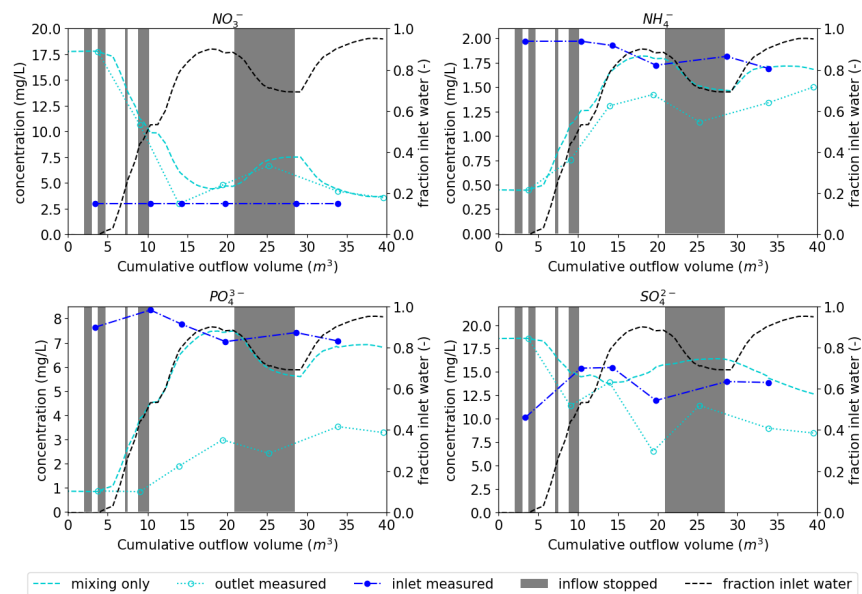
Figure 52: Measured nutrient concentrations on 06-07-2020, plotted together with their estimated concentration based on mixing only.
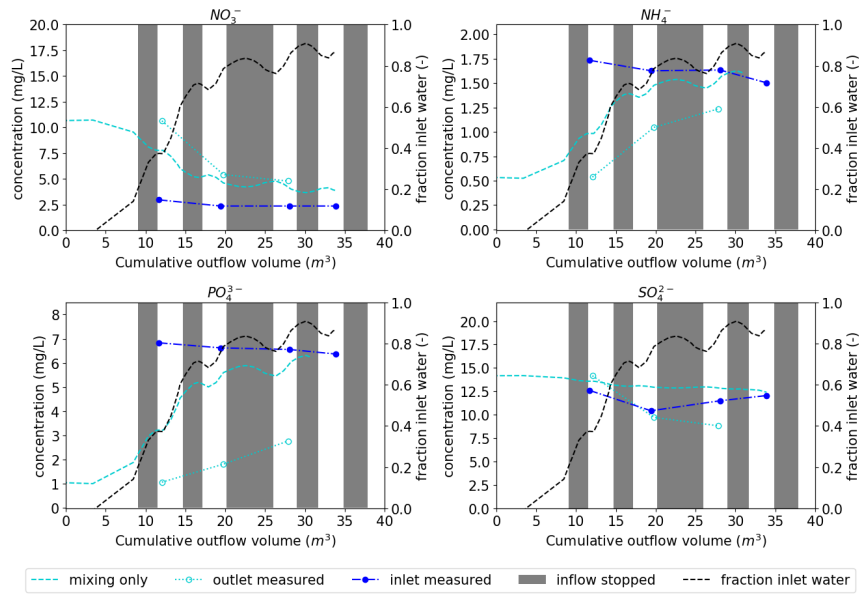
Figure 53: Measured nutrient concentrations on 14-07-2020, plotted together with their estimated concentration based on mixing only.
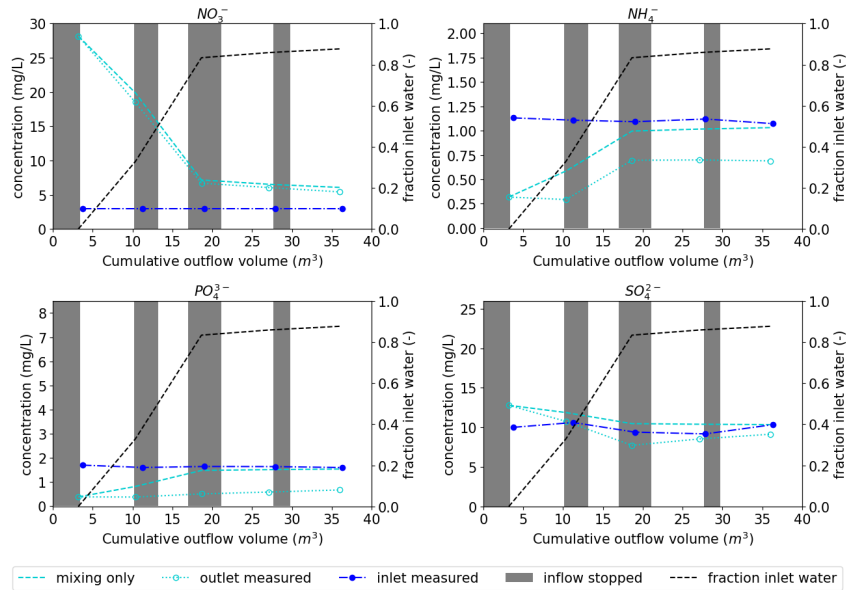
Figure 54: Measured nutrient concentrations on 18-08-2020, plotted together with their estimated concentration based on mixing only.
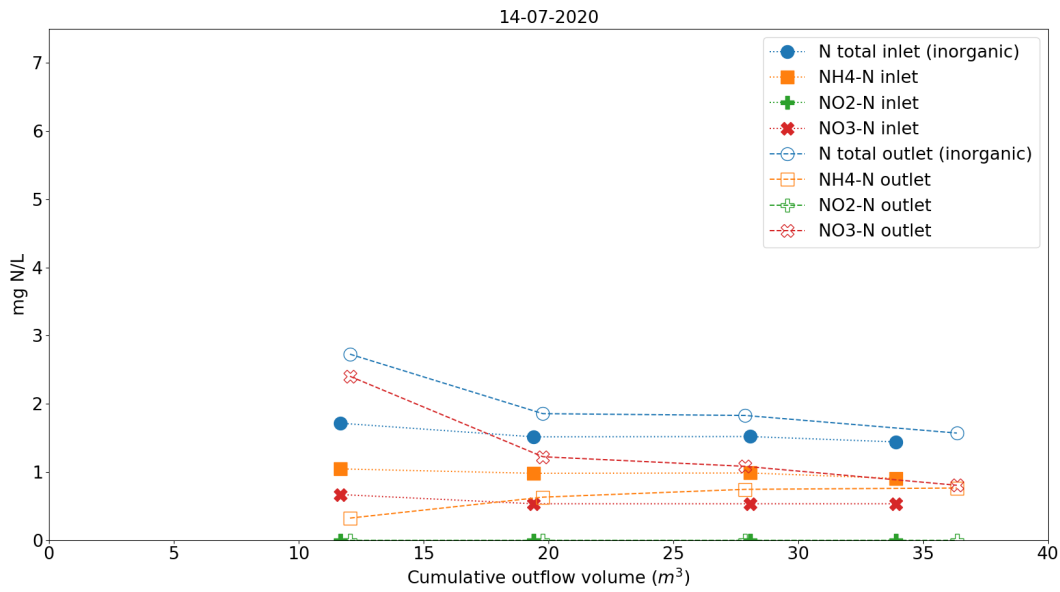
B.3.2 nitrogen conversions
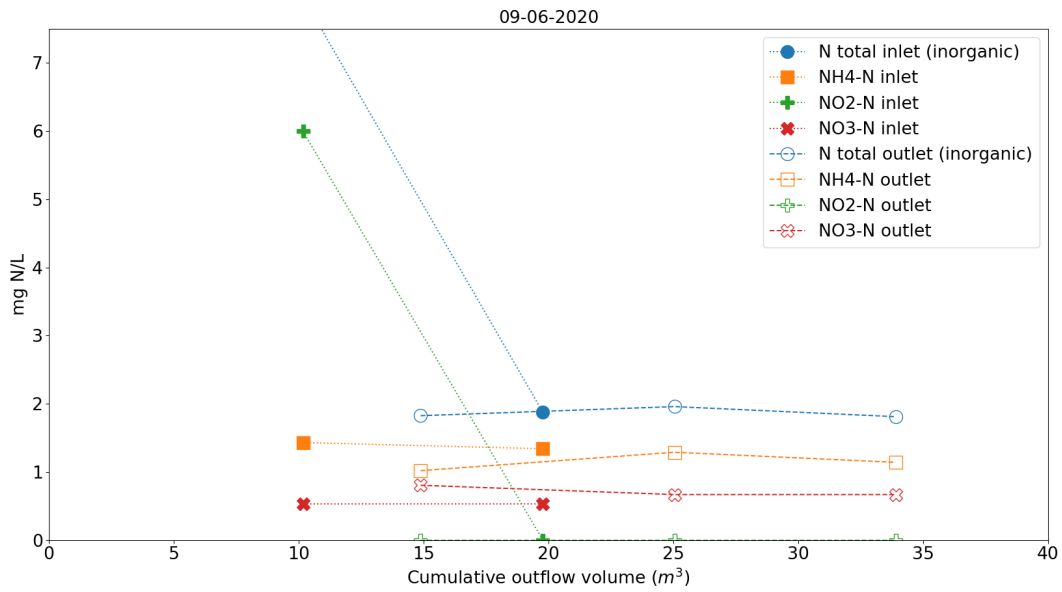
Figure 55: Comparsion of N-concentrations at inlet and outlet on 09-06-2020
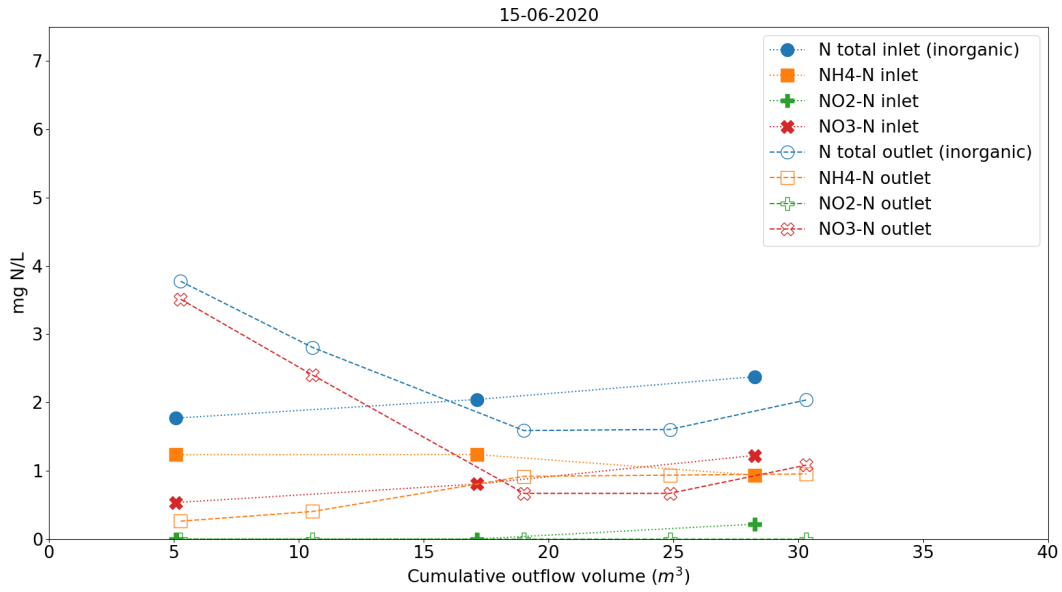
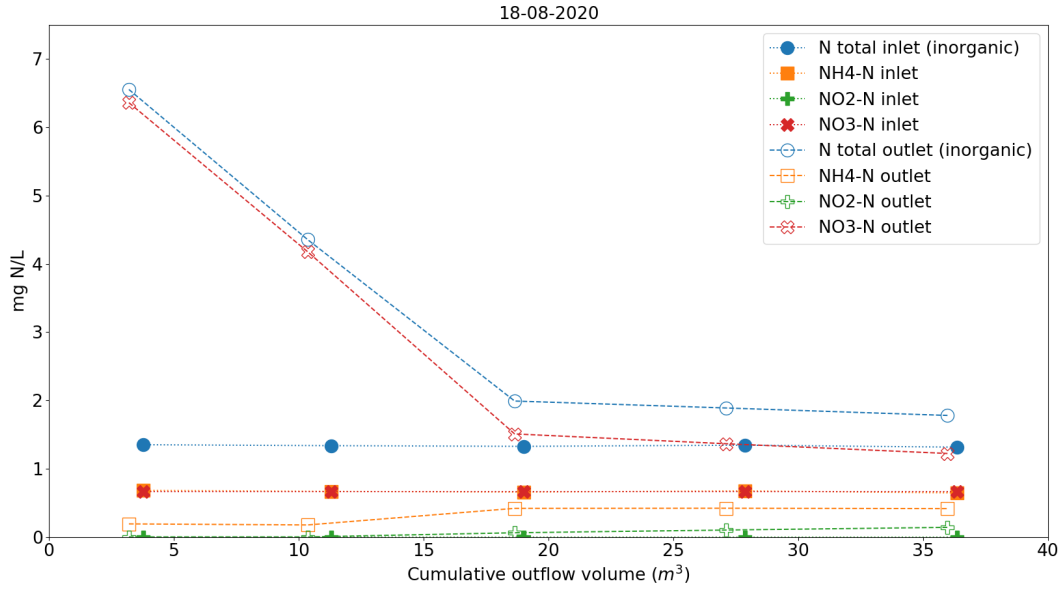Figure 56: Comparsion of N-concentrations at inlet and outlet on 15-06-2020
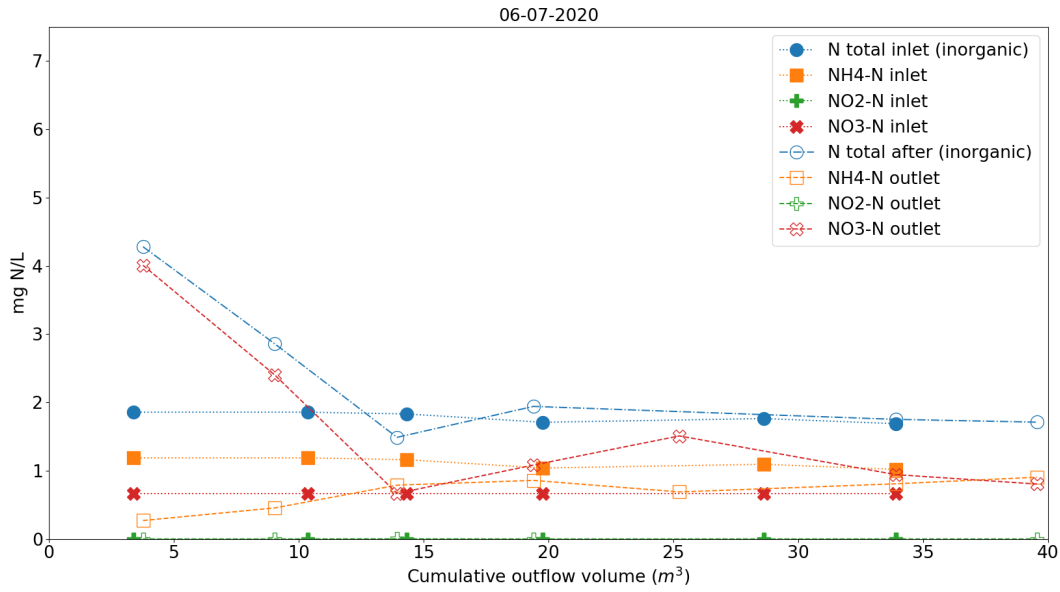
Figure 57: Comparsion of N-concentrations at inlet and outlet on 06-07-2020

Figure 58: Comparsion of N-concentrations at inlet and outlet on 14-07-2020

Figure 59: Comparsion of N-concentrations at inlet and outlet on 18-08-2020
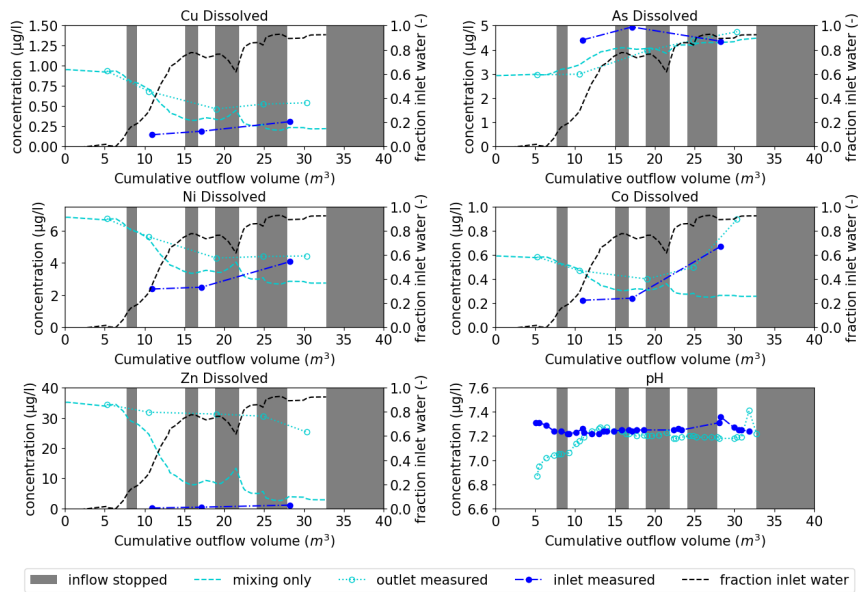
B.4 Metals

B.4.1 Dissolved

Figure 60: Measured dissolved concentrations, on 15-06-2020, of Cu, As, Ni, Co & Zn, plotted together with their estimated concentration based on mixing only.
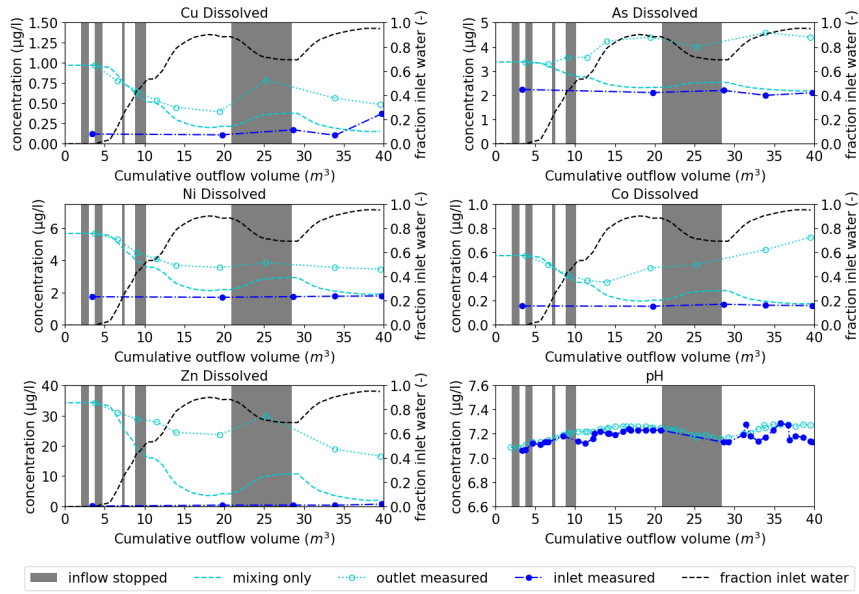
Figure 61: Measured dissolved concentrations, on 06-07-2020, of Cu, As, Ni, Co & Zn, plotted together with their estimated concentration based on mixing only.
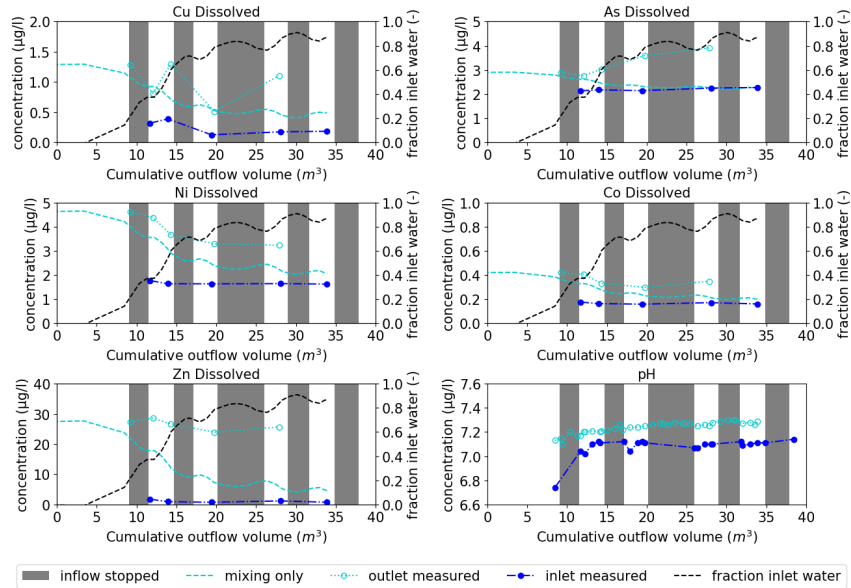

Figure 62: Measured dissolved concentrations, on 06-07-2020, of Cu, As, Ni, Co & Zn, plotted together with their estimated concentration based on mixing only.
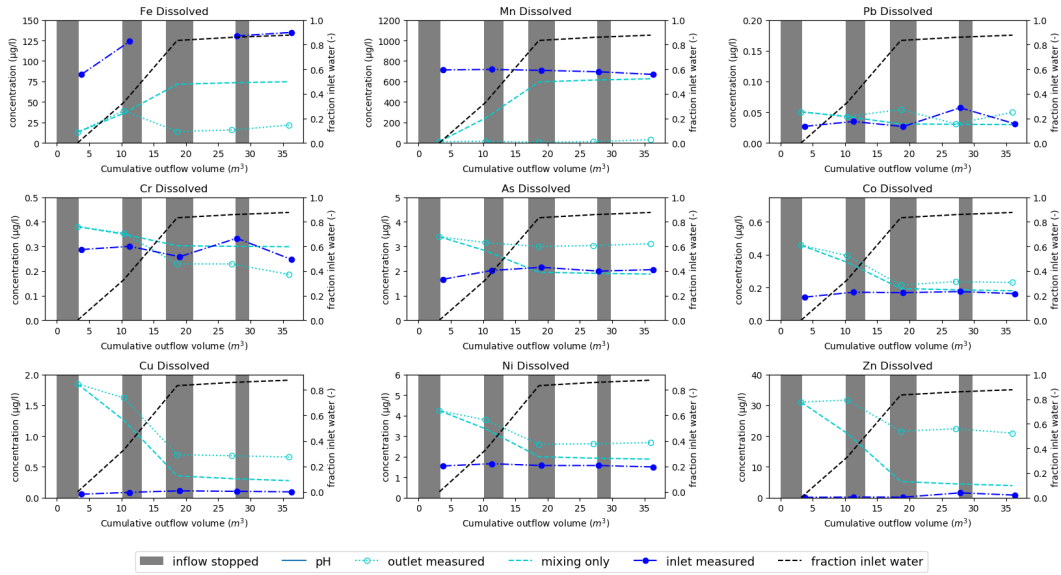
Figure 63: Measured dissolved concentrations, on 18-08-2020, of Cu, As, Ni, Co, Zn, Fe, Mn, Pb & Cr, plotted together with their estimated concentration based on mixing only.
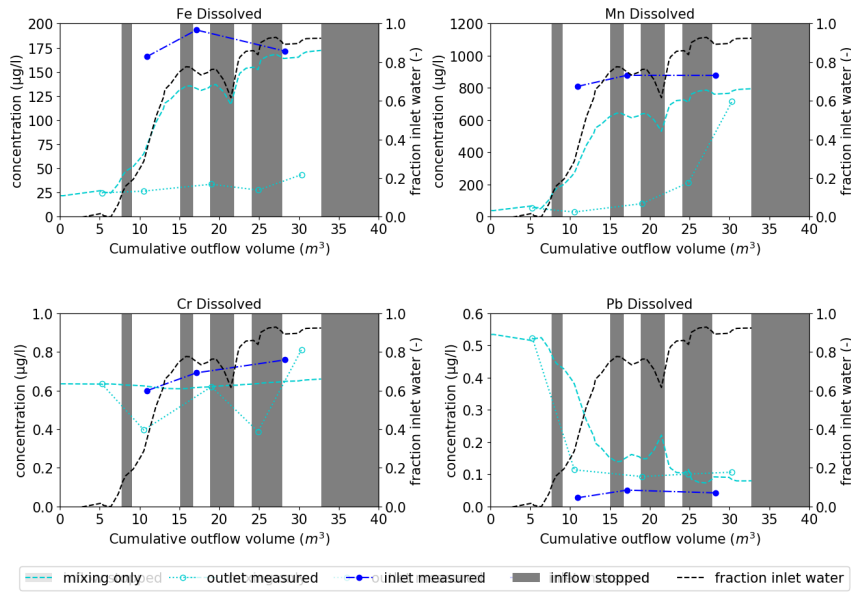

Figure 64: Measured dissolved concentrations, on 15-06-2020, of Fe, Mn, Cr & Pb, plotted together with their estimated concentration based on mixing only.

Figure 65: Measured dissolved concentrations, on 06-07-2020, of Fe, Mn, Cr & Pb, plotted together with their estimated concentration based on mixing only.

Figure 66: Measured dissolved concentrations, on 14-07-2020, of Fe, Mn, Cr & Pb, plotted together with their estimated concentration based on mixing only.
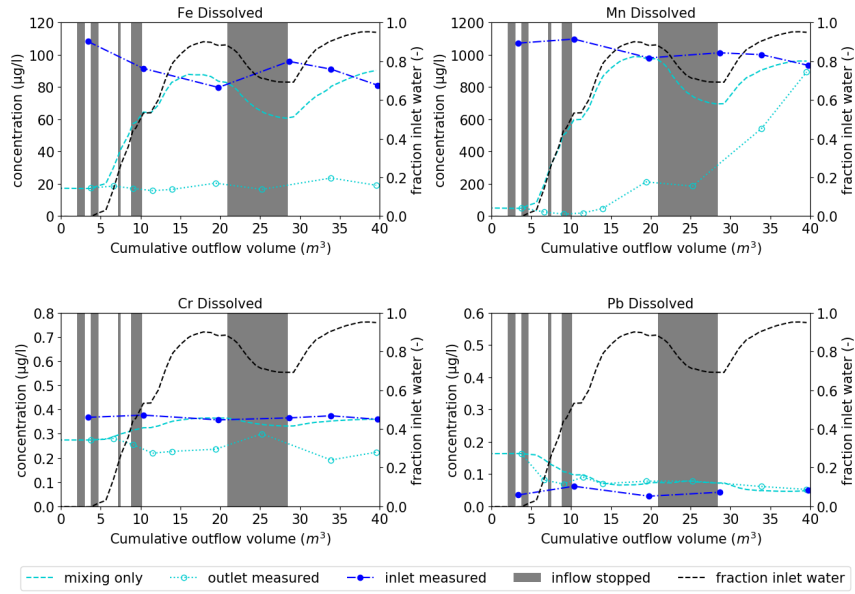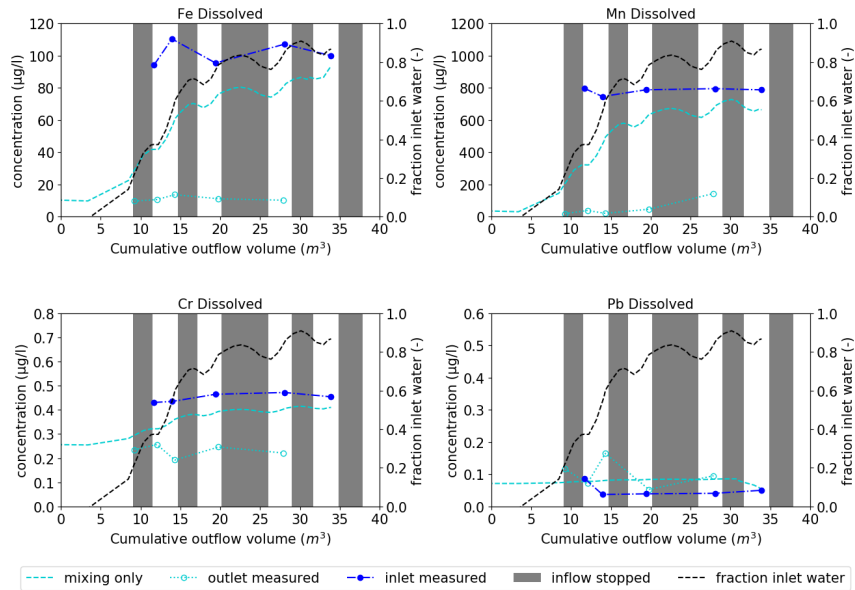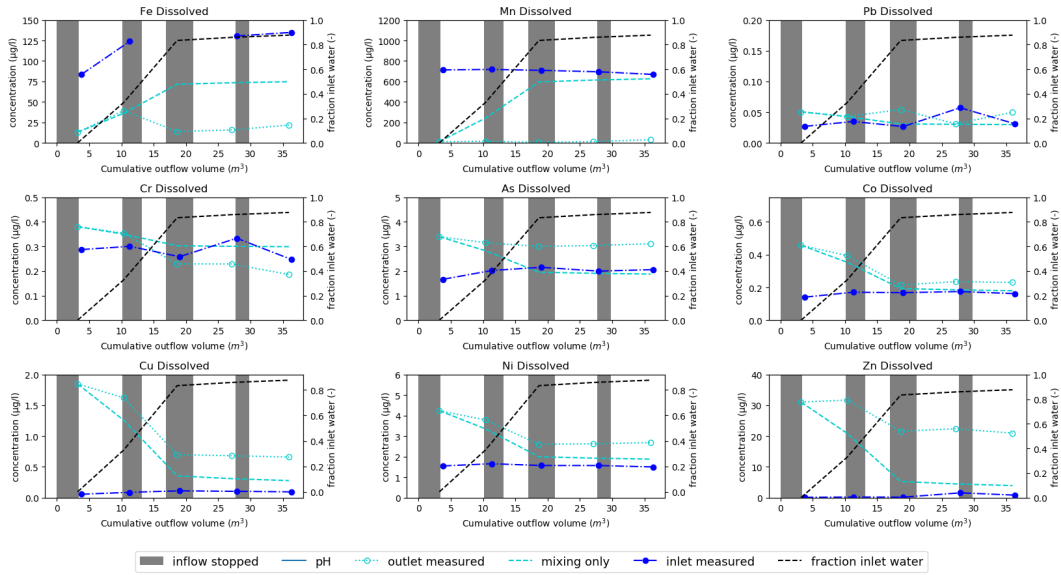
Figure 67: Measured dissolved concentrations, on 18-08-2020, of Fe, Mn, Cr & Pb, plotted together with their estimated concentration based on mixing only.

B.4.2 Suspended

Figure 68: Measured suspended concentrations, on 15-06-2020, of Cu, As, Ni, Co & Zn, plotted together with their estimated concentration based on mixing only.

Figure 69: Measured suspended concentrations, on 06-07-2020, of Cu, As, Ni, Co & Zn, plotted together with their estimated concentration based on mixing only.
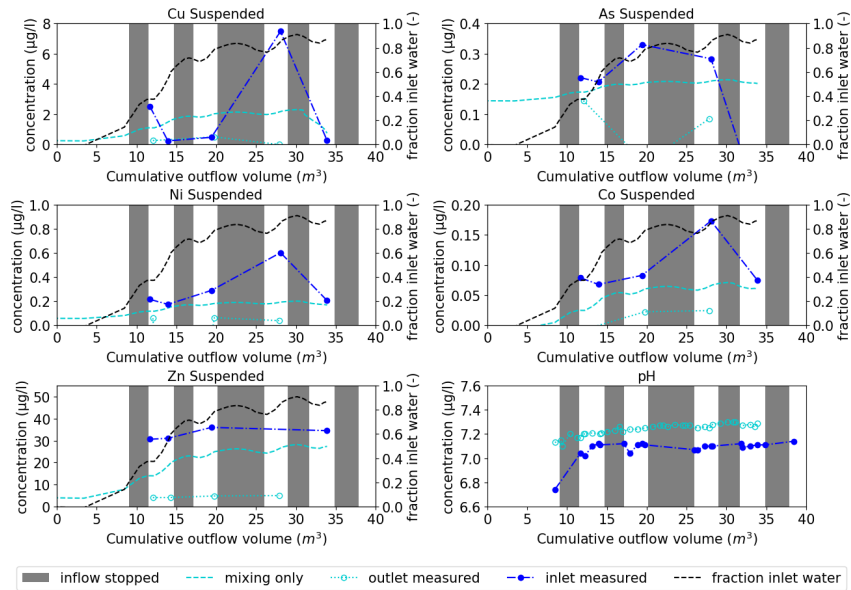
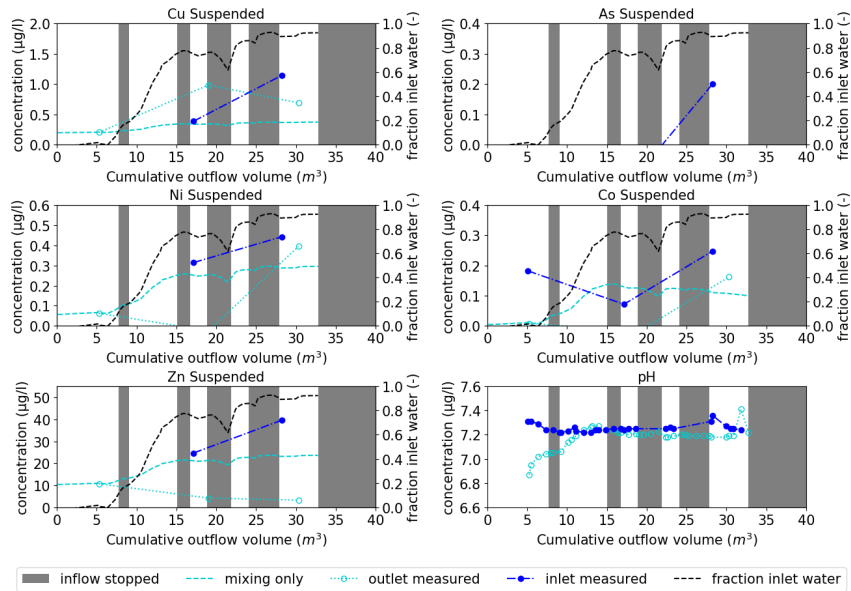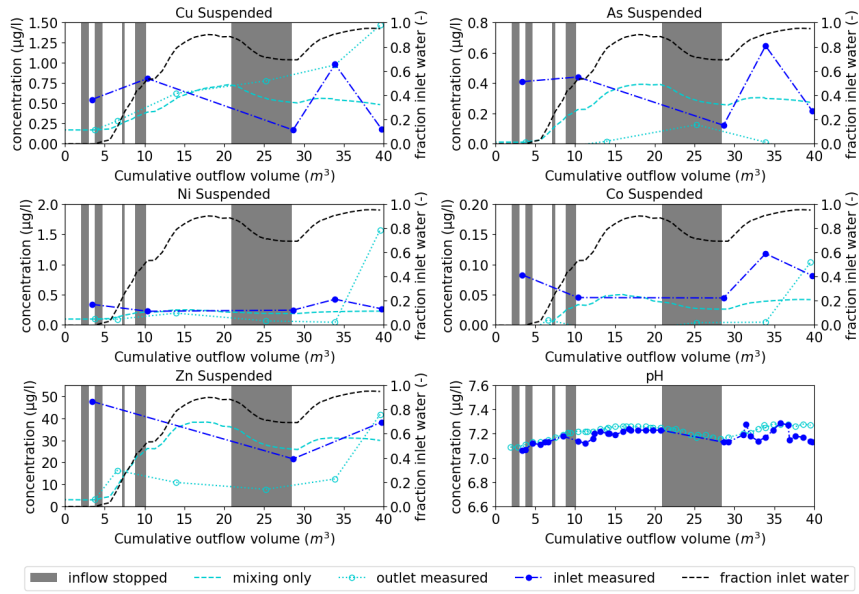Figure 70: Measured suspended concentrations, on 06-07-2020, of Cu, As, Ni, Co & Zn, plotted together with their estimated concentration based on mixing only.
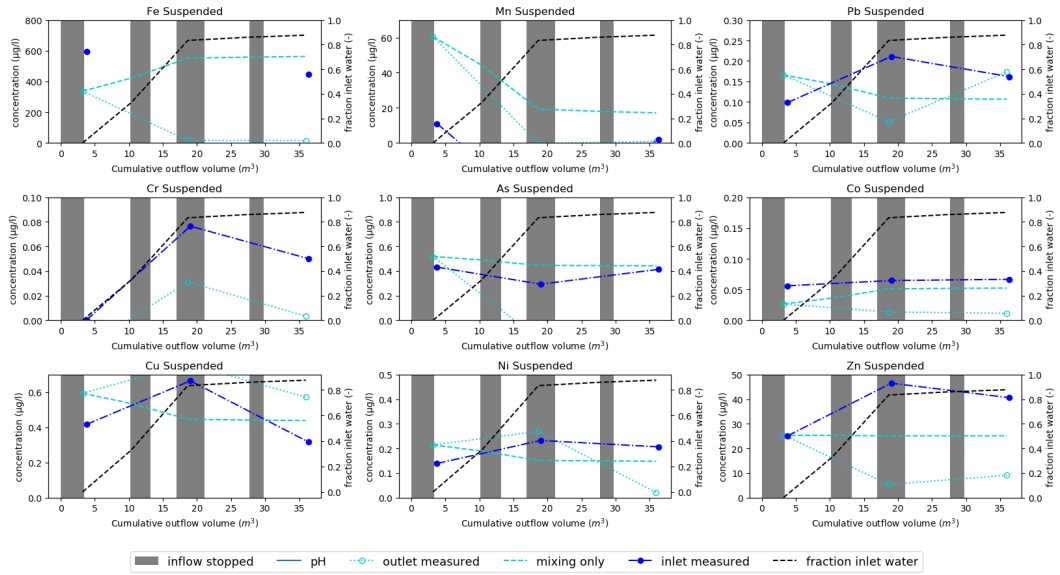
Figure 71: Measured suspended concentrations, on 18-08-2020, of Cu, As, Ni, Co, Zn, Fe, Mn, Pb & Cr, plotted together with their estimated concentration based on mixing only.
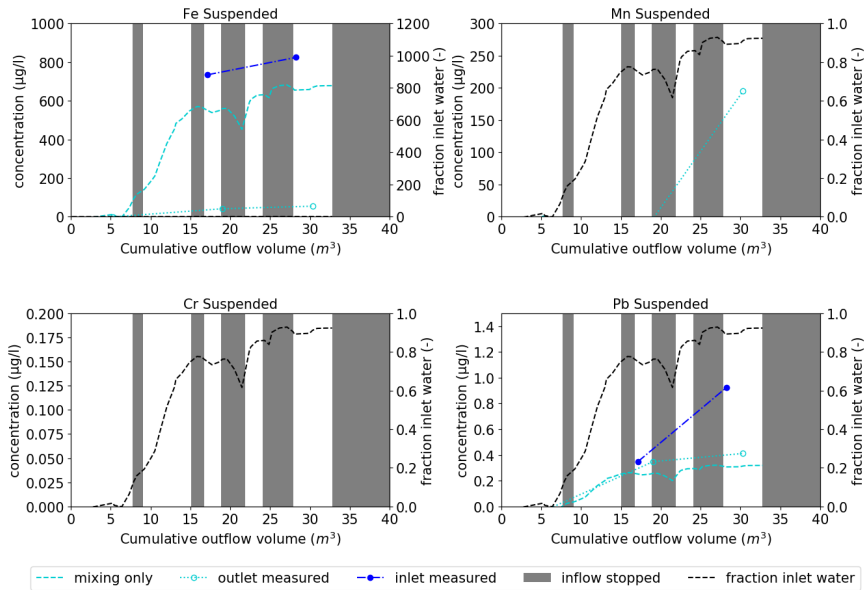
Figure 72: Measured suspended concentrations, on 15-06-2020, of Fe, Mn, Cr & Pb, plotted together with their estimated concentration based on mixing only.

Figure 73: Measured suspended concentrations, on 06-07-2020, of Fe, Mn, Cr & Pb, plotted together with their estimated concentration based on mixing only.

Figure 74: Measured suspended concentrations, on 14-07-2020, of Fe, Mn, Cr & Pb, plotted together with their estimated concentration based on mixing only.
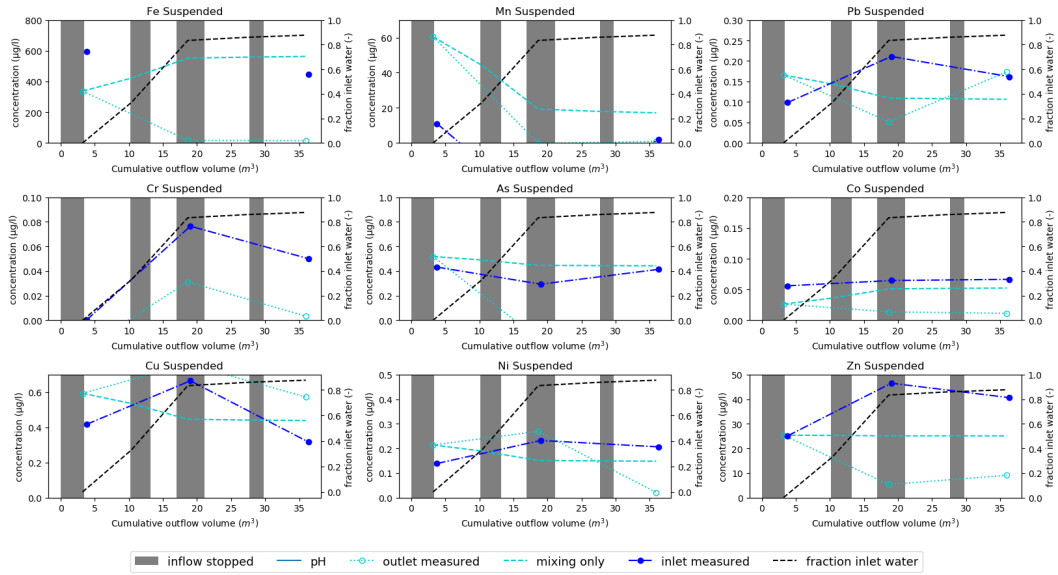
Figure 75: Measured suspended concentrations, on 18-08-2020, of Fe, Mn, Cr & Pb, plotted together with their estimated concentration based on mixing only.
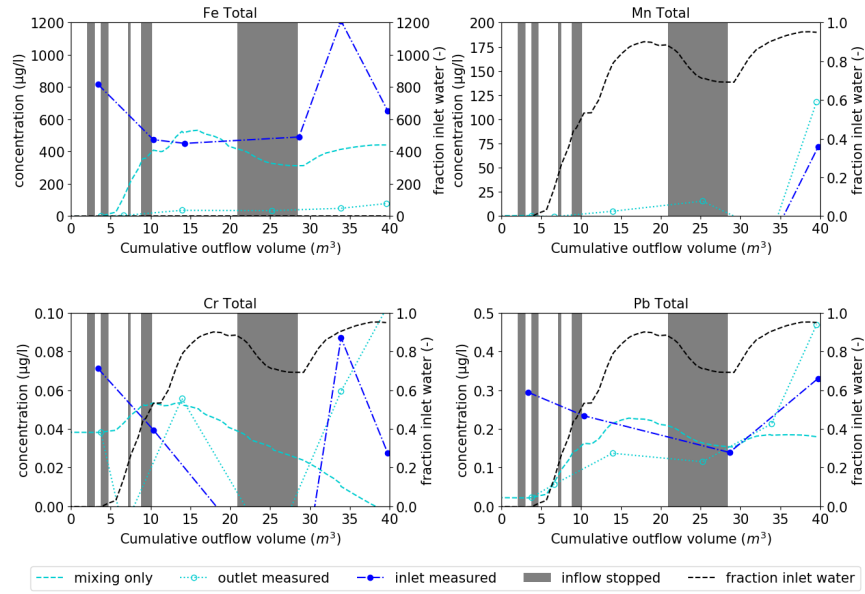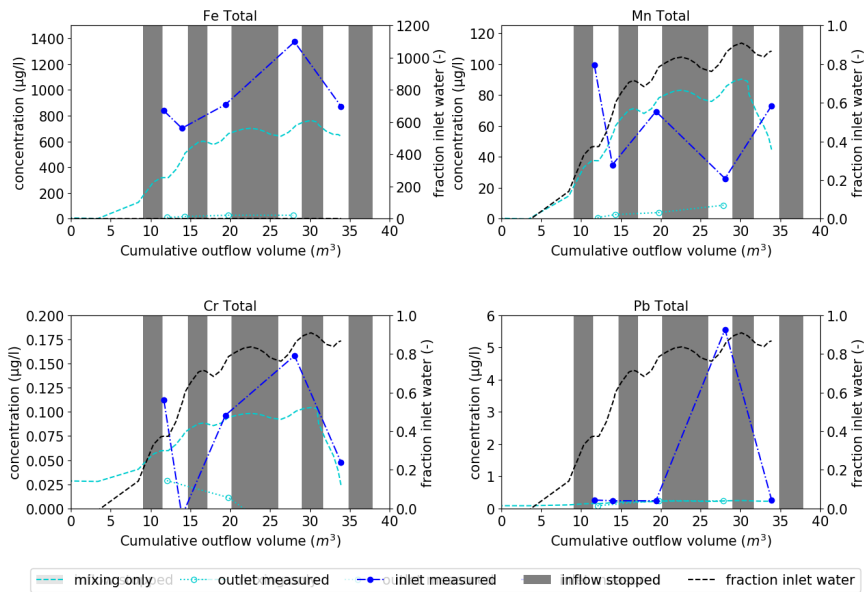
C   Stormwater runoff quality from Literature

Table 23: Metal and nutrient concentrations in stormwater runoff in the Netherlands

	Roofs in residential areas		Roofs and Roads in Residential Areas		Roofs and roads in industrial areas	
	mean [139]	median [139]	mean [139, 140]	median [139, 140]	mean [139]	median [139]
Metals ($\mu g/L$)						
Cr	2.0 [6]	-	2.0 [6], 6.2 [140]	1.1 [140]	-	-
Ni	3.4	1.9	4.1, 5.6	2.1, 3.6	12	1.3
Cu	34	22	21, 19	12, 11	6.7	22
Zn	95	23	144, 102	75, 60	594	65
Pb	324	40	21, 18	8, 6	68	4.2
Cd	0.29	0.16	0.18, 0.27	0.10, 0.15	1.4	0.05
As	0.85 [6]	-	1.32 [6]	-	-	-
Fe	-	-	1.8 [6]	1.1[6]	-	-
Nutrients (mg/L) [139]						
NO_3^-	-	-	1.5	0.93	0.66	0.59
Total-P			0.30	0.20	0.52	0.18

D   Reaction Equations

Nitrification

$$2NH_4^+ + 3O_2 \longrightarrow 2NO_2 + 4H^+ + 2H_2O \tag{21a}$$

$$2NO_2^- + O_2 \longrightarrow 2NO_3^- \qquad (21b)$$

$$NH_4^+ + 2O_2 \longrightarrow 2H^+ + H_2O + NO_3^- \qquad (21)$$

Denitrification

$$2NO_3^- + 10e^- + 12H^+ \longrightarrow N_2 + 6H_2O \qquad (22)$$
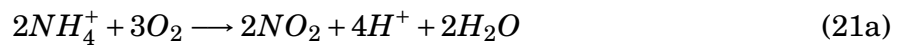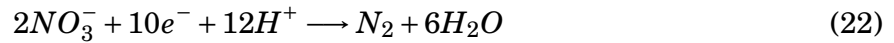
Oxidation of pyrite (iron(II) disulfide)

$$2FeS_2 + 6NO_3^- + 4H_2O \longrightarrow 3N_2 + 4SO_4^{2-} + 2Fe(OH)_3 + 2H^+ \qquad (23)$$

$$4FeS_2 + 14H_2O + 15O_2 \longrightarrow 8SO_4^{2-} + 4Fe(OH)_3 + 16H^+ \qquad (24)$$

Oxidation of iron

$$4Fe^{2+} + O_2 + 2H_2O \longrightarrow 4Fe^{3+} + 4OH^- \qquad (25a)$$

$$4Fe^{3+} + 4OH^- + 8H_2O \longrightarrow 4Fe(OH)_3 + 8H^+ \qquad (25b)$$

$$4Fe^{2+} + O_2 + 10H_2O \longrightarrow 4Fe(OH)_3 + 8H^+ \qquad (25)$$
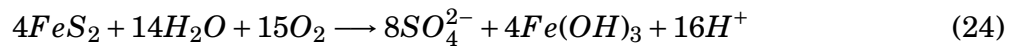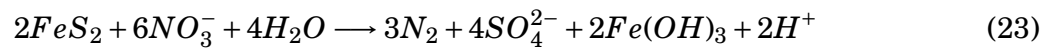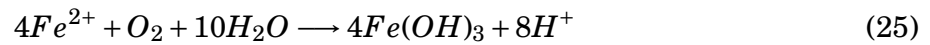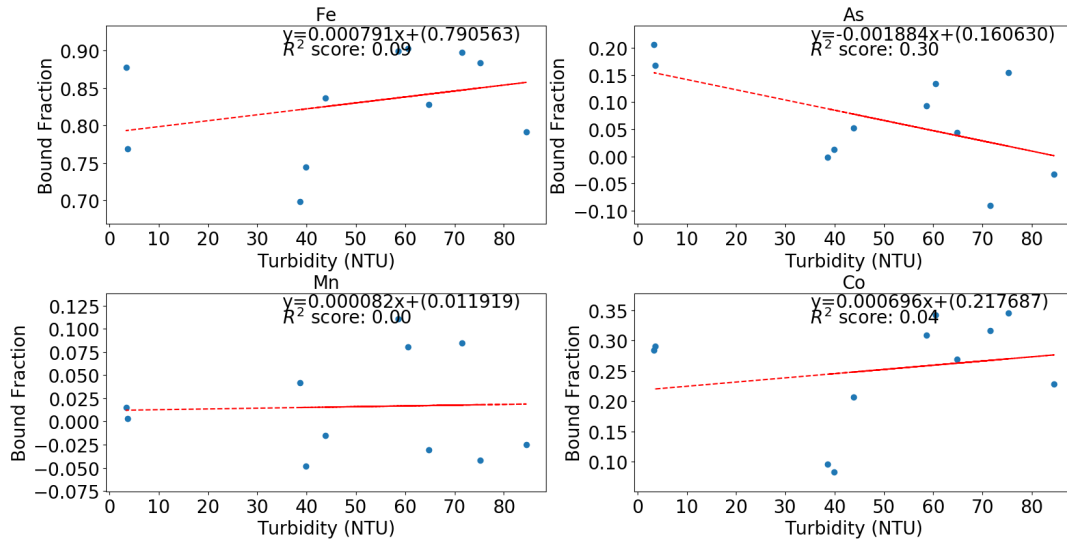
E   Correlations

Figure 76: Correlation between turbidity and the bound fraction of Fe, As, Mn and Co, using linear regression.
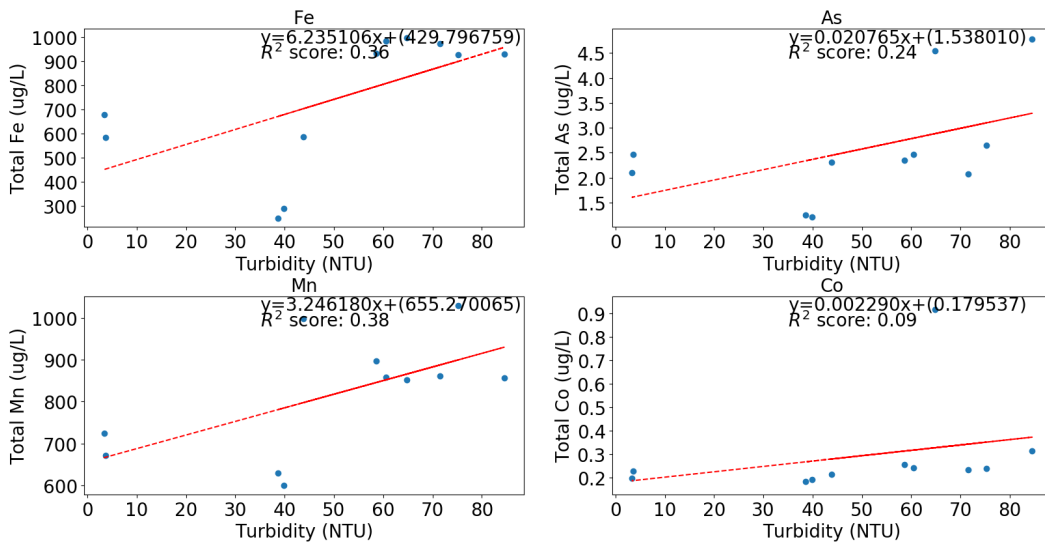
Figure 77: Correlation between turbidity and the total concentration of Fe, As, Mn and Co, using linear regression.
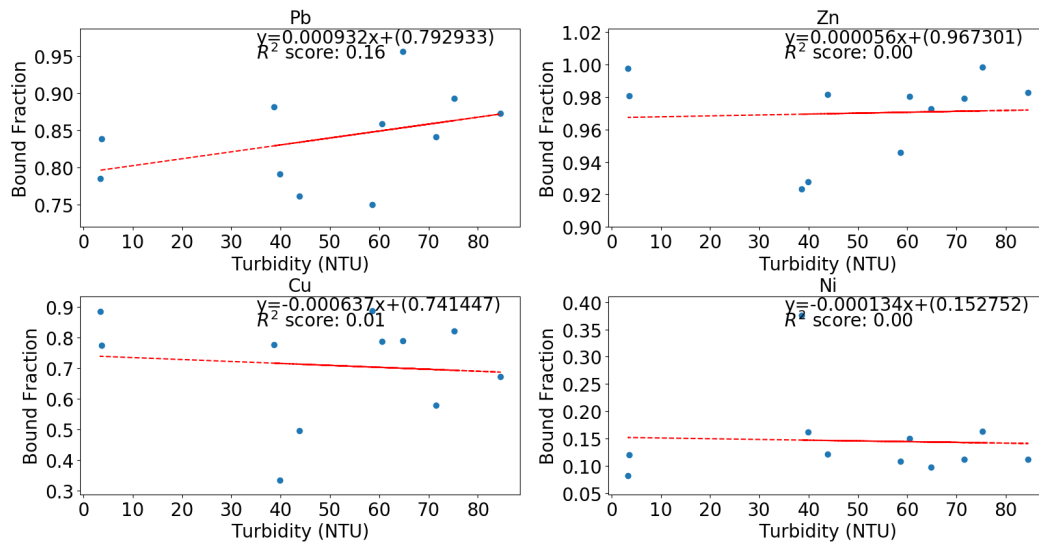
Figure 78: Correlation between turbidity and the bound fraction of Pb, Ni, Zn and Cu, using linear regression.
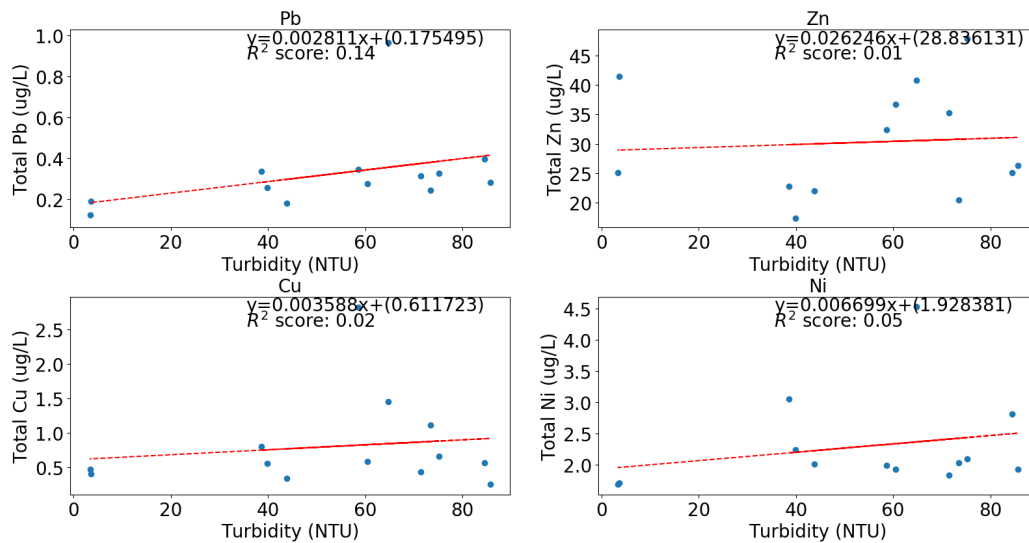
Figure 79: Correlation between turbidity and the total concentration of Pb, Ni, Zn and Cu, using linear regression.
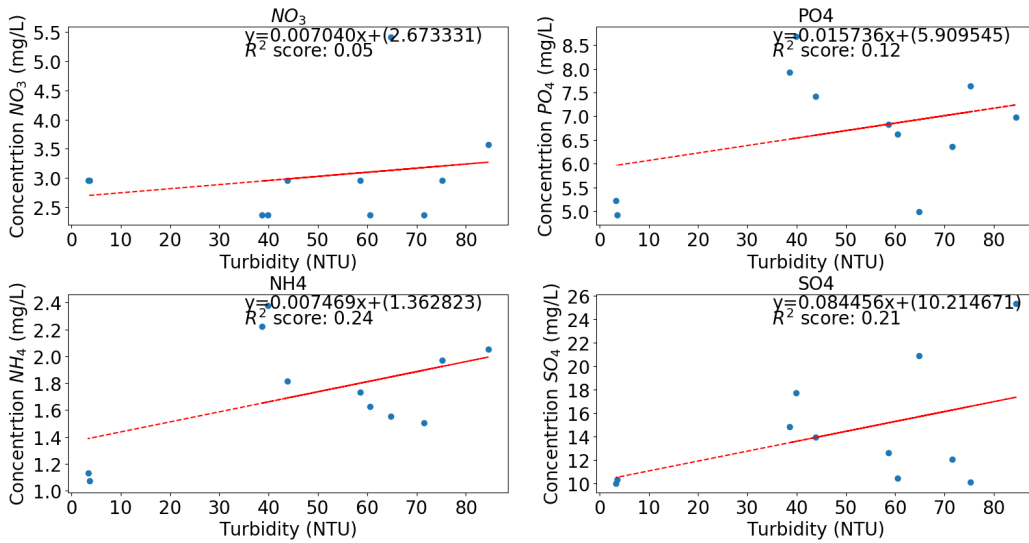
Figure 80: Correlation between turbidity and the total concentration of NO_3, NH_4, PO_4 and SO_4 using linear regression.
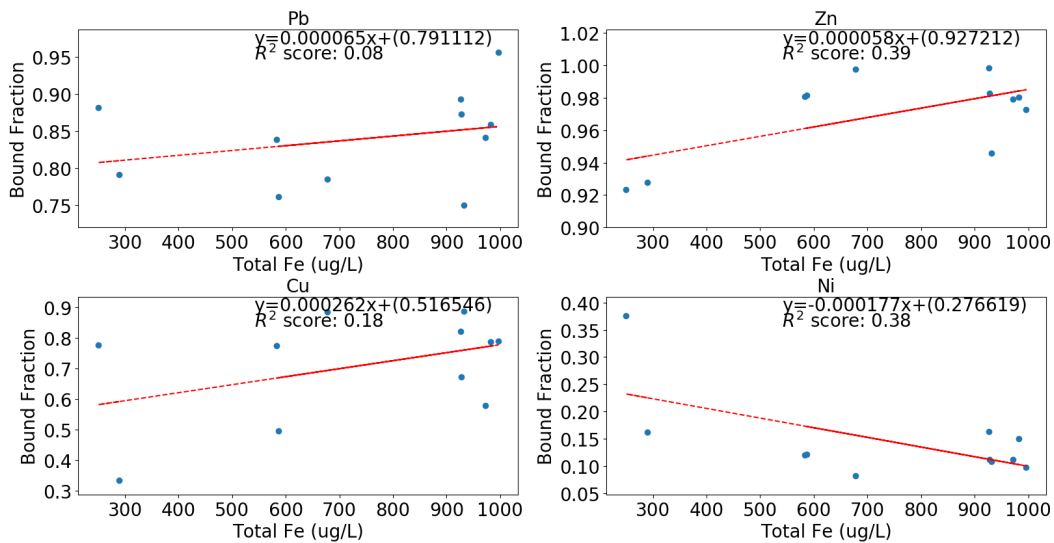
Figure 81: Correlation between total Fe and the bound fractions of Pb, Ni, Zn and Cu using linear regression.

110
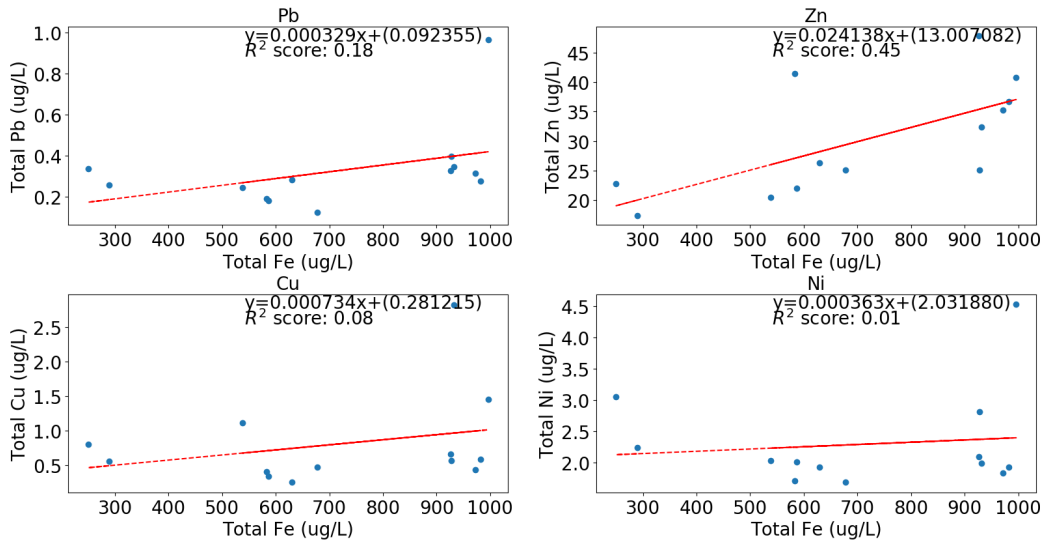
Figure 82: Correlation between total Fe and the total concentrations of Pb, Ni, Zn and Cu using linear regression.
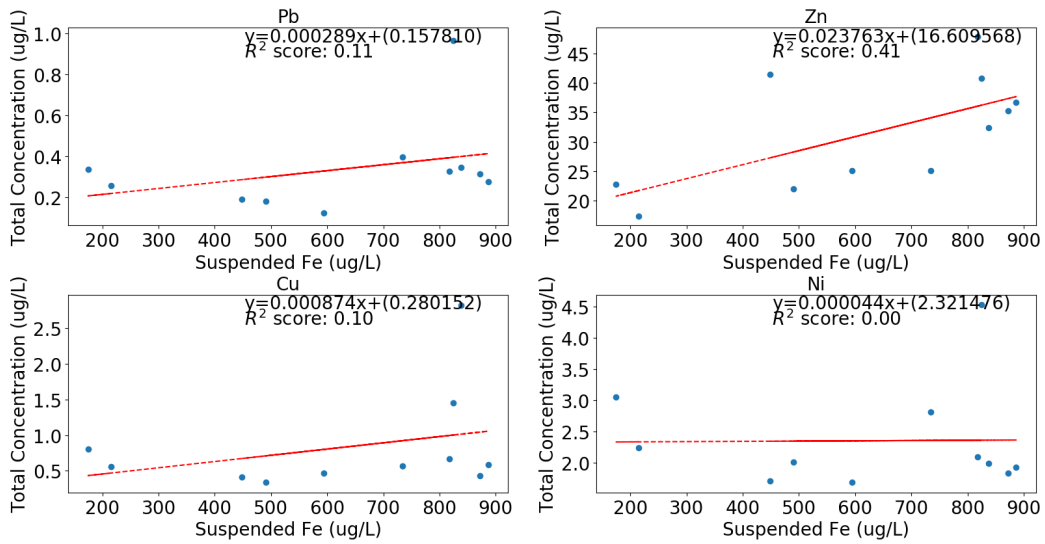
Figure 83: Correlation between suspended Fe and the total concentrations of Pb, Ni, Zn and Cu using linear regression.

Table 24: Samples taken at inlet and outlet and time since the system started running.

|	9/06/2020		15/06/2020		6/07/2020		14/07/2020		18/08/2020	
Sample	Before	After	Before	After	Before	After	Before	After	Before	After
1		0:40	0:27	0:28	0:18	0:20		0:49	0:20	0:17
2	0:54	0:52	0:48	0:42	0:33	0:35	1:02	1:04	0:48	0:38
3	1:16	1:19	0:58	0:56	0:55	0:48	1:14	1:16	1:00	0:55
4	1:45	1:43	1:12	1:10	1:06	1:01	1:31	1:28	1:11	1:09
5		2:13	1:31	1:27	1:16	1:14	1:43	1:45		1:24
6		2:31	2:02	1:41	1:29	1:27		1:57	1:41	1:39
7		2:45		2:00	1:45	1:43	2:18	2:12	1:55	1:54
8		3:00		2:12		1:58	2:29	2:28		2:09
9			2:30	2:28		2:14	2:49	2:44	2:28	2:24
10			2:42	2:41	2:32	2:30	3:00	2:58	2:43	2:40
11				2:58	2:47	2:45	3:24	3:13		2:57
12					3:00	3:00			3:13	3:11
13					3:16	3:15				
14					3:31	3:30				
15										
	Win		Win		Win		Win		Win	

Only Dissolved   Total and dissolved   Total only (analysis error on dissolved)

112

F   Analysis Frequency

G   PHREEQC Scripts

G.1   Conceptual Model

G.1.1   Inlet Water

DATABASE D:\Users\Kirsten\Documents\Kirsten\TU_Delft\MasterThesis\Urban Water Buf
INCLUDE$ Metal_sorption_Solution_Master_Species.phr
INCLUDE$ Metal_sorption_Solution_Species.phr
INCLUDE$ Metal_sorption_Surface_Species.phr
INCLUDE$ Metal_sorption_Phases.phr

SOLUTION 1 #Inlet Water
−units mg/l
Temp   17.8
pH   7.06
pe   6.44   #N−couple
#pe   −3.11   #S−couple
Alkalinity   289.7   as CaCO3
As   2.08   ug/L
Cd   0   ug/L
Cr   0.37   ug/L
Cu   0.17   ug/L
Co   0.19   ug/L
Fe(2)   90.75   ug/L
Mn   1025.70 ug/L
Ni   1.78   ug/L
Pb   0.04   ug/L
Zn   0.47   ug/L
Ba   61.48   ug/L
Ca   84.5
K   12.1
Mg   11.5
Na   56.1
Li   6.15   ug/L
B   113.84   ug/L
Al   16.39   ug/L
Se   1.82   ug/L
Sr   350.46   ug/L
F   0.28
Cl   67.14

```
N(3)                0                      #NO2-N
N(5)                0.67                   #NO3-N
N(−3)               1.44                   #NH4-N
P                   2.46     as PO4   #PO4-P
Br                  0.01
S(6)                13.47                  #SO4
#S(−2)              0.001
O(0)                0.015
Si                  4.9
#END


EXCHANGE 1
 X 0.06# X is  the  exchanger ,  value  is  cation  exchange  capacity  (CEC)  in  eq/L − 60
 −equilibrate 1            # equilibrate  with  solution  number 1


SURFACE 1      #QUARTZ (A) OR IOCS (B)
Hfo_wOH 0.207    600        93.3                   #Quartz: 0.207 600 93.3 − IOCS: 2.01 600
Hfo_sOH 0                                          #
−equilibrate 1

# PRINT
# −reset false
# −totals true
# −exchange true
END                             #


## G.1.2   Initial concentrations in outlet water

DATABASE D:\Users\Kirsten\Documents\Kirsten\TU_Delft\MasterThesis\Urban Water Buf
INCLUDE$ Metal_sorption_Solution_Master_Species.phr
INCLUDE$ Metal_sorption_Solution_Species.phr
INCLUDE$ Metal_sorption_Surface_Species.phr
INCLUDE$ Metal_sorption_Phases.phr


SOLUTION 2 #Initial  water  in  biofilter
−units mg/l
Temp                16.6
pH                  7.11
pe                  6.62     #N−couple
#pe                 −3.098   #S−couple
```

```
Alkalinity      344        as CaCO3
As              3.37       ug/L
Cd              0          ug/L
Cr              0.27       ug/L
Co              0.57       ug/L
Cu              0.97       ug/L
Fe              17.4       ug/L
Mn              51.6       ug/L
Ni              5.76       ug/L
Pb              0.16       ug/L
Zn              34.18      ug/L
Ba              67.63      ug/L
Ca              135.4
K               16.02
Mg              31.00
Na              235
Li              10.32      ug/L
B               203.9      ug/L
Al              3.28       ug/L
Se              2.95       ug/L
Sr              648.3      ug/L
F               0.25
Cl              358.84
N(3)            0                      #NO2-N
N(5)            4.0                    #NO3-N
N(-3)           0.35                   #NH4-N
P               0.285      as PO4  #PO4-P
Br              1.83
S(6)            18.56                  #SO4
#S(-2)          0.001
O(0)            1.64
Si              6.7


EXCHANGE 1
 X 0.06           # X is the exchanger, value is cation exchange capacity (CEC) in
 -equilibrate 2          # equilibrate with solution number 2


SURFACE 1     QUARTZ (A) OR IOCS (B) Pim Transport Values
Hfo_wOH 0.207   600       93.3              #Quartz: 0.207 600 93.3 - IOCS: 2.01 600
Hfo_sOH 0                                   #
```

```
−equilibrate 2

#  PRINT
#  −reset false
#  −totals  true
#  −exchange  true
END



#  END
```

G.2   Transport Model

G.3   Multi-pathway

```
DATABASE  WATEQ4F.dat
TITLE  .  −Metal Sorption by various media in  biofilter
INCLUDE$  Metal_sorption_Solution_Master_Species.phr
INCLUDE$  Metal_sorption_Solution_Species.phr
INCLUDE$  Metal_sorption_Surface_Species.phr
INCLUDE$  Metal_sorption_Phases.phr


SURFACE_SPECIES
Hfo_wOH  +  Cd+2  =  Hfo_wOCd+  +  H+
          log_k    −2.0      #−2.91
END


PHASES
    fix_pH                                        #fixed pH
    H+  =  H+
    log_k  0
END


SOLUTION  0   STORMWATER  RUNOFF  (SPANGEN)  −  Dissolved
−units  mg/l
Temp              17.8
pH                7.2
pe                6.52      #N−couple
#pe               −3.11     #S−couple
Alkalinity        289.74    as  CaCO3
As                2.08      ug/L
Cd                0         ug/L
```

```
Cr              0.37      ug/L
Cu              0.17      ug/L
Co              0.19      ug/L
Fe(2)           90.75     ug/L
Mn              1025.70 ug/L
Ni              1.78      ug/L
Pb              0.04      ug/L
Zn              0.47      ug/L
Ba              61.48     ug/L
Ca              84.5
K               12.1
Mg              11.5
Na              56.1
Li              6.15      ug/L
B               113.84  ug/L
Al              16.39     ug/L
Se              1.82      ug/L
Sr              350.46    ug/L
F               0.28
Cl              67.14     charge
#N(3)           0                        #NO2-N
#N(5)           2.96                     #NO3
#N(5)           0.67                     #NO3-N
#N(-3)          1.44                     #NH4-N
P               2.46      as PO4  #PO4-P
Br              0.01
S(6)            13.47                    #SO4
#S(-2)          0.001
#O(0)           0.015
Si              4.9
END


SOLUTION 1-5   Initial  solution  for  column
-units mg/l
Temp            16.6
pH              7.2
pe              6.71      O2(g)     -0.68 #N-couple, O in equilibrium with atmosphere
Alkalinity      121 as HCO3
Ca              49
Cl              51        charge
K               4.4
```

```
Mg                 8.8
Na                 31

END

EXCHANGE 1−5
 X 0.06# X is the exchanger, value is cation exchange capacity (CEC) − 60 meq/L
 −equilibrate 1          # equilibrate with solution number 1

SURFACE 1    QUARTZ (A) OR IOCS (B)
Hfo_wOH 0.207    600      93.3                  #Quartz
#Hfo_wOH 2.01    600      892                   #IOCS
Hfo_sOH 0                                       #
−equilibrate 1                                  #
END

SURFACE 2−5     QUARTZ
Hfo_wOH 0.207    600      93.3                  #Quartz
#Hfo_wOH 2.01    600      892                   #IOCS
Hfo_sOH 0                                  #
−equilibrate 1                             #
END

EQUILIBRIUM_PHASES 1−5
fix_pH −7.2 HCl 10                              #fix_pH fix_pH −7.2 NaOH 10
END

TRANSPORT
        −cells          5                                        # 5 cells
        −lengths        0.12                                     # 5∗ 0.12
        −shifts         25641                                    #Plug: 25
Fast_Corner: 102564 Slow_Middle:6410
        −time_step      2356                                     #Plug: 23
Fast_Corner: 589 Slow_Middle: 9423
        #timestep ∗ shifts = total time
        −flow_direction   forward
        −boundary_conditions    flux      flux
        −diffc          0.0e−9
        −dispersivities  0
        −correct_disp    true
        −print          5
        −print_frequency 10
```

```
            −punch_cells        5
            −punch_frequency 5




SELECTED_OUTPUT
            −file               Biofilter_Sorption_Quartz_Spangen.csv
            −reset              false
            −step
            −pH                 true
            −totals             Pb Cu Ni Zn Co #P

USER_PUNCH
−headings   total_residence_time bed_volume bed_volume2
−start
10 PUNCH (TOTAL_TIME + time_step /2)
11 PUNCH ((STEP_NO + .5) /5)*0.39                   #Bed volume = Pore Volume * poros
# Pore volume = (STEP_NO + .5) / cells
12 PUNCH TOTAL_TIME/(3.27*3600)*0.39                #Bed Volume = Total Time/(Time pe

USER_GRAPH 1
−headings time Zn pH Ni Cu
−axis_titles Bed_Volumes ug/L pH
−initial_solutions false
−chart_title "Try 1"
−plot_concentration_vs t
#−plot_tsv_file data_P.txt                  # plot data from tab delimited text file
−axis_scale y_axis         0 1.5 0.1        # a b c from a to b with steps of c
−axis_scale sy_axis        6 10 0.2                 # pH
−axis_scale x_axis         0 1000 10        # bed volumes
−start
10 graph_x total_time/(3.27*3600)*0.39   # BV
20 graph_y (tot("Zn")*1e6) / 7.19e−03    #normalised
30 graph_sy −la("H+")
40 graph_y (tot("Ni")*1e6)/3.03e−02
50 graph_y (tot("Cu")*1e6)/2.68e−03
−end

END
```